Optimization Techniques for Reliable Data Communication in Multi-Antenna Wireless Systems

by

Ramadan Elsabae

A Doctoral Thesis submitted in partial fulfilment
of the requirements for the degree of
Doctor of Philosophy

July 2018

Signal Processing and Networks Research Group
Wolfson School of Mechanical, Electrical and
Manufacturing Engineering
Loughborough University

To my late parents Grera and Oum Alkhair

and late brothers Mohammed and Ahmed

Declaration

This is to certify that I am responsible for the work submitted in this thesis, that the original work is my own except as specified in acknowledgements or in footnotes, and that neither the thesis nor the original work therein has been submitted to this or any other institution for a degree.

..... (Signed)

Ramadan Elsabae

July 2018

Acknowledgements

I would like to thank my first and second supervisor Dr. Yu Gang and Prof. Sangarapillai Lambotharan for their guidance and support throughout my years of PhD studies.

My thanks to my colleagues and staff at the Signal Processing and Networks Research Group at Loughborough University for their help and friendship throughout my PhD studies.

Finally, I would like to thank my wife for her support and encouragement to complete my PhD study.

Abstract

The field of wireless communication has witnessed tremendous growth and attracted increasing attention over the past decades. Some of these successes are due to the possibility of implementing different wireless antenna configurations as well as exploiting signal processing capabilities and mathematical optimization techniques. Utilizing multiple antenna configuration techniques such as MIMO offers such advantages including increasing channel capacity as well as combating interference and fading. Furthermore, signal processing and mathematical optimization techniques offer smart approaches to improve performance, security, efficiency and robustness in wireless communication systems. This thesis aims to combine the advantages of different antenna configurations with the advantages of signal processing and optimization techniques to develop new techniques that offer improvements in wireless communication systems. Specifically, this thesis looks at new methods of achieving reliable data communication in wireless communication systems using different antenna transmission optimization methods. In particular, the problems of exploitation of MIMO communication channel diversity, secure downlink beamforming techniques, adaptive beamforming techniques, resource allocation methods, simultaneous

power and information transfer and energy harvesting within the context of multi-antenna wireless systems are addressed.

Firstly, a new optimization technique for use in coordinated multi-cell beamforming in the presence of local users and a global user is proposed. In this approach, the local users are served by only the corresponding base station (BS), while the global user is served by multiple basestations. The global user is able to, with the aid of multiple antennas, decode multiple data streams transmitted by various transmitters through singular value decomposition of the channels at the receiver and using left dominant singular vectors as the receiver beamforming. The coordinating base stations employ semidefinite programing based transmitter beamforming and agree to perform optimal data rate split for the global user in order to minimise the transmission power.

In the second contribution, the problem of maximising the worst case user signal-to-interference-plus-noise-ratio (SINR) in multi-input single-output (MISO) system within the context of energy harvesting is addressed. The interference channel is exploited by users for radio frequency energy harvesting (RFEH), while satisfying quality of service (QoS) and power constraints within a framework of beamforming and resource allocation. A power splitting technique, in which each user divides the received signal into data information and energy charging is considered. The minimum SINR of all users in the MISO network that meets the transmitted power and energy harvesting constraints is maximised.

In order to achieve simultaneous wireless information and power transfer (SWIPT) in a wireless powered communication (WPC) system,

a downlink beamforming design with simultaneous energy and secure information transmission approach is employed. The WPC system consists of the wireless device (WD) and an information receiver (IR). The SWIPT system simultaneously serves one IR while transferring power to a WD. Both systems operate on the same frequency band. As a result, the WD is able to jointly take advantage of the wireless energy transfer from the SWIPT BS, interference power from the BS due to transmission of signals to IRs and the recycled power for energy harvesting. This approach aim to minimize the total transmitted power of the SWIPT BS subject to the SINR target at the information receivers. In order to preserve the secrecy of the information transmitted by BS to IRs on the BS, we introduce a set of constraints SINR less than the SINR threshold values.

In the final work, the SWIPT system simultaneously serves one information receiver (IR1) while transferring power to a WD. In addition, a second information receiver (IR2) is considered and served by the WD. The WD is charged by the wireless energy signal power from the SWIPT BS plus the loop information signal transmitted from the WD, which received by one antenna energy receiver (ER) located at the WD. Additionally, it is assumed that IR1 is an eavesdropper for the WD, and IR2 is an eavesdropper for the BS and both systems operate on the same frequency band. In this approach, the secrecy rate maximisation problem is non-convex due to the non-concavity of the secrecy rate function, thus two alternative algorithms are proposed to reformulate the optimization to a convex problem, which are the null space based optimization and Taylor series approximated optimization.

The aforementioned proposed techniques are evaluated using different performance measures in order to demonstrate their performance and improvements as compared to existing techniques.

Table of Contents

List of Symbols

a	Lower case denotes a scalar
$\mathbf{a}$	Lower case bold denotes a vector
$\mathbf{H}$	Upper case bold denotes a matrix
$\mathbf{I}$	Identity matrix
$\lvert\mathbf{A}\rvert$	Determinant of matrix $\mathbf{A}$
$\lVert\cdot\rVert_2$	Euclidean norm
$\lVert\cdot\rVert_F$	Frobenius norm
$\mathbb{C}$	The set of complex numbers
$\mathbb{C}^n$	n-dimensional complex $\mathbb{C}^n$
$\mathbb{R}$	The set of real numbers
$\mathbb{R}^n$	Real vectors $\mathbb{R}^n$
$\mathbb{H}^n$	Complex hermitian matrix $\mathbb{H}^n$
$\mathbf{A} \succeq \mathbf{B}$	$\mathbf{A}$ - $\mathbf{B}$ is a positive semi-definite matrix
$\mathbf{A} \succeq 0$	$\mathbf{A}$ is a positive semi-definite
$(\cdot)^T$	Transpose operator
$(\cdot)^H$	Hermitian
$(\cdot)^{-1}$	Inverse
$(\cdot)^*$	Complex conjugate
$\mathbb{E}(\cdot)$	Expectation operator

$\mathrm{Tr}(\cdot)$	Trace operator
$\mathrm{rank}(\cdot)$	Rank operator
$\mathbf{0}$	Vector of zeros
$\mathbf{1}$	Vector of ones
$\mathbf{dom}$	Domain of a function
$\cup$	Union of a set
$\cap$	Intersection of a set
$\mathrm{diag}(\cdot)$	Diagonal elements of a square matrix
$\log(\cdot)$	Natural logarithm
$\Pr(\cdot)$	Probability operator
$\exp(\cdot)$	Exponential operator
$\log_2(\cdot)$	Logarithm to base 2
$\min(\cdot)$	Minimum value
$\max(\cdot)$	Maximum value
$\otimes$	Kronecker product

List of Acronyms

AWGN	Additive White Gaussian Noise
BPSK	Binary Phase Shift Keying
BER	Bit Error Rate
BSs	Base Stations
CSCG	circularly Symmetric Complex Gaussian
CPU	Central Processing Unit
CSI	Channel State Information
DC	Direct Current
DPC	Dirty Paper Coding
DPSK	differential Phase Shift Keying
ER	Energy Receiver
ET	Energy Transmitter
GSVD	Generalized Singular Value Decomposition
IR	Information Receiver
IT	Information Transmitter
MIMO	Multiple-Input Multiple-Output
MISO	Multi Input Single Output
MMSE	Minimum Mean Square Error
MRC	Maximum Ratio Combining

MU-MIMO	Multiuser Multi-input Multi-output
MU-MISO	Multiuser Multi-input Single-output
OFDM	Orthogonal Frequency division Multiplexing
PMU	Power Management Unit
QoS	Quality of Service
RF	Radio Frequency
SIMO	Single Input Multi Output
SINR	Signal-to-Interference-Ratio
SISO	Single-Input Single-Output
STBC	Space Time Block Code
SNR	Signal To Noise Ratio
SDMA	Space Division Multiple Access
SDP	Semidefinite Programming
SWIPT	Simultaneously Wireless Information and Power Transfer
SVD	Singular Value Decomposition
WD	Wireless Device
WET	Wireless Energy Transfer
WIT	Wireless Information Transfer
WPC	Wireless Power Communication
ZF	Zero-Forcing

List of Figures

Chapter 1

Introduction

Over the last three decades, the communications industry has witnessed unprecedented growth in it's history [2–5]. This owes largely to the advancements in both the architecture and technology of wireless communications. This in turn has raised a lot of expectations in the field leading to even further research and development of new ideas. Consequently, numerous cutting edge applications have emerged from theoretical research ideas through to commercialisation. These include, wireless fidelity (WI-FI), smart grids, the global positioning system (GPS), wireless sensor networks (WSN) and a host of mobile electronic devices such as mobile phones, tablets etc. More so, this devices are expected to offer high speed data communication and transfer with limited resources such as frequency etc. However, due to the ever increasing demand of consumers for mobile electronic devices, existing resources are becoming overloaded and meeting this ever increasing demand keeps getting more challenging. Therefore, new techniques and approaches are needed in order to meet current demands as well

as future wireless communications systems. In addition, the demand for portable wireless devices is on the increase. More so, these devices are expected to offer high speed data communication and transfer with limited resources such as frequency etc. There is the possibility of using the technology to increase the data rate. Given that these devices require power to operate, hence, the power demand by these devices is also on the increase as the number of devices increases. Therefore, we have a situation where the number of wireless device is on the increase which means more energy is becoming abundant. Harvesting this readily available energy to produce power could help mitigate the power demand by helping power the devices.

In proffering new solutions to meeting these demand challenges, it is crucial to identify key areas associated with such demands. A careful study of the wireless communication systems may reveal transmit/receive antenna configuration, energy efficiency, reliability (or the quality of service (Qos)) and security as the key factors that have played important roles in the evolution witnessed in the wireless communications field. Furthermore, it may seem that these requirements can be satisfied easily by increasing the transmit power and the transmission bandwidth. However, leveraging frequency reuse becomes a useful approach to serve an increasing number of users within the availability of scarce radio spectrum resource. Therefore, increasing transmit power cannot always be a good solution as this will in turn lead to increase in the interference power of the co-channel. Furthermore, power saving in cellular networks can help to reduce emission of the greenhouse gases in addition to alleviating the financial burden to service providers [6].

1.1 Motivation

Multi-antenna transmission has been considered an effective method for capacity improvement of wireless communication systems when it comes to coping with the wireless access consumers ever increasing demand of high speed data communication [7–9] and [10].

Multiple-antenna approaches form a key aspect for modern wireless communications. These techniques provide a trade-off between superior error performance and higher data rates for increased system complexity and cost. A number of transmission principles that exploit the multiple-antenna configuration employs such configurations at either the transmitter, the receiver, or both. A technique known as spatial modulation (SM) is a new multiple-antenna transmission technique. This technique, with a very low system complexity, can offer improved data rates when compared to non-multiple-antenna systems i.e. single-input single-output (SISO) systems. Additionally, it can offer improved and robust error performance even in environments with correlated channels. The SM approach is an entirely new modulation concept that is able to exploit the uniqueness and randomness properties of the wireless channels for communication purposes. Simple but effective coding mechanism that establishes one-to-one mapping between blocks of information bits that are to be transmitted and the spatial positions of the transmit-antenna in the antenna-array is employed to achieve SM [11].

Multiple-antenna usage for wireless communication systems has received an increased interest by researchers during the last decade [12]. Multiple-antenna in multiple-input multiple-output (MIMO) systems

configuration can be exploited in different ways to achieve antenna gains, diversity, or multiplexing. In addition, MIMO techniques have important advantages, developing new approaches for multiple antenna transmission in order to mitigate the practical limitations while retaining the key advantages of a MIMO systems is essential.

In wireless communication systems there has been an increase in the demand for data traffic and throughput. This has been due to the fact that mobile devices are usually constrained by their limited battery life. Additionally, it is often costly to replace or recharge their batteries. Thus, energy harvesting (EH) has become attractive for realizing perpetual communications.

As a possible application context, EH is employed in fifth-generation (5G) wireless communication networks as a way of bypassing the energy limitation issues in mobile devices. This is also a way to improve the energy efficiency of the 5G networks by extracting energy from the external natural environment (e.g., wind energy, solar power, etc.) [13, 14].

Energy is and has been harvested directly from external sources without exploiting the resources of the communication network itself. However, the natural environment may not be able to provide stable energy. When this is the case, wireless mobile receivers may have to find alternative energy sources in the communication network for example information-carrying radio-frequency (RF) signal radiated by fixed transmitters (hot spots, base stations, etc.) [15–17]. In such a situation, the transmitter not only act as a sender of signals to the mobile receivers, but will also need to transfer power that can be used

to charge these receivers' batteries. As a result, the idea of simultaneous wireless information and power transfer (SWIPT) becomes a promising concept to provide power for communication devices as a way to mitigate the energy scarcity and extend the lifetime of wireless networks [17, 15].

As mentioned earlier, security is a key criteria in wireless networks and consequently plays a significant role in wireless communications. This is because it ensures that important messages are confidential enough so as to prevent eavesdropping from unauthorized users.

There are some crucial reasons which lead to security issues including vulnerability of wireless channels is to channel jamming making it easy for an eavesdropper to jam and prevent legitimate users from accessing the network. Another reason is when an active attacker obtains illegal access to network resources thereby bypassing secure infrastructures without the authentication mechanisms. Another might be eavesdropping without advanced technological devices due to the open nature of wireless channels [18].

Considering security in SWIPT, a number of researches have been carried out in this regard. Particularly, secure communication in SWIPT has been investigated in [19–26]. The authors in [19] considered a MISO secure SWIPT system with two optimization problems: i) energy harvesting maximization with a secrecy rate constraint for the IR, and ii) secrecy rate maximization of IR with individual harvested energy constraints of energy receivers (ERs), have been developed to guarantee a reliable information transmission to the IR and the target harvested energy simultaneously transferred to the ERs are satisfied by optimally designing the beamformer vectors and the power allocation at the legit-

imate transmitter. The authors in [20] addressed the problem of secure communication system with SWIPT when two types of eavesdroppers (potential eavesdroppers and passive eavesdroppers) coexist. A total transmit power minimization problem was formulated to jointly optimize the transmit beamforming, and energy beamforming, thereby achieving secure communications with a target amount of harvested power by incorporating channel uncertainties of the potential eavesdroppers. In [23], the authors considered a multiuser MISO SWIPT system with multi-antenna energy harvesting potential eavesdroppers only, where an energy harvesting maximization problem is proposed to guarantee secure communications. The authors also show the existence of a rank-one optimal transmit covariance solution and proposed one efficient algorithm to construct an equivalent rank-one optimal solution [19, 23]. In [19, 23] however, the authors considered the case where the CSI is assumed to be available, i.e. only the CSI of the potential eavesdropper is unavailable at the transmitter [20, 21], for which there are practical difficulties to obtain the CSI of the link between the transmitter and the users. Robust secure transmission for a MISO SWIPT system has been proposed without Artificial Noise (AN) in [22] and with AN [24], by incorporating the channel uncertainties of all channels. Semi-definite programming (SDP) relaxation was used in [22, 24, 26] to solve the secrecy rate maximization problem. However, the suboptimal solution has been proposed to guarantee the solution of the relaxed problem is rank-one [22], whereas in [24, 26], the authors have shown the optimal solution of the relaxed problem is rank-two, which is not exact to the optimal condition for the SDP relaxation. The authors in

[25] used a two-step algorithm with conic reformulation proposed to circumvent the rank-one solution in the MISO secure SWIPT system, while a new SDP relaxation is investigated to guarantee that the relaxed problem yields rank-one solution in the AN-aided MISO secure SWIPT system. The optimal resource allocation in the AN-aided secure Orthogonal Frequency-Division Multiple Access (OFDMA) systems with SWIPT was investigated in [27].

Overall, exploitation of MIMO communication channel diversity, secure downlink beamforming techniques, adaptive beamforming techniques, resource allocation methods, simultaneous power and information transfer and energy harvesting provide promising grounds for improvements in multi-antenna wireless communication systems. This thesis presents and describes new methods associated with the aforementioned approaches.

1.2 Thesis Outline

Optimal beamforming, interference attenuation, secure downlink communication, simultaneous power and information transfer and energy harvesting are crucial challenges facing reliable data communication in multi-antenna wireless systems. This is especially so when one takes into consideration the ever increasing demand for secure portable wireless devices with multi-antenna, fast data rates and high throughputs. The work in this thesis therefore focuses on techniques for addressing the aforementioned challenges and improving the respective solutions. The proposed solutions as well as improvements to solutions are presented

and detailed in the subsequent chapters. Specifically, the outline of this thesis is as follows:

In Chapter 1, the focus is on introducing the motivation, overview as well as the contributions of the thesis. A list of publications steming from this thesis can be found also in Chapter 1.

In Chapter 2, background material and key concepts related to reliable data communication in multi-antenna wireless systems are introduced. In addition, some solution concepts used to offer improvements in relation to wireless communication systems are studied . In particular, the idea of multi-antenna wireless communication is examined along with beamforming techniques followed by the introduction of some key fundamentals of convex optimization techniques.

In Chapter 3, mathematical optimization techniques for coordinated multi-cell beamforming in the presence of local users and a global user are investigated. The global user is served by multiple bases tations (BS) while the local users are served by only the corresponding basestation. With the aid of multiple antennas, the global user is able to decode multiple data streams transmitted by various transmitters through singular value decomposition of the channels at the receiver while using left dominant singular vectors as the receiver beamforming. The coordinating basestations employ semidefinite programing based transmitter beamforming and agree to perform optimum data rate split for the global user in order to minimise the transmission power.

In Chapter 4, study the problem of maximizing the worst-case user signal-to-interference-plus-noise ratio (SINR) in a multi input single output (MISO) system within the context of energy harvesting. The

interference channel is exploited by users for radio frequency energy harvesting (RFEH) while satisfying QoS and power constraints within a framework of beamforming and resource allocations. The power splitting technique where each user divides the received signal into data information and energy charging is considered. The worst-user case SINR is maximized while satisfying the transmission power and energy harvesting constraints in addition to meeting the RFEH constraints.

Chapter 5 focuses on the study of a downlink wireless network consisting of wireless powered communication (WPC) system and a simultaneous wireless information and power transfer (SWIPT) system. The SWIPT system simultaneously serves one information receiver (IR) while transferring power to a wireless device (WD). The wireless powered system consists of the WD and its IR. Both systems operate on the same frequency band. The WD is therefore able to take advantage of the wireless energy transfer from the SWIPT basestation (BS), interference power from the BS due to transmission of signals to IRs and the recycled power for energy harvesting. The aim is to minimize the total transmitted power of the SWIPT BS subject to the signal-to-interference-and-noise ratio (SINR) target at the information receivers. Furthermore, a set of constraints SINR less than one are introduced in order to preserve the secrecy of the information transmitted by BS to IRs on the BS.

Chapter 6 considers secrecy rate optimizations for a simultaneous wireless information and power transfer (SWIPT) and wireless powered communication (WPC)system. The SWIPT system simultaneously serves one information receiver (IR1) and transfers power to a wireless

device (WD). The second information receiver (IR2) is served by the WD. Additionally, it is assumed that the (IR1) is an eavesdropper for the information signal transmitted by the (WD), and the (IR2) is an eavesdropper for the information signal transmitted by the (BS). The secrecy rate maximization problem is non-convex due to the non-concavity of the secrecy rate function. As a result, Taylor series approximation of the secrecy rate function is employed to reformulate the problem as a convex one.

Chapters 3 to 6 form the heart of the original contributions of this thesis.

Finally, concluding remarks are drawn and possible future research challenges are discussed in Chapter 7.

1.3 Publications List

The main contributions of this thesis are based on the under listed publications.

1.3.1 Journals

1. **Ramadan. Elsabae,**, A. Deligiannis Y. Gong and S. Lambotharan,“Secrecy Wireless Information and Power Transfer in MIMO Channels," in *IEEE Transactions on Vehicular Technology*, (Submitted).

1.3.2 Conferences

1. **Ramadan Elsabae**, Bokamoso Basutli, Kinan Ghanem, Yu. Gong and Sangarapillai Lambotharan, “"Coordinated Multicell Beamforming with Local and Global Data Rate Constraints". In: *24th European Signal Processing Conference (EUSIPCO)*, Budapest, Hungary, 2016, pp. 1388 - 1392.

2. **Ramadan Elsabae**, Bokamoso Basutli, Yu Gong, and Sangarapillai Lambotharan, “Downlink Beamforming Design with Simultaneous Energy and Secure Information Transmission". In: *2017 IEEE Wireless Communications and Networking Conference (WCNC)*, San Francisco, USA, 2017, pp. 1-5.

3. Kinan Ghanem, **Ramadan Elsabae**, Bokamoso Basutli, and Sangarapillai Lambotharan,„ “Lambotharan,"SINR Balancing for MISO System Model with Energy Harvesting Constraints". (Ready for Submission).

Chapter 2

Literature Review and Technical Background

2.1 Introduction

In this chapter, background material and key concepts related to data communication in multi-antenna wireless systems are introduced. In addition, some solution concepts used to offer improvements in relation to wireless communication systems are studied. In particular, the idea of multi-antenna wireless communication is examined along with different multi-antenna types. Exploitable techniques often used to derive the benefits in multi-antenna wireless systems including beamforming and singular value decomposition are studied. This chapter further looks at the convex optimization theory where the idea of convex and non-convex problems is introduced along with techniques for handling such problems.

2.2 Communication in Multi-Antenna Wireless Systems

In wireless systems, multi-antenna transmission has been employed largely as way of increasing and improving the system robustness, capacity and error rate performance [9, 8]. A multi-antenna wireless system usually involves equipping both the transmitter and receiver with multiple antennas. The multi-antenna wireless system configuration has garnered attention and raised expectations in the wireless communication community owing to the promising improvements it offers as a way of countering challenges due to resource availability constraints and channel impairments. The most important advantages of multiple antenna systems are array gain, interference reduction, and diversity gain. A typical configuration of the multi-antenna types is

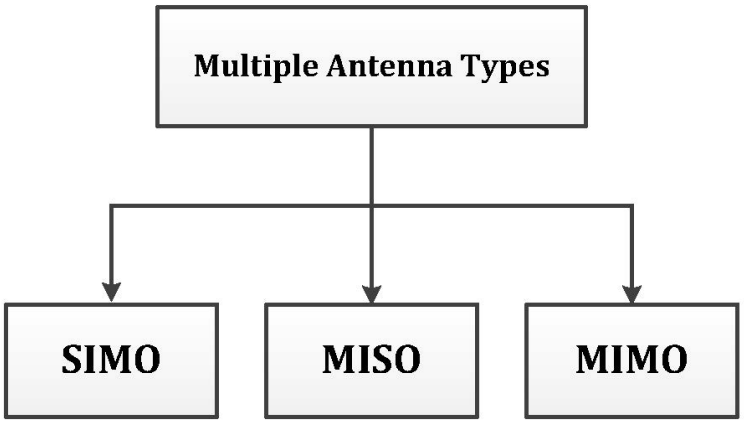

Fig. 2.1 Different types of multi-antenna configurations.

shown in Fig. 2.1. For the purpose of this thesis, the single-input multiple-output (SIMO) version of multi-antenna wireless system is not

considered. Although it offers receive diversity and help combat fading and channel interference.

2.2.1 Multiple-Input Single-Output (MISO)

The MISO configuration is such that there are more than one antennas at the transmitter and one antenna is present at the receiver. An example MISO configuration is shown in Fig. 2.2. This configuration allows for transmit diversity where data are transmitted redundantly from the two or more transmit antennas and the receive receives the optimum signal. The MISO configuration offers desirable properties

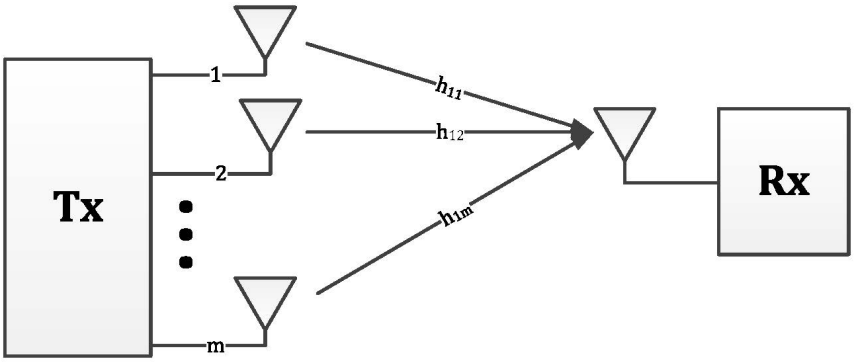

Fig. 2.2 Exapmle MISO configuration.

which include the redundancy coding and processing being done at the transmitter end. This property is of significant advantage to wireless mobile devices because it helps to reduce the processing levels required at the receiver and also less space is required for the receiver.

2.2.2 Multiple-Input Multiple-Output (MIMO)

The MIMO system configuration consists of two or more antennas at both the transmitter and receiver ends. The MIMO system configuration

offers many advantages including providing improvement in channel capacity and robustness, data throughput and additional diversity to help combat fading ([7–9]). Furthermore, the a MIMO system offers what is known as multiplexing gain compared to the traditional antenna array systems in addition to being able to exploit the transmit and receive multi-antenna benefits simultaneously [28]. An example MIMO

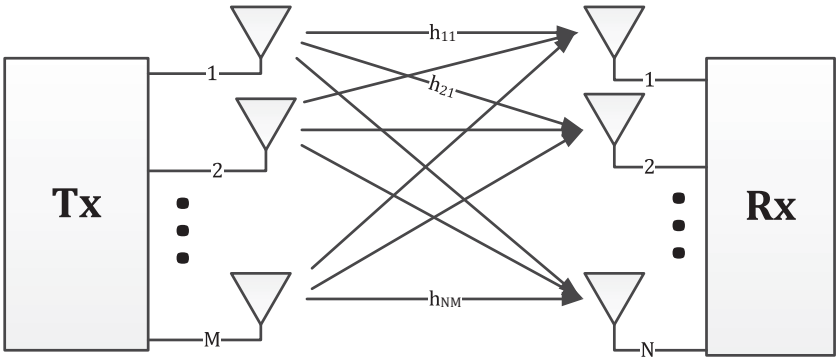

Fig. 2.3 Example MIMO configuration with M transmit antennas and N receive antennas.

configuration is shown in Fig. 2.3. From the Figure, there are M transmit antennas and N receive antennas. The MIMO channel gain, H is expressed as an $N \times M$ matrix given as

$$\mathbf{H} = \begin{bmatrix} h_{1,1} & \cdots & h_{1,M} \\ \vdots & \ddots & \vdots \\ h_{N,1} & \cdots & h_{N,M} \end{bmatrix}, \tag{2.1}$$

and the received signal is given by

$$\mathbf{y} = \mathbf{H}\mathbf{x} + \mathbf{n}, \tag{2.2}$$

where $\mathbf{H} \in \mathbb{C}^{N \times M}$ with $h_{n,m}$ being the single -input single-output (SISO) channel gain between the n-th receive and the m-th transmit antenna pair. The vector $\mathbf{y} \in \mathbb{C}^{N \times 1}$ denotes the received signal, $\mathbf{x} \in \mathbb{C}^{M \times 1}$ represents the transmit signal vector, and $\mathbf{n} \in \mathbb{C}^{N \times 1}$ denotes an additive white complex Gaussian noise vector.

2.2.3 Singular Value Decomposition (SVD)

SVD is a valuable tool that can be employed in a wireless MIMO system to help handle data transmission issues including interference elimination thereby enhancing data throughput and coverage. The SVD technique can be thought of as a way to look at the MIMO channel as a set of independent channel. SVD involves the specific decomposition of the wireless MIMO channel matrix, $\mathbf{H}$ of (2.1). The SVD technique is useful for analysing/characterising the behaviour of a MIMO channel matrix and it can be applied to a non-square matrix. In addition, SVD has the advantage of achieving parallelization in a MIMO channel. Using SVD, the channel gain matrix of (2.1), can be decomposed into a product of three matrices as [Jie Tang 64]:

$$\mathbf{H} = \mathbf{U}\mathbf{\Sigma}\mathbf{V}^H, \tag{2.3}$$

where $\mathbf{U} \in \mathbb{C}^{M \times M}$ is an $M \times M$ matrix and $\mathbf{V} \in \mathbb{C}^{N \times N}$ is an $N \times N$ matrix. $\mathbf{\Sigma} \in \mathbb{C}^{M \times N}$ is an $M \times N$ diagonal matrix. These singular

values are non-negative and arranged in decreasing order of magnitude. The number of non-zero singular values denotes the rank of the matrix. The SVD technique is valid for $N \geq M$.

2.2.4 Null Spaces

Null space is a technique which applies to linear transformations. The right null space (or simply the null space) of a matrix $\mathbf{G} \in \mathbb{R}^{n \times m}$ is that matrix, $\mathbf{X}$ such that

$$\mathbf{GX} = 0, \tag{2.4}$$

where $\mathbf{X} \in \mathbb{R}^{m \times (m-r)}$ with $r = \text{rank}(\mathbf{G}) \leq \min(n, m)$. The left null space of $\mathbf{G}$ is that matrix $\mathbf{Y}$ such that

$$\mathbf{YG} = 0, \tag{2.5}$$

where $\mathbf{Y} \in \mathbb{R}^{(n-r) \times n}$ with $r = \text{rank}(\mathbf{G}) \leq \min(n, m)$. Therefore, the left null space of the channel matrix of (2.1) $\mathbf{H}$ is the columns of $\mathbf{U}$ (of (2.3)) corresponding to singular values equal to zero, transposed. The null space (or the right null space) of $\mathbf{H}$ are the columns of $\mathbf{V}$ corresponding to where singular values equal to zero.

2.2.5 Beamforming Techniques

Beamforming, also known as a spatial filtering technique is a signal processing method used to achieve transmission or reception directionality control in the physical layer of a multi-antenna system. In addition to improve transmission/reception gain, this technique is utilized at the transmit and receive end of a MIMO system to achieve spatial

selectivity. Furthermore, beamforming exploits interference in order to change the directionality of the transmit/receive array [Tang 44].

Transmitter Beamforming

In transmit beamforming, the data in each symbol period is multiplied by a set of weighting coefficients. This is to precompensate for the channel effects before transmission. When transmitting, the beamformer controls the relative phase and the amplitude of the signal at each transmitter so as to form a constructive radiation pattern and destructive interference in the wave front. Beamforming at the transmitter is also known as downlink beamforming. In the transmitter beamforming, beamformers for all users within a coverage area must be jointly designed so as to avoid interference to unintended users within that area. Furthermore, in order to be able to estimate channel coefficients, channel knowledge is needed and this could be provided by sending the estimates of what is known as the channel state information (CSI) from the receiver through a finite rate feedback channel [Tang 45–48]. Fig. 2.4 shows an illustration of transmit beamforming. Let $\mathbf{w} = [w_1, w_2, \cdots, w_M]^T$ be the weighting factors imposed on the set of M transmit antennas, respectively. The signal transmitted on the m-th antenna is given by

$$\mathbf{x}_m(n) = w_m \mathbf{s}(n), \tag{2.6}$$

where $\mathbf{x}_m(n)$ is the transmitted signal, $\mathbf{s}(n)$ is the information stream and w_m is the weighting factor

Suppose user i is a recipient of the signal from the transmit beamformer, therefore, the signal received by the user i can be written

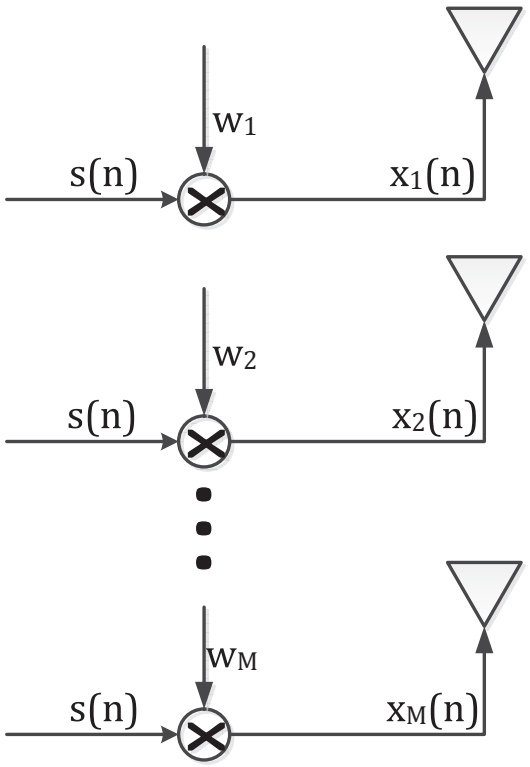

Fig. 2.4 Example transmitter beamformer format.

as

$$y_i(n) = \mathbf{h}_i^H \mathbf{x} + v_i(n), \tag{2.7}$$

where $\mathbf{h}_i$ denotes the channel coefficient vector between the transmitter and the user i and v_i denotes the receiver noise.

Receiver Beamforming

In receive beamforming, the goal is to estimate the desired signal in the presence of interference and noise. When receiving, the different signals from each of the receiving antennas are combined such that what is observed is the expected pattern of radiation. Fig. 2.5 shows an illustration of receiver beamforming. Let $\mathbf{w}^* = [w_1^*, w_2^*, \cdots, w_N^*]^T$

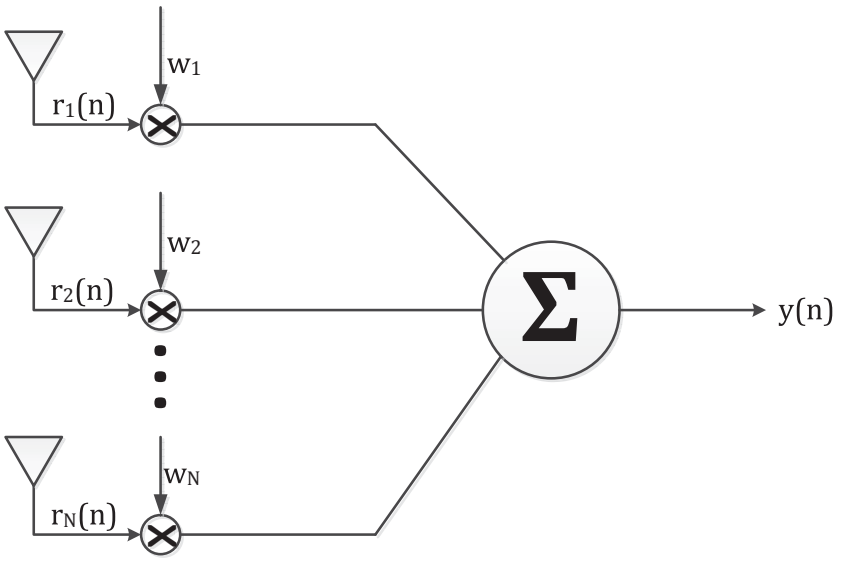

Fig. 2.5 Example receiver beamformer format.

be the complex weighting vector imposed on the set of N receive antennas, where $[\cdot]^T$ denotes the transpose operator; and denote $\mathbf{r}(n) = [r_1(n), r_2(n), \cdots r_N(n)]^T$ as a $N \times 1$ vector of array observations. The received signal, $y[n]$ is given by

$$y(n) = \mathbf{w}^H \mathbf{r}(n), \tag{2.8}$$

where the array observation vector, $\mathbf{r}(n)$ given as

$$\mathbf{r}(n) = \mathbf{d}(n) + \boldsymbol{\iota}(n) + \boldsymbol{\gamma}(n), \tag{2.9}$$

and the terms $\mathbf{d}(n), \boldsymbol{\iota}(n)$ and $\boldsymbol{\gamma}(n)$ are the desired signal, the receiver noise and the interference respectively.

2.3 Emerging Concepts

Owing to the to advances witnessed in the evolution of wireless communication systems and the prospects of multiple-antenna wireless systems over the last three decades; some new concepts have emerged as a way of exploring new dimensions and as well as proffering solutions to some of the challenges associated with these advances. Some of these new dimensions include wireless energy harvesting and simultaneous wireless energy transfer and ensuring secure communication in the presence of an eavesdropper. These concepts are briefly introduced.

2.3.1 Summary of Wireless Power Transfer (WPT)

Energy harvesting for wireless communication networks is a new system that allows wireless terminal and devices to recharge their batteries from wireless energy sources. There has been alot of requirement and interest to implement energy harvesting technologies into communication networks. Many researchers and studies concentrate on WPT and energy harvesting. The efforts on WPT have concentrated on high power applications and long distance. However health consideration and poor transmission process prevent further development. Thus most studies on WPT work on short distance transmission such as charging mobile , wireless phones, electrical vehicle and some medical applications. In the literature [29], many experimental results for different WPT scenarios are presented. In terms of energy consumption and interference management, (SWIPT) can give better result by superposing information and power transfer. For example, with the same signal

wireless device receiver can be charged and receive information from the information and energy transmitter on the same time. The need for SWIPT technologies will increase in the field of Internet of Things in small cells, MIMO technologies and new generation mobile networks to overcome path loss effect and support energy sustainability and high throughput. A typical WEH enabled sensor device usually consists of a WEH unit, a transceiver, an antenna, a power management unit, a sensor/processor unit, and possibly an onboard battery [30].

2.3.2 WPT Module

There are three different modules of WPT system, near field, far field directive power and far field low power. For far field low power type, the distance and communication range up to several kilometers and the collected and harvested power are about microwatts. In this chapter, the far field low power WPT module will be considered. WD is a wireless device can receive wireless energy and use this harvested energy to transmit it is own information to specific information receiver. In figure 2.6, block diagram of a WD in WPC far field low power module. The WD consist of special antenna array system call Rectenna, which is include RF power collection antenna, matching network and a radio frequency to direct current (RF to DC) converter, an energy storage unit and the power management unit (PMU). The rechargeable battery will provide power to the central processing unit (CPU) [31], the transmitter will use this power to transmit information through transmitter antenna.

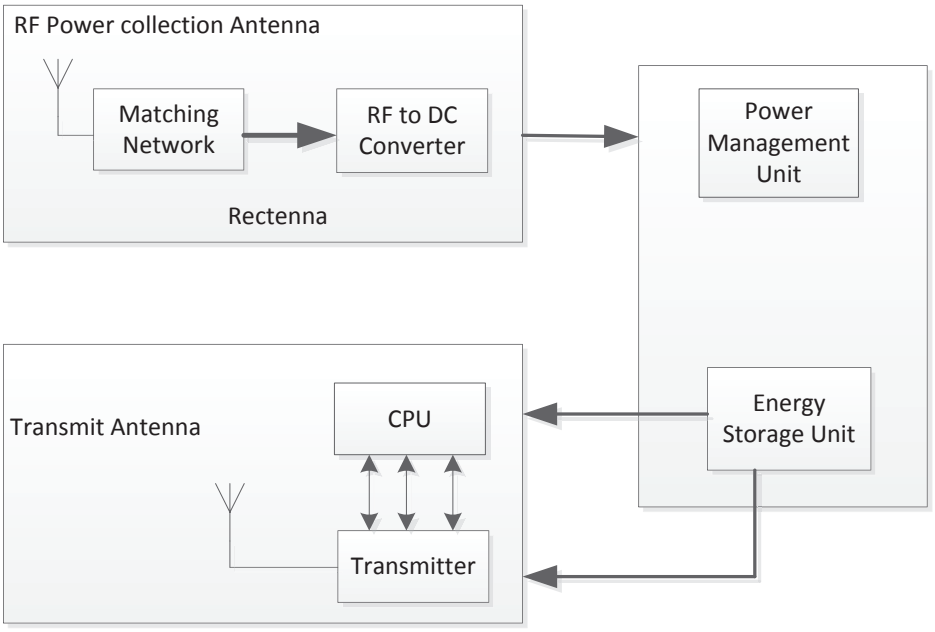

Fig. 2.6 Block diagram of a WD in WPC far field low power module.

2.3.3 Simultaneous Wireless Information and Power Transfer (SWIPT)

SWIPT is a promising technology for multi-antenna wireless systems where remote receivers simultaneously extract information and power from the common transmit signal [32, 33, 16, 34, 35]. The SWIPT approach exploits the same emitted electromagnetic wave field in order to deliver both energy and information at the same time. The SWIPT technique offers such advantages as: energy scavenging ability by wireless devices while receiving data, hence prolonging their life time and interference control [35] An example SWIPT setting is depicted in Fig. 2.7. It is seen from this figure that a single multi-antenna transmitter transmits both information and power signal to different receivers simultaneously.

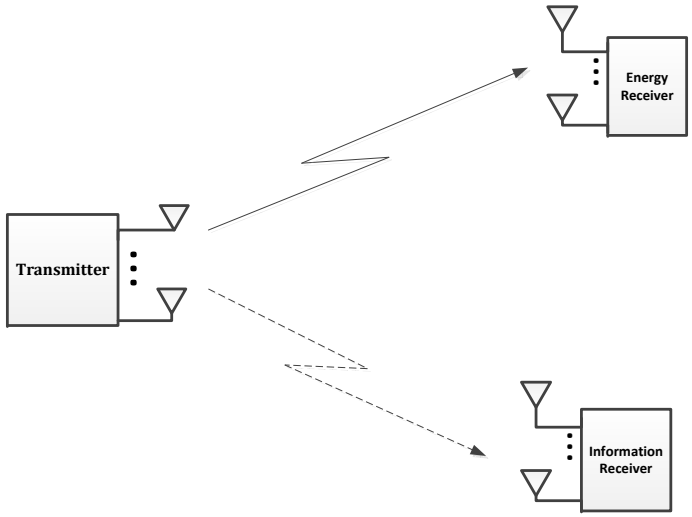

Fig. 2.7 An example MIMO system for SWIPT.

2.3.4 Secure Communications for Multi-Antenna Transceiver

This subsection introduces the concept of reliable and secure communications for multi-antenna systems. Particularly, in the case where a transmitter equipped with multiple antennas is required to transmit securely to a multi-antenna receiver in the presence of an eavesdropper. The concept of secure communications in multi-antenna systems has also been researched widely; see [36–40] for more details. The problem of a transmitter communicating with a receiver in the presence of an eavesdropper can be considered as a wiretap channel problem. Consider the diagram of Fig. 2.8. In this figure, a legitimate transmitter communicates with a legitimate receiver while an eavesdropper attempts to listen in on the communication. Suppose the legitimate transmitter and receiver consist of M and N transmit and receive antennas, respectively, and the eavesdropper has N_e receive antennas. The channel

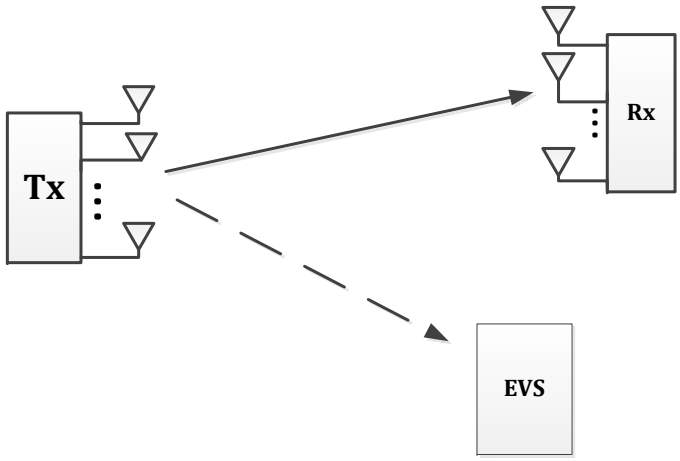

Fig. 2.8 A simple wiretap channel. Tx is the legitimate transmitter, Rx is the legitimate receiver and EVS is the eavesdropper.

coefficients between the legitimate transmitter and receiver and the eavesdropper can be represented as $H_l \in \mathbb{C}^{M\times N}$ and $H_e \in \mathbb{C}^{M_e\times N_e}$, respectively. Denote P as the maximum available transmit power at the legitimate transmitter. The signal received at the legitimate receiver can be expressed as

$$\mathbf{y}_l = \mathbf{H}_l^H \mathbf{x} + \mathbf{v}_l, \quad \mathbf{y}_e = \mathbf{H}_e^H \mathbf{x} + \mathbf{v}_e, \tag{2.10}$$

with $\mathbf{x} \in \mathbb{C}^{M\times 1}$ denoting the desired signal intended to the legitimate receiver. The covariance of the transmit matrix is expressed as $Q_l = \mathbb{E}\{\mathbf{x}\mathbf{x}^H\}$. The two noise terms $\mathbf{v}_l$ and $\mathbf{v}_e$ are zero mean circularly symmetric complex Gaussian random variables with identity covariance matrices. Achievable transmission rate to both the legitimate receiver and the eavesdropper can be written as [8]:

$$R_l = \log\left|\mathbf{I} + \frac{1}{\sigma_l^2}\mathbf{H}_l^H \mathbf{Q}_l \mathbf{H}_l\right|, \quad R_e = \log\left|\mathbf{I} + \frac{1}{\sigma_e^2}\mathbf{H}_e^H \mathbf{Q}_l \mathbf{H}_e\right| \tag{2.11}$$

respectively. The achievable secrecy rate at the legitimate receiver is: [37]

$$R = [R_l - R_e]^+. \tag{2.12}$$

The notation $[\cdot]^+$ denote $\max\{\cdot, 0\}$. The secrecy rate maximization is then formulated as:

$$\begin{aligned} \max_{\mathbf{Q}_l \succeq 0} \quad & R, \\ \text{s.t.} \quad & \text{Tr}(\mathbf{Q}_l) \leq P, \end{aligned} \tag{2.13}$$

where, $\mathbf{Q}_l, \text{Tr}(\mathbf{Q}_l)$ and P are the information signal covariance matrix at the transmitter, the trace of the information signal covariance matrix at the transmitter and the maximum transmit power at the transmitter respectively.

2.4 Convex Optimization Theory

The use of mathematical optimization techniques to facilitate analytical and numerical solutions in the field of multi-antenna wireless communication and other engineering problems has grown widely within the last three decades [41]. These techniques have been used to perform design and analysis of communication systems and development of signal processing algorithms. This is mainly because many communication problems can either be cast as or be converted into mathematical optimization problem. One of such optimization techniques is known

as convex optimization. Convex optimization generally refers to the minimization of a convex objective function subject to one or more convex constraints [41]. In convex optimization problems, a local optimum is also a global optimum. This key feature make convex optimization techniques attractive and important in many communications and engineering problems. More so, the optimal solution of a convex problem can be verified by employing rigorous optimality conditions known as the Karush-Kuhn-Tucker (KKT) conditions and duality theory. Once a problem has been formulated as a convex one, software tools such as CVX [newcastle 90], MATLAB, Yalmip [newcastle 89] can be used to to solve convex optimization problems. This in turn make solutions to convex problems in communication and engineering more implementable. Most problems are however not convex and hence cannot be solved directly. However, some non-convex problems can be recast as a convex problem and solved using convex optimization problems solving methods. It is therefore key to be able recognize problems which can be solved directly using convex optimization approaches and those that require reformulation into a convex problem in order to apply convex optimization techniques. Subsequently, the key concepts of convex optimization techniques for both convex and non-convex problem will be introduced.

2.4.1 Basic Concepts in Optimization

Being familiar with the basic concepts of convexity as well as the convex optimization models is a key step in understanding and recognizing convex optimization problems in communication and engineering

applications [41]. Some of these basic concepts are introduced next, particularly the idea of convex sets, cones and functions.

Convex Sets

A set $\mathcal{S}$ is said to be convex if the line segment joining any two points $x_1, x_2 \in \mathcal{S}$ also lies in $\mathcal{S}$. This property is defined mathematically as

$$\mu = \theta x_1 + (1-\theta)x_2 \in \mathcal{S}, \quad \forall \theta \in [0,1], \tag{2.14}$$

where $\theta \in \mathbb{R}$ with the parameter value $\theta = 0$ and $\theta = 1$ corresponding to when $\mu = x_2$ and $\mu = x_1$ respectively [1].

Convex Cones

A set $\mathcal{C}$ is referred to as a cone or nonnegative homogeneous if there exists $\alpha \geq 0$ and for every $y \in \mathcal{C}$, αy is such that $\alpha y \in \mathcal{C}$. The set $\mathcal{C}$ is called a convex cone if the set is convex and a cone. This implies that for any $y_1, y_2 \in \mathcal{C}$ and $\alpha_1, \alpha_2 \geq 0$, the following holds [1]:

$$\alpha_1 y_1 + \alpha_2 y_2 \in \mathcal{C}. \tag{2.15}$$

Convex cones can be realised in different forms in communication and engineering applications. The most common forms of convex cones are [41]:

i. Second-order cone (SOC). This is also known as ice cream cone.

ii. Nonnegative orthant $\mathbb{R}^n_+$

iii. Positive semidefinite matrix cone.

Convex Functions

A function $f(y) : \mathbb{R}^n \to \mathbb{R}$ is said to be convex if its domain, $\mathbf{dom}f(y)$ is a convex set and if $\forall y_1, y_2 \in \mathbf{dom}f(y)$, and α with $0 \leq \alpha \leq 1$ the following inequality holds [1]:

$$f(\alpha y_1 + (1-\alpha)y_2) \leq \alpha f(y_1) + (1-\alpha)f(y_2). \tag{2.16}$$

Considering Fig. 2.9, the inequality of (2.16) geometrically implies that

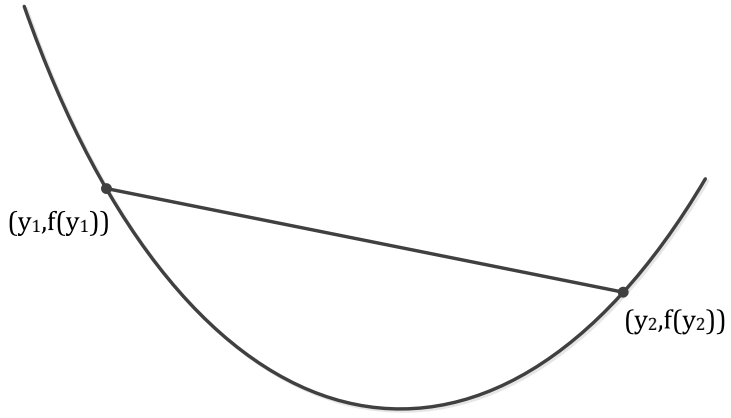

Fig. 2.9 An example graph of a convex function. The line segment (i.e., chord) between any two points on the graph lies above the graph [1].

the chord from y_1 to y_2 i.e. the line segment between $(y_1, f(y_1))$ and $(y_2, f(y_2))$ lies above the graph of $f(y)$ as seen in Fig. 2.9. Moreover, a function $f(y)$ is termed *strictly convex* if strict inequality holds in (2.16) whenever $y_1 \neq y_2$ and $0 < \alpha < 1$. Furthermore, the function $f(y)$ is concave if $f(y)$ is *convex*, and *strictly concave* if the function $f(y)$ is strictly convex. In addition, a function is convex iff it is convex when restricted to any line that intersects its domain. That is to say $f(y)$ is convex iff for all $y_1 \in \mathbf{dom}f(y_1)$ and all b, the function $g(v) = f(y_1 + vb)$ is convex (on its domain, $\{v | y_1 + vb \in \mathbf{dom}f(y_1)\}$).

The above is a useful property as it allows for the convexity check of a function by restricting it to a line [1].

2.4.2 Convex Optimization Problems

In this subsection, the basic format of a convex optimization problem as well as some basic terminologies used in formulating such problem are introduced. In addition, some example types of convex optimization problems are presented.

A generic convex optimization problem can be coined in the following form [1]:

$$\begin{aligned} \min_{y} \quad & f_0(y) \\ \text{subject to} \quad & f_j(y) \leq 0, \quad j = 1, \cdots, p, \\ & h_j(y) = 0, \quad j = 1, \cdots, r, \end{aligned} \tag{2.17}$$

where $y \in \mathbb{R}^n$ denotes the *optimization variable*, the function $f_0 : \mathbb{R}^n \to \mathbb{R}$ is the *objective function* or *cost function* and the functions $f_0, \cdots, f_p : \mathbb{R}^n \to \mathbb{R}$ and $h_1, \cdots, h_r$ are convex and linear functions respectively; $f_j(y) \leq 0$ and $h_j(y) = 0$ are termed as the *inequality constraint* and *equality constraint* respectively. The corresponding functions $f_j : \mathbb{R}^n \to \mathbb{R}$ and $h_j : \mathbb{R}^n \to \mathbb{R}$ are called the *inequality constraint functions* and *equality constraint functions* respectively. Note that in some convex optimization problems, the terms in the first and second line of (2.17) are shortened from *minimize* and *subject to* to *min* and *s.t.* respectively. The set of points for which all constraint functions and the objective function are defined is known as the *domain*,

$\mathcal{D}$ of the example optimization problem of (2.17). This domain, $\mathcal{D}$ is given as

$$\mathcal{D} = \bigcap_{j=0}^{p} \mathbf{dom} f_j \cap \bigcap_{j=1}^{r} \mathbf{dom} h_j. \tag{2.18}$$

If a point $y \in \mathcal{D}$ satisfies the inequality and equality constraints $f_j(y) \leq 0$ and $h_j = 0$ then it is *feasible*. The problem in (2.17) is feasible if at least one feasible point exists, else it is *infeasible*. The set of all points that are feasible is called the *constraint set* or the *feasible set*. The optimal solution to the problem of (2.17) can be achieved at the optimal point y^* such that the following inequality holds

$$f_0(y^*) \leq f_0(y), \quad \forall y \in \mathcal{D}. \tag{2.19}$$

The example optimization problem described in (2.17) is said to be convex if the following conditions are true:

i. The functions $f_j(j = 0, 1, \cdots, p)$ are convex;

ii. $h_j(x)$ are affine functions, and

iii. The set domain of the optimization problem is convex.

In what follows, some example types of convex optimization problems are presented.

Linear Programming

In a convex optimization problem, when the objective and all constraint functions are affine, this type of problem is then called *linear*

programming. A linear programming problem can be written as:

$$\begin{aligned} \min_{\mathbf{y}} \quad & \mathbf{a}^T\mathbf{y} \\ \text{s.t.} \quad & \mathbf{b}_j^T\mathbf{y} \preceq \mathbf{c}_j, \quad j = 1, \cdots, p, \end{aligned} \tag{2.20}$$

where vectors $\mathbf{a},\ \mathbf{b}_1, \cdots, \mathbf{b}_p \in \mathbb{R}^n$ and scalars $\mathbf{c}_1, \cdots, c_p \in \mathbb{R}$ are the parameters of the optimization problem that specify the objective and constraint functions.

Quadratic Programming

Another example of a type of convex optimization problem is quadratic programming. In this type of problem, the objective function is quadratic (or convex) and the constraint functions are affine. A quadratic programming problem can be written as:

$$\begin{aligned} \min_{\mathbf{y}} \quad & \mathbf{y}^T\mathbf{Q}\mathbf{y} + \mathbf{p}^T\mathbf{y} + l \\ \text{s.t.} \quad & \mathbf{P}\mathbf{y} \preceq \mathbf{h}, \\ & \mathbf{G}\mathbf{y} = \mathbf{b}, \end{aligned} \tag{2.21}$$

where $\mathbf{Q} \in \mathbb{S}_+^n$, $\mathbf{P} \in \mathbb{R}^{m\times n}$ and $\mathbf{G} \in \mathbb{R}^{m\times n}$. Linear programming is a special case of quadratic programming when $\mathbf{Q}$ from first line of (2.21) is zero.

Second-Order Cone Programming

A convex optimization problem in the following form is called a second-order cone programming (SOCP) problem [1]:

$$\begin{aligned} \min_{\mathbf{y}} \quad & \mathbf{f}^T\mathbf{y} \\ \text{s.t.} \quad & ||\mathbf{A}_j\mathbf{y} + \mathbf{b}_j||_2 \leq \mathbf{c}_j^T\mathbf{y} + d_j, \quad j = 1, \cdots, p, \\ & \mathbf{F}\mathbf{y} = \mathbf{g}, \end{aligned} \tag{2.22}$$

where $\mathbf{y} \in \mathbb{R}^n$ is called the optimization variable, $\mathbf{A} \in \mathbb{R}^{n_j \times n}$, and $\mathbf{F} \in \mathbb{R}^{m \times n}$. The constraint $||\mathbf{A}\mathbf{y} + \mathbf{b}||_2 \leq \mathbf{c}^T\mathbf{y} + d$, is called as second-order cone constraint, since it is the same as requiring the affine function $\mathbf{A}\mathbf{y} + \mathbf{b}, \mathbf{c}^T\mathbf{y} + d$ to lie in the second-order cone in $\mathbb{R}^{k+1}$. If $A_j = 0,\ j = 1, \cdots, p$ then the SOCP problem of (2.22) reduces to a (general) linear programming problem.

2.4.3 Quasi-Convex Problem

Some convex optimization problems can be *quasi-convex* (or *unimodal*). A function $f : \mathbb{R}^n \to \mathbb{R}$ is called quasi-convex if for a certain $\alpha \in \mathbb{R}$, its domain and all its sub-level sets

$$\mathcal{S}_\alpha = y \in \mathbf{dom} f | f(y) \leq \alpha, \tag{2.23}$$

are convex [1]. The standard for a quasi-convex problem can be written as [1]:

$$\begin{aligned} \min_{y} \quad & f(y) \\ \text{s.t.} \quad & f_j(y) \leq 0, \quad j = 1, \cdots, p, \\ & \mathbf{A}y = \mathbf{b}. \end{aligned} \tag{2.24}$$

A function is called *quasi-concave* if the function f is *quasi-convex*, i.e., every super-level set $\{y|f(y) \geq \alpha\}$ is convex. A function that is quasi-convex and also quasi-concave is termed quasi-linear. For quasi-linear function f, its domain, and every level set $\{y|f(y) = \alpha\}$ are all convex [1].

2.4.3.1 Bisection Method

A quasi-convex optimization problem can be solved by solving a sequence of convex optimization problems. This relies on the fact that the sub-level sets of a quasi-convex function can be represented by a family of convex inequalities. Define a non-increasing function, $\psi_t(\mathbf{y}) : \mathbb{R}^n \rightarrow \mathbb{R}$, $t \in \mathbb{R}$, as a family of convex functions which has the following property:

$$f(\mathbf{y}) \leq t \Leftrightarrow \psi_t(\mathbf{y}) \leq 0. \tag{2.25}$$

The quasi-convex optimization problem in (2.24) can be formulated to consider the feasibility problem below:

$$\begin{aligned} \text{find} \quad & y \\ \text{s.t.} \quad & \psi_t(\mathbf{y}) \leq 0, \\ & f_j(\mathbf{y}) \leq 0, \quad j = 1, \cdots, p, \\ & \mathbf{A}\mathbf{y} = \mathbf{b}. \end{aligned} \tag{2.26}$$

The equation in (2.26) is a convex feasibility problem due to its equality constraints being linear and inequality constraints being convex. Suppose x^* is the optimal value of the quasi-convex optimization problem of (2.24); then $x^* \leq t$ or $x^* \geq t$ if (2.24) is feasible or infeasible respectively. The inequality $x^* \leq t$ means that for any given t, any feasible point $\mathbf{y}$ is also feasible for the problem of (2.24). Therefore, the problem of (2.24) can be solved using the bisection method by solving (2.26) at each step [1, 42]. The bisection method in this case is based on the assumption that (2.26) is feasible and the optimal value x^* lies within an initial interval $[u, v]$.

- Assume $t = \frac{(u+v)}{2}$ and use to solve (2.26).
- If $x^* \leq t$, the optimal value is in the lower half of the interval, then update the interval $[u, v]$ by reducing v.
- If $x^* \geq t$, the optimal value is in the upper half of the interval, then update the interval $[u, v]$ by increasing u.
- The optimal value x^* can be obtained when $v - u \leq \tau$, where $\tau > 0$ is a tolerance value [42].

2.4.4 Convex Optimization for Non-Convex Problems

Having a convex problem is desired as there are a variety of methods that can be employed to solve them and these problems can usually be solved directly. However, most of problems are generally not convex and a reformulation is required to recast the problem to a convex one. Once a problem is formulated in a convex manner, it can be solved at least from a numerical perspective. Convex optimization techniques play an important role in non-convex problems. Convex optimization can be applied to problems that are not convex in various ways which include combining convex optimization with a local optimization method as a way of handling initialization point issues for local optimization method [1]. Another useful role convex optimization plays in solving non-convex problems is in terms of bounds for global optimization. Many techniques used for global optimization require an inexpensive computable lower bound on the optimal value of the non-convex problem [1]. The (two) standard approaches for achieving this are based on convex optimization. The first involves *relaxation* where each non-convex constraint is replaced with a looser or relaxed, but convex, constraint. The second involves what is called *Lagrangian relaxation* where the Lagrangian dual problem is solved. This is a convex problem which provides a lower bound on the optimal value of the non-convex problem [1]. Some basic convex optimization concept which are required especially in terms of bounds for global optimization are discussed next.

2.4.4.1 Semi-definite Programming (SDP)

Denote K to be a pointed, closed convex cone. when K is $\mathbb{S}^k_+$, the associated conic form problem is called *semi-definite programming* and has the form [1]:

$$\begin{aligned} \min_{\mathbf{y}} \quad & \mathbf{a}^T\mathbf{y} \\ \text{s.t.} \quad & \mathbf{y}_1\mathbf{F}_1 + \mathbf{y}_2\mathbf{F}_2 + \cdots + \mathbf{y}_m\mathbf{F}_m + \mathbf{G} \succeq 0, \\ & \mathbf{A}\mathbf{y} = \mathbf{b}, \end{aligned} \tag{2.27}$$

where $\mathbf{y} \in \mathbb{R}^m$, $\mathbf{A} \in \mathbb{R}^{p\times m}$. . The inequality constraint in (2.27) is called the linear matrix inequality (LMI) [1] with $\mathbf{G}, \mathbf{F}_1, \cdots, \mathbf{F}_m \in \mathbb{S}^k$. If the matrices $\mathbf{G}, \mathbf{F}_1, \cdots, \mathbf{F}_m$ of (2.27) are all diagonal, then the LMI in (2.27) is equivalent to a set of m linear inequalities, and the SDP problem of (2.27) reduces to linear programming problem [1].

2.4.4.2 Semi-definite Relaxation (SDR)

Consider a non-convex quadratically constrained quadratic programming (QCQP) problem of the form

$$\begin{aligned} \min_{\mathbf{y}} \quad & \mathbf{y}^T\mathbf{Q}_0\mathbf{y} + \mathbf{p}_0^T\mathbf{y} + r_0 \\ \text{s.t.} \quad & \mathbf{y}^T\mathbf{Q}_j\mathbf{y} + \mathbf{p}_j^T\mathbf{y} + r_j \leq 0, \quad j = 1, \cdots, m, \end{aligned} \tag{2.28}$$

where $\mathbf{y} \in \mathbb{R}^n$, $\mathbf{Q} \in \mathbb{S}^n$ $\mathbf{p} \in \mathbb{R}^n$ and $r \in \mathbb{R}^{m\times n}$. The above problem is not convex when at least one of the $\mathbf{Q}_j$ is not positive semi-definite. The SDR method utilizes the property, $\mathbf{Y} = \mathbf{y}\mathbf{y}^T$ to linearise (2.28). This definition of $\mathbf{Y}$ implies that $\text{rank}(\mathbf{Y}) = 1$ and $\mathbf{y}^T\mathbf{Q}_j\mathbf{y} = \text{tr}(\mathbf{Q}_j\mathbf{Y})$.

As a result, (2.28) can be reformulated as

$$\begin{aligned} \min_{\mathbf{Y}} \quad & \mathrm{tr}(\mathbf{Q}_0\mathbf{Y}) + \mathbf{p}_0^T\mathbf{y} + r_0 \\ \text{s.t.} \quad & \mathrm{tr}(\mathbf{Q}_j\mathbf{Y}) + \mathbf{p}_j^T\mathbf{y} + r_j \leq 0, \quad j = 1, \cdots, m, \\ & \mathbf{Y} = \mathbf{y}\mathbf{y}^T \end{aligned} \tag{2.29}$$

The equality constraint $\mathbf{Y} = \mathbf{y}\mathbf{y}^T$ of (2.29) is a non-convex constraint. This constraint can however be relaxed introducing a looser positive semi-definite inequality constraint $\mathbf{Y} \succeq \mathbf{y}\mathbf{y}^T$. Afterwards, the problem of (2.29) can be rewritten as:

$$\begin{aligned} \min_{\mathbf{Y}} \quad & \mathrm{tr}(\mathbf{Q}_0\mathbf{Y}) + \mathbf{p}_0^T\mathbf{y} + r_0 \\ \text{s.t.} \quad & \mathrm{tr}(\mathbf{Q}_j\mathbf{Y}) + \mathbf{p}_j^T\mathbf{y} + r_j \leq 0, \quad j = 1, \cdots, m, \\ & \mathbf{Y} - \mathbf{y}\mathbf{y}^T \succeq 0 \end{aligned} \tag{2.30}$$

Using a property known as the Schur complement, the last constraint in (2.30) can be rewritten as

$$\begin{aligned} \min_{\mathbf{Y}} \quad & \mathrm{tr}(\mathbf{Q}_0\mathbf{Y}) + \mathbf{p}_0^T\mathbf{y} + r_0 \\ \text{s.t.} \quad & \mathrm{tr}(\mathbf{Q}_j\mathbf{Y}) + \mathbf{p}_j^T\mathbf{y} + r_j \leq 0, \quad j = 1, \cdots, m, \\ & \begin{bmatrix} \mathbf{Y} & \mathbf{y} \\ \mathbf{y}^T & 1 \end{bmatrix} \succeq 0. \end{aligned} \tag{2.31}$$

The problem seen in (2.31) is known as the SDP relaxation of the original non-convex problem in (2.28). The optimal value of the relaxed

problem gives the lower bound on the optimal value of the original non-convex QCQP.

2.4.4.3 Lagrangian Duality and KKT Conditions

As earlier stated, the Lagrangian duality is one of the techniques used to computable lower bound on the optimal value of the non-convex problem. Here, the Lagrangian duality and the *Karush-Kuhn-Tucker* (KKT) conditions are introduced.

Consider the problem of (2.17). Lagrange duality involves combining the objective function with a weighted sum of the constraint functions. For the problem of (2.17), the Lagrange dual problem $\mathcal{L} : \mathbb{R}^n \times \mathbb{R}^m \times \mathbb{R}^p \to \mathbb{R}$ can be expressed as:

$$\mathcal{L}(\mathbf{y}, \boldsymbol{\lambda}, \boldsymbol{\nu}) = f_0(\mathbf{y}) + \sum_{j=1}^{m} \lambda_j f_j(\mathbf{y}) + \sum_{j=1}^{p} \nu_j h_j(\mathbf{y}), \tag{2.32}$$

where $\nu_j \geq 0$, and $\lambda_j \geq 0$ are the Lagrange dual multipliers that are associated with the j-th equality $h_j(y) = 0$ and inequality $f_j(y) \leq 0$ constraints, respectively. The objective function $f_0(y)$ of (2.17) and the optimization variable $\mathbf{y}$ are called the primal objective and the primal variable respectively. The Lagrange dual multipliers $\boldsymbol{\lambda}$ and $\boldsymbol{\nu}$ known as the dual variables. The Lagrange dual objective or the Lagrange dual function $g : \mathbb{R}^m \times \mathbb{R}^p \to \mathbb{R}$

$$g(\mathbf{y}, \boldsymbol{\lambda}, \boldsymbol{\nu}) = \inf \mathcal{L}(\mathbf{y}, \boldsymbol{\lambda}, \boldsymbol{\nu}), \tag{2.33}$$

is the minimum value of the Lagrange dual function over y for $\lambda \in \mathbb{R}^m, \nu \in \mathbb{R}^p$. The function $g(\mathbf{y}, \boldsymbol{\lambda}, \boldsymbol{\nu})$ is always concave irrespective of

the convexity or otherwise of the original problem. This is because the dual function, $g(y, \lambda, \nu)$ is the pointwise infimum of a series of affine functions in $(\boldsymbol{\lambda}, \boldsymbol{\nu})$. $g(\mathbf{y}, \boldsymbol{\lambda}, \boldsymbol{\nu})$ produces a lower bound on the optimal value $f_0(\mathbf{y}*)$ to (2.17). Given any $\boldsymbol{\nu}$ and $\boldsymbol{\lambda} \geq 0$, the following is true:

$$g(\boldsymbol{\lambda}, \boldsymbol{\nu}) \leq f_0(\mathbf{y}*). \tag{2.34}$$

The difference between the primal objective $f_0(\mathbf{y})$ and the dual objective $g(\boldsymbol{\lambda}, \boldsymbol{\nu})$ is known as the duality gap. Weak duality occurs when strict inequality holds in (2.34), strong duality holds when the inequality is satisfied with equality between the primal problem and the dual problem. Solving the dual problem below can ensure best lower bound of the original problem is achieved:

$$\begin{aligned} \max_{\boldsymbol{\lambda}, \boldsymbol{\nu}} \quad & g(\boldsymbol{\lambda}, \boldsymbol{\nu}) \\ \text{s.t.} \quad & \boldsymbol{\lambda} \geq 0. \end{aligned} \tag{2.35}$$

KKT Conditions

The under listed are known as KKT conditions, and they confirm the optimality of the solutions

i. The primal inequality and and equality constraints: $f_j(y) \leq 0,\ j = 1, \cdots, m\ h_j(y) = 0,\ j = 1, \cdots, p$

ii. The dual constraints: $\lambda \geq 0$

iii. Complementary slackness: $\lambda_j f_j(y) \leq 0,\ j = 1, \cdots, m$

iv. Gradient of the Lagrange dual function with respect to y:

$$\bigtriangledown f_0(y) + \sum_{j=1}^{m} \lambda_j \bigtriangledown f_j(y) + \sum_{j=1}^{p} \nu_j \bigtriangledown h_j(y) = 0. \tag{2.36}$$

These conditions are necessary optimality conditions but not sufficient for general optimization. With optimization problems, the KKT conditions can be satisfied when strong duality holds. For convex optimization problems however, strong duality holds between the dual problem and the primal problem (both of which are optimal) if the KKT conditions hold [1].

2.5 Summary

In this chapter, fundamental concepts of multi-antenna wireless communication are outlined. Different configurations used in wireless communication systems were introduced and discussed in addition to spatial and signal processing methods used to derive useful performance benefits. Lastly, mathematical optimization methods used to facilitate numerical and analytical solutions in communications and engineering were introduced. In particular, convex optimization theory and its basic concepts and ideas for handling both convex and non-convex problems were discussed.

In the next chapter, a coordinated multicell beamforming technique will be proposed for achieving required data rate by a local and global user in a multi-antenna setting.

Chapter 3

Coordinated Multicell Beamforming with Local and Global Data Rate Constraints

In the previous chapter, background material and key concepts related to data communication in multi-antenna wireless systems as well as mathematical optimization techniques for solving both convex and non-convex problem have been introduced.

In this chapter, optimization techniques for coordinated multi-cell beamforming in the presence of local users and a global user are proposed. The local users are served by only the corresponding base station (BS), while the global user is served by multiple base stations. The global user, with the aid of multiple antennas, is able to decode multiple data streams transmitted by various transmitters through singular value

decomposition of the channels at the receiver and using left dominant singular vectors as the receiver beamforming. The coordinating bases tations employ semidefinite programing based transmitter beamforming and agree to perform optimum data rate split for the global user in order to minimise the transmission power.

3.1 Introduction

With technology trends of today, where wireless networks have data hungry users, it is necessary to consider cell densification that enhances frequency reusage [43, 44]. Multiantenna deployment at both mobile users and BSs also enables the mobile network to take advantage of the spatial diversity in order to increase the overall performance of the network. Various coordinated beamformer techniques have been developed for downlink beamforming in multiantenna wireless systems [45–47]. The use of generalized singular value decomposition (GSVD) for coordinated beamforming in MIMO system was examined in [48]. In [49], a multiuser multi-input multi-output (MU-MIMO) network was considered. The work in [49] showed that by introducing a limited number of zero-forcing constraints, the SINRs of all streams are decoupled and this reduces the problem to a multiuser multi-input single-output (MU-MISO) problem. The setback of this approach is the reduced degrees-of-freedom and inefficiency. Coordinated beamforming design with weighted power minimization was considered in [50] using Lagrangian duality theory. The work in [51] considered power minimization problem in a network wherein users are served by joint

non-coherent multiflow beamforming. The authors in [51] emphasized that even though the users can be served by multiple transmitters, the information symbols are coded and transmitted independently. Coordinated beamforming with user fairness based SINR balancing techniques were also considered in [52–55]. In this paper, we aim to study joint downlink beamforming using power minimization approach. The users have known specific data rate targets that need to be satisfied. We consider optimal solution that meets the target SINRs for all users. The set of users considered in this work consist of single antenna local users and a single multiantenna global user. The global user is served by multiple BSs. By using SVD, we decompose the multi-input multi-output (MIMO) channels between the BSs and the global user to form parallel and independent multi-input single-output (MISO) channels. The approach requires no phase synchronization between the BSs that are serving the global user. According to the proposed scheme, certain users are served by only a single base station (BS). However, one multiantenna terminal is served by two BSs. The latter user is known as global user which receives data from both BSs simultaneously. Hence, optimum split of data rate from different BS is also considered in this paper. Even though one global user is considered in this paper, it is possible to extend it to multiple global users who can benefit from different channel conditions of both BSs, especially when the users are at the cell edge.

3.2 Detection and Precoding for Multiple Input Multiple Output Channels

Figure 3.1 shows singular value decomposition-based MIMO transmission systems. Precoding is a generalization of beamforming to support multi-layer transmission in multi-antenna wireless communications. In conventional beamforming, the same signal is emitted from each of the transmit antennas with appropriate weighting such that the signal power is maximized at the receiver output [49]. Thus, in order to maximize the throughput in multiple receive antenna systems, multi-layer beamforming is required. The benefits of beamforming are to increase the received signal gain, by making signals emitted from different antennas add up constructively, and to reduce the multipath fading effect. The

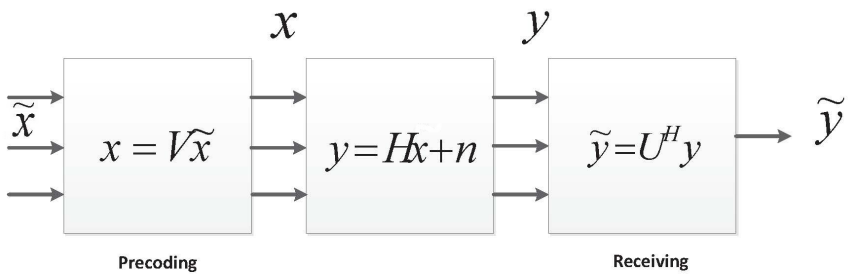

Fig. 3.1 Singular value decomposition-based MIMO transmission systems.

Precoding can be separated by two classifications which are precoding for single user MIMO and precoding for multi user MIMO. SVD is a mathematical application that lets us create an alternate structure of the MIMO signal. In particular the MIMO signal is examined by looking at the eigenvalues of the **H** matrix. The received signal is given

by

$$\mathbf{y} = \mathbf{H}\mathbf{x} + \mathbf{n} \tag{3.1}$$

The $\mathbf{H}$ matrix can be written in SVD form as

$$\mathbf{H} = \mathbf{U}\mathbf{\Lambda}\mathbf{V}^T \tag{3.2}$$

where $\mathbf{U}$ and $\mathbf{V}$ are orthogonal matrices and $\mathbf{\Lambda} = \text{diag}(\lambda_1, \lambda_2....., \lambda_n)$ a diagonal matrix of the singular values. Then received signal can be rewritten as

$$\mathbf{y} = (\mathbf{U}\mathbf{\Lambda}\mathbf{V}^T)\mathbf{x} + \mathbf{n} \tag{3.3}$$

Then the received signal $\mathbf{y}$ is multiplied by $\mathbf{U}^H$ which gives

$$\mathbf{r} = \mathbf{U}^H\mathbf{y} \tag{3.4}$$

The parallel decomposition is essentially a linear mapping function performed by pre-coding the input signal $\mathbf{s}$, consisting of multiplying it with matrix $\mathbf{V}$, such that $\mathbf{x} = \mathbf{V}\tilde{\mathbf{x}}$. Therefore, the received signal $\mathbf{r}$ can be written as

$$\mathbf{r} = \mathbf{U}^H[\mathbf{U}\mathbf{\Lambda}\mathbf{V}^T]\mathbf{V}\tilde{\mathbf{x}} + \mathbf{n}, \tag{3.5}$$

where $\mathbf{U}$ and $\mathbf{V}$ are unitary matrices ($\mathbf{U}^H\mathbf{U} = \mathbf{I}$ and $\mathbf{V}\mathbf{V}^T = \mathbf{I}$) and $\mathbf{\Lambda}$ is a diagonal matrix of singular values (λ_i) of H matrix.

$$\mathbf{r} = \mathbf{\Lambda}\tilde{\mathbf{x}} + \mathbf{n} \tag{3.6}$$

where

$$\mathbf{\Lambda} = \begin{bmatrix} \lambda_1 & 0 & . & . \\ 0 & \lambda_2 & 0 & . \\ . & . & . & . \\ 0 & . & . & \lambda_n \end{bmatrix} \tag{3.7}$$

In general, the singular value decomposition (SVD) is used to get the orthogonal and the best channel gain.

3.2.1 Precoding for Single User MIMO

In single user multiple-input multiple-output (MIMO) systems as shown in figure 3.2, a transmitter equipped with multiple antennas communicates with a receiver that has multiple antennas. Most classic precoding results assume narrowband, slowly fading channels, meaning that the channel for a certain period of time can be described by a single channel matrix. In practice, such channels can be achieved, for example, through orthogonal frequency division multiplexing (OFDM). The precoding strategy that maximizes the throughput, called channel capacity, depends on the channel state information available in the system.

3.2.2 Precoding for Multi User MIMO

In multi-user MIMO, a multi-antenna transmitter communicates simultaneously with multiple receivers (each having one or multiple antennas) as illustrated in Figure 3.3. This is known as space-division multiple access (SDMA). From an implementation perspective, precoding algorithms for SDMA systems can be sub-divided into linear and nonlinear precoding types. The capacity achieving algorithms are

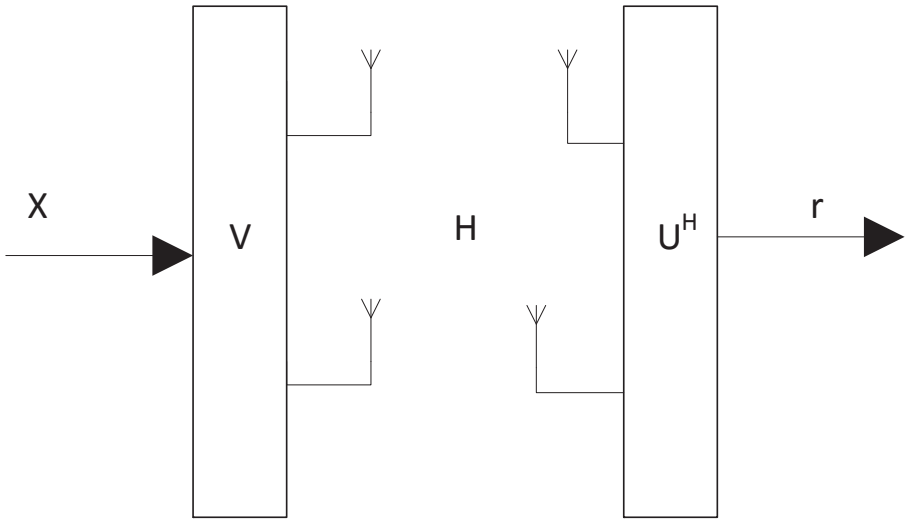

Fig. 3.2 One signal input singular value decomposition-based MIMO transmission systems.

nonlinear, but linear precoding approaches usually achieve reasonable performance with much lower complexity. Linear precoding strategies include minimum mean square error (MMSE) precoding and the simplified zero-forcing (ZF) precoding. There are also precoding strategies tailored for low-rate feedback of channel state information, for example random beamforming. Nonlinear precoding is designed based on the concept of dirty paper coding (DPC), which shows that any known interference at the transmitter can be subtracted without the penalty of radio resources [49] if the optimal precoding scheme can be applied on the transmit signal.

The model systems SISO, SVD-MIMO and Alamouti schemes were explained on previous section perform good performance. Figure (3.4) shows the comparison of average bit error rate (BER) performance between singular value decomposition-based MIMO transmission, Alamouti and SISO schemes. All the schemes use Binary Phase Shift Keying

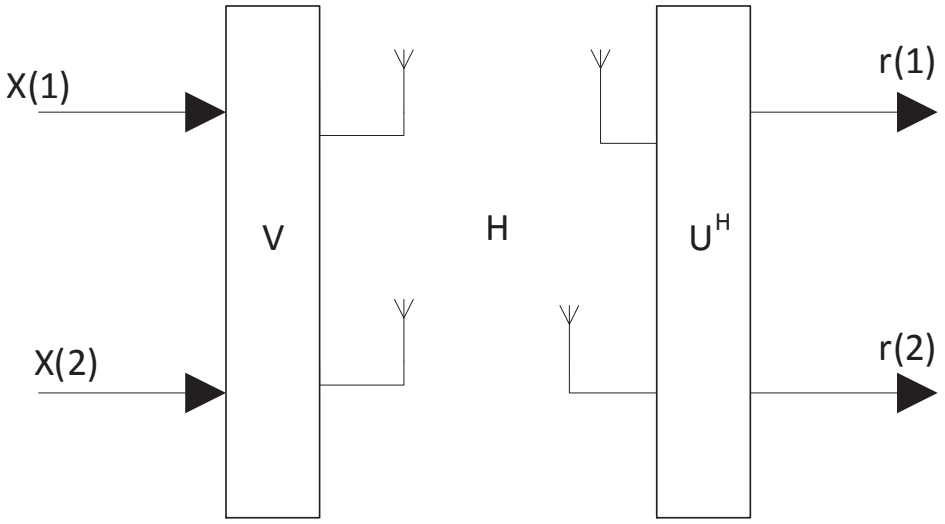

Fig. 3.3 Two signal input singular value decomposition-based MIMO transmission systems.

(BPSK) modulation. From the figure it can be seen that, SVD scheme with one signal input gives best performance comparing to SISO, Alamouti (2x2) and SVD with two signals input schemes due to that the SVD with one signal and Alamouti have divesity of four whereas SVD with two signals has diversity of two and SISO has no diversity. Since the singular values are often of very different magnitudes, this approach proves beneficial.

3.3 System Model and Assumptions

Considers a network comprising of two base-stations denoted by $n \in 1, 2$ as depicted in Figure 3.5. Each BS is equipped with M antennas and it serves L_n single antenna local users in the cell n. T sets of all local users and all BSs are denoted by $\mathcal{L}$ and $\mathcal{N}$ respectively. There is a global user denoted by g, being served by both BSs. The global user is

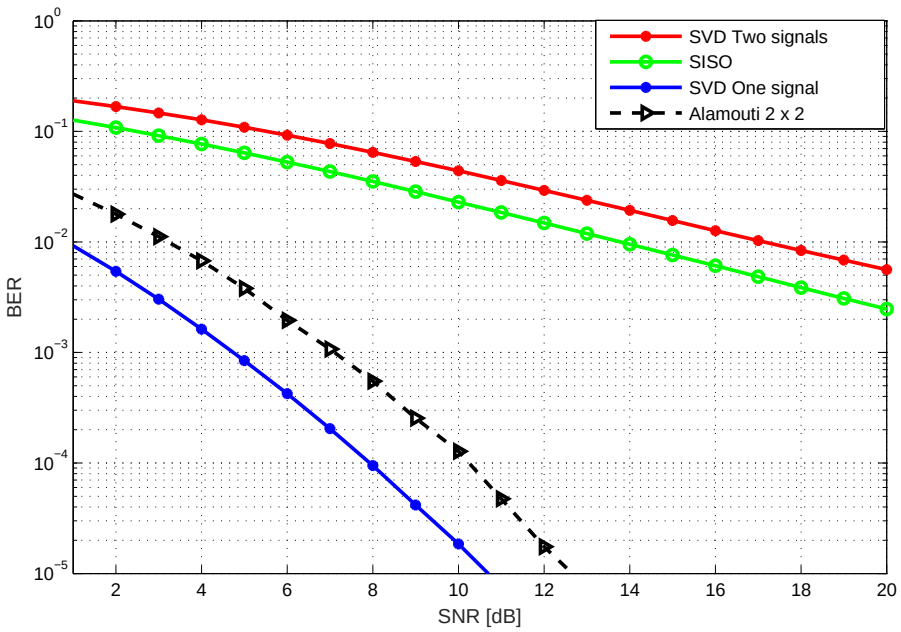

Fig. 3.4 Singular value decomposition-based MIMO transmission systems.

equipped with N_r antennas to be able to receive multi signals from multi transmitters. Assume that all the BSs operate in the same frequency and that all users experience considerable intercell interference.

3.4 Problem Formulation

In the downlink, the transmitted signal for l-th local user from n-th BS can be written as

$$\mathbf{x}_{nl}(t) = \mathbf{w}_{nl} s_l(t), \tag{3.8}$$

where $s_l(t) \in \mathbb{C}$ represents the information symbol at time t and $\mathbf{w}_{nl} \in \mathbb{C}^M$ is the transmit beamforming vector, the squared ℓ_2-norm of which represents the transmission power, for user l at n-th BS. Without loss of generality assume that $s_l(t)$ is normalised such that

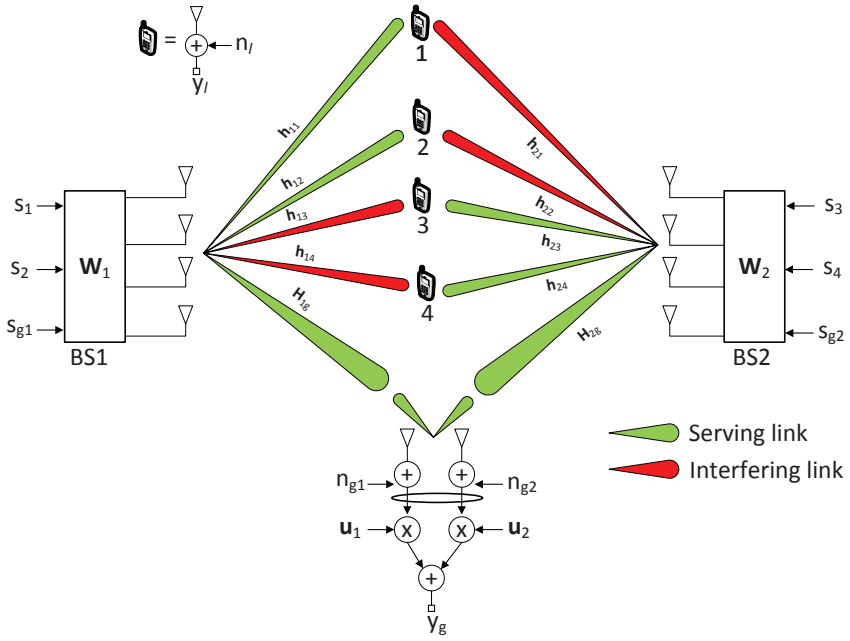

Fig. 3.5 Network topology. Both BS1 and BS2 serve two local user and one global user.

$\mathbb{E}\{|s_l(t)|^2\} = 1$ and that all data streams are independent such that $\mathbb{E}\{s_l(t)s_j(t)^*\} = 0$ if $l \neq i$. Perfect channel state information (CSI) is assumed at both the transmitter and the receiver. The MIMO channel between the n-th BS and the global user g denoted as $\mathbf{H}_{ng} \in \mathbb{C}^{N_r \times M}$, where N_r is the number of receive antennas at the global user. The intended signal at the global user is given by

$$\mathbf{r} = \mathbf{H}_{1g}\mathbf{w}_{1g_1}\mathbf{s}_{g_1}(n) + \mathbf{H}_{2g}\mathbf{w}_{2g_2}\mathbf{s}_{g_2}(n), \tag{3.9}$$

where, $\mathbf{s}_{g_1}$ is the transmitted signal from BS1 through channel g_1 to the global user and $\mathbf{s}_{g_2}$ is the transmitted signal from BS2 through channel g_2 to the global user The global user deploys the receive beamformers $\mathbf{U}_1$ and $\mathbf{U}_2$. By using SVD, the channel matrices between the BSs can

be written as

$$\mathbf{H}_{1g} = \mathbf{U}_1 \mathbf{\Lambda}_1 \mathbf{V}_1^H, \tag{3.10}$$

$$\mathbf{H}_{2g} = \mathbf{U}_2 \mathbf{\Lambda}_2 \mathbf{V}_2^H, \tag{3.11}$$

where $\mathbf{U}_1 \in \mathbb{C}^{N_r \times N_r}$ (respectively $\mathbf{U}_2 \in \mathbb{C}^{N_r \times N_r}$) and $\mathbf{V}_1 \in \mathbb{C}^{M \times M}$ (respectively $\mathbf{V}_2 \in \mathbb{C}^{M \times M}$) are the unitary matrices and $\mathbf{\Lambda}_1 \in \mathbb{C}^{N_r \times M}$ (respectively $\mathbf{\Lambda}_2 \in \mathbb{C}^{N_r \times M}$) is the diagonal matrix of the singular values of $\mathbf{H}_{1g}$ (respectively $\mathbf{H}_{2g}$) sorted in descending order. The SVD of the MIMO channels allows us to represent the global user as two virtual users denoted as g_1 and g_2. Denote $\mathbf{u}_1$ and $\mathbf{u}_2$ as the singular vectors corresponding to the largest singular values of $\mathbf{H}_{1g}$ and $\mathbf{H}_{2g}$ respectively. The decomposed received signal at the virtual users g_1 and g_2 can be written as

$$\begin{aligned} y_{g_1} = \mathbf{u}_1^H \Big[& \mathbf{H}_{1g}\mathbf{w}_{1g}sg_1 + \mathbf{H}_{2g}\mathbf{w}_{2g}sg_2 + \mathbf{H}_{1g}\left(\mathbf{w}_{11}s_1 + \mathbf{w}_{12}s_2\right) \\ & + \mathbf{H}_{2g}\left(\mathbf{w}_{23}s_3 + \mathbf{w}_{24}s_4\right) + n_{g_1} \Big], \end{aligned} \tag{3.12}$$

$$\begin{aligned} y_{g_2} = \mathbf{u}_2^H \Big[& \mathbf{H}_{2g}\mathbf{w}_{2g}sg_2 + \mathbf{H}_{1g}\mathbf{w}_{1g}sg_1 + \mathbf{H}_{2g}\left(\mathbf{w}_{23}s_3 + \mathbf{w}_{24}s_4\right) \\ & + \mathbf{H}_{1g}\left(\mathbf{w}_{11}s_1 + \mathbf{w}_{12}s_2\right) + n_{g_2} \Big], \end{aligned} \tag{3.13}$$

where n_{g_1} and n_{g_2} denote the additive white Gaussian noise for virtual users g_1 and g_1, respectively, with zero mean and variance $\sigma_{g_1}^2$ and $\sigma_{g_2}^2$, respectively. Let us denote the effective channel vector between the n-th BS and the virtual user g_v as $\mathbf{q}_{n,g_v}$. The effective channels

between the BSs and the virtual users can be written as

$$\mathbf{q}_{11} = \mathbf{u}_1^H \mathbf{H}_{1g}, \tag{3.14}$$

$$\mathbf{q}_{12} = \mathbf{u}_2^H \mathbf{H}_{1g}, \tag{3.15}$$

$$\mathbf{q}_{21} = \mathbf{u}_1^H \mathbf{H}_{2g}, \tag{3.16}$$

$$\mathbf{q}_{22} = \mathbf{u}_2^H \mathbf{H}_{2g}. \tag{3.17}$$

3.5 System Metric Design

All the users have specific data rate requirements in order to establish successful connections. A set of local users belonging to the n-th BS are denoted as $\mathcal{L}_n \subset \mathcal{L}$. The correlation matrix of the channel from the n-th BS to l-th local user is defined as $\mathbf{R}_{nl} = [\mathbf{h}_{nl}\mathbf{h}_{nl}^H]$. The correlation matrix of the channel from the n-th BS to the virtual user g_v is denoted as $\mathbf{G}_{ng_v} = [\mathbf{q}_{ng_v}\mathbf{q}_{ng_v}^H]$. The intracell and intercell interference powers experienced by the l-th local user are given as

$$I_n = \sum_{\substack{i=1 \\ i \neq l}}^{L_n} \mathbf{w}_{ni}^H \mathbf{R}_{nl} \mathbf{w}_{ni} + \mathbf{w}_{1g_1}^H \mathbf{R}_{nl} \mathbf{w}_{1g_1}, \tag{3.18}$$

$$I_p = \sum_{\substack{j=1 \\ p \neq n}}^{L_p} \mathbf{w}_{pj}^H \mathbf{R}_{pl} \mathbf{w}_{pj} + \mathbf{w}_{2g_2}^H \mathbf{R}_{pl} \mathbf{w}_{2g_2}, \tag{3.19}$$

respectively. The downlink SINR of the l-th local user at n-th BS is given by

$$\mathrm{SINR}_l^n = \frac{\mathbf{w}_{nl}^H \mathbf{R}_{nl} \mathbf{w}_{nl}}{I_n + I_p + \sigma_l^2}. \tag{3.20}$$

where $\mathbf{h}_{nl} \in \mathbb{C}^{M \times 1}$ is the channel vector between the n-th BS and the l-th local user, and σ_l^2 is the noise variance at the l-th local user.

Respectively, the SINR of the virtual users g_{v1} and g_{v2} are given by

$$\mathrm{SINR}_{g_1} = \frac{\mathbf{w}_{1g_1}^H \mathbf{G}_{11} \mathbf{w}_{1g_1}}{\sum\limits_{i=1}^{L_1} \mathbf{w}_{1i}^H \mathbf{G}_{11} \mathbf{w}_{1i} + \sum\limits_{j=1}^{L_2} \mathbf{w}_{2j}^H \mathbf{G}_{21} \mathbf{w}_{2j} + \sigma_{g_1}^2}. \tag{3.21}$$

$$\mathrm{SINR}_{g_2} = \frac{\mathbf{w}_{2g_2}^H \mathbf{G}_{22} \mathbf{w}_{2g_2}}{\sum\limits_{i=1}^{L_1} \mathbf{w}_{1i}^H \mathbf{G}_{12} \mathbf{w}_{1i} + \sum\limits_{j=1}^{L_2} \mathbf{w}_{2j}^H \mathbf{G}_{22} \mathbf{w}_{2j} + \sigma_{g_2}^2}. \tag{3.22}$$

According to [56], the total data rate of the global user is given by

$$R_g = R_{g1} + R_{g2} = \log_2(1 + \mathrm{SINR}_{g_1}) + \log_2(1 + \mathrm{SINR}_{g_2}). \tag{3.23}$$

3.6 Transmission Beamforming Design

The aim is to operate with the minimum total transmission power that will guarantee all the users their specific data rate target. The specific data rate for the l-th local user and the global user is denoted as r_l and r_g respectively. Our optimization problem is formulated as

$$\begin{aligned} \min_{\mathbf{W1},\mathbf{W2}} & \sum_{n\in\mathcal{N}} \sum_{l\in\mathcal{L}} \|\mathbf{w}_{nl}\|_2^2 + \|\mathbf{w}_{1g_1}\|_2^2 + \|\mathbf{w}_{2g_2}\|_2^2, \\ \text{s.t} \quad & \log_2(1 + \mathrm{SINR}_l) \geq r_l, \quad \forall l, \\ & R_g \geq r_g. \end{aligned} \tag{3.24}$$

In [46], it was proved that at optimality, the constraints in (3.24) will be satisfied with equality. For analysis purpose, the data rates are converted in (3.24) to SINRs. The local user SINR is determined as $\mathrm{SINR}_l = 2^{r_l} - 1$. By setting the data rate at virtual user g_1 as a variable θ, where $0 \leq \theta \leq r_g$, the SINRs of the virtual users g_1 and g_2 can be

written as $\text{SINR}_{g_1} = 2^{\theta} - 1$ and $\text{SINR}_{g_2} = 2^{(r_g - \theta)} - 1$, respectively. let us define the total interference experienced by the l-th local user and virtual users g_1 and g_2 as

$$I_l = \sum_{n\in\mathcal{N}} \sum_{k\neq l} \mathbf{w}_{pk}^H \mathbf{R}_{nk} \mathbf{w}_{pk} + \mathbf{w}_{1g_1}^H \mathbf{R}_{pg_1} \mathbf{w}_{1g_1} + \mathbf{w}_{2g_2}^H \mathbf{R}_{2g_2} \mathbf{w}_{2g_2}, \tag{3.25}$$

$$I_{g_1} = \sum_{n\in\mathcal{N}} \sum_{l\in\mathcal{L}} \mathbf{w}_{nl}^H \mathbf{R}_{nl} \mathbf{w}_{nl} + \mathbf{w}_{2g_2}^H \mathbf{G}_{1g_2} \mathbf{w}_{2g_2}, \tag{3.26}$$

$$I_{g_2} = \sum_{n\in\mathcal{N}} \sum_{l\in\mathcal{L}} \mathbf{w}_{nl}^H \mathbf{R}_{nl} \mathbf{w}_{nl} + \mathbf{w}_{1g_1}^H \mathbf{G}_{2g_1} \mathbf{w}_{1g_1}. \tag{3.27}$$

Given the SINR thresholds of the l-th local user and the virtual user g_v as γ_l and γ_{g_v}, we rewrite (3.24) as

$$\begin{aligned} \min_{\mathbf{W1},\mathbf{W2}} \; & \sum_{n\in\mathcal{N}} \sum_{l\in\mathcal{L}} \mathbf{w}_{nl}^H \mathbf{w}_{nl} + \mathbf{w}_{1g_1}^H \mathbf{w}_{1g_1} + \mathbf{w}_{2g_2}^H \mathbf{w}_{2g_2} \\ \text{s.t} \; & \mathbf{w}_{nl}^H \mathbf{R}_{nl} \mathbf{w}_{nl} - \gamma_l I_l \geq \gamma_{nl} \sigma_l^2, \quad \forall l, \\ & \mathbf{w}_{1g_1}^H \mathbf{G}_{1g_1} \mathbf{w}_{1g_1} - \gamma_{g_1} I_{g_1} \geq \gamma_{g_1} \sigma_{g_1}^2, \quad \forall l, \\ & \mathbf{w}_{2g_2}^H \mathbf{G}_{2g_2} \mathbf{w}_{2g_2} - \gamma_{g_2} I_{g_2} \geq \gamma_{g_2} \sigma_{g_2}^2, \quad \forall l, \end{aligned} \tag{3.28}$$

where $\gamma_l I_l$ is the SINR thresholds of the l-th local user and the γ_{g_1}, γ_{g_2} are the SINR threshold of the global user. The constraints set in (3.24) makes the whole problem non-convex but after necessary manipulations [57], the problem can be convexified. Denote $\mathbf{W}_{nl} = \mathbf{w}_{nl}\mathbf{w}_{nl}^H$, $\mathbf{W}_{1g_1} = \mathbf{w}_{1g_1}\mathbf{w}_{1g}^H$ and $\mathbf{W}_{2g_2} = \mathbf{w}_{2g_2}\mathbf{w}_{2g}^H$. using the rule $\mathbf{w}^H\mathbf{R}\mathbf{w} = \text{Tr}[\mathbf{R}\mathbf{w}^H\mathbf{w}] =$

$\mathrm{Tr}[\mathbf{RW}]$ to rewrite the (3.25)-(3.28) as

$$\begin{aligned} I_l = &\sum_{n\in\mathcal{N}}\sum_{k\neq l}\mathrm{Tr}[\mathbf{R}_{nk}\mathbf{W}_{pk}] + \mathrm{Tr}[\mathbf{G}_{1g_1}\mathbf{W}_{1g_1}] \\ &+ \mathrm{Tr}[\mathbf{G}_{2g_2}\mathbf{W}_{2g_2}], \end{aligned} \tag{3.29}$$

$$I_{g_1} = \sum_{n\in\mathcal{N}}\sum_{l\in\mathcal{L}}\mathrm{Tr}[\mathbf{R}_{nl}\mathbf{W}_{nl}] + \mathrm{Tr}[\mathbf{G}_{2g_2}\mathbf{W}_{2g_2}], \tag{3.30}$$

$$I_{g_2} = \sum_{n\in\mathcal{N}}\sum_{l\in\mathcal{L}}\mathrm{Tr}[\mathbf{R}_{nl}\mathbf{W}_{nl}] + \mathrm{Tr}[\mathbf{G}_{1g_1}\mathbf{W}_{1g_1}], \tag{3.31}$$

$$\begin{aligned} &\min_{\mathbf{W1},\mathbf{W2}} \sum_{n\in\mathcal{N}}\sum_{l\in\mathcal{L}}\mathrm{Tr}[\mathbf{W}_{nl}] + \mathrm{Tr}[\mathbf{W}_{1g_1}] + \mathrm{Tr}[\mathbf{W}_{2g_2}] \\ &\text{s.t}\ \ \mathrm{Tr}[\mathbf{R}_{nl}\mathbf{W}_{nl}] - \gamma_l I_l \geq \gamma_{nl}\sigma_l^2, \quad \forall l, \\ &\qquad \mathrm{Tr}[\mathbf{G}_{1g_1}\mathbf{W}_{1g_1}] - \gamma_{g_1} I_{g_1} \geq \gamma_{g_1}\sigma_{g_1}^2, \quad \forall l, \\ &\qquad \mathrm{Tr}[\mathbf{G}_{2g_2}\mathbf{W}_{2g_2}] - \gamma_{g_2} I_{g_2} \geq \gamma_{g_2}\sigma_{g_2}^2, \quad \forall l, \\ &\qquad \mathbf{W}_{nl} \succeq 0, \quad \mathbf{W}_{nl} = \mathbf{W}_{nl}^H, \quad \mathrm{rank}[\mathbf{W}_{nl}] = 1, \quad \forall n, \forall l, \\ &\qquad \mathbf{W}_{1g_1} \succeq 0, \quad \mathbf{W}_{1g_1} = \mathbf{W}_{1g_1}^H, \quad \mathrm{rank}[\mathbf{W}_{1g_1}] = 1, \\ &\qquad \mathbf{W}_{2g_2} \succeq 0, \quad \mathbf{W}_{2g_2} = \mathbf{W}_{2g_2}^H, \quad \mathrm{rank}[\mathbf{W}_{2g_2}] = 1, \end{aligned} \tag{3.32}$$

where, $\mathbf{W} \succeq 0$ means $\mathbf{W}$ positive semidefinite. The ranks of $\{\mathbf{W}_{nl}\}_{\forall n,\forall l}$, $\mathbf{W}_{1g_1}$, and $\mathbf{W}_{2g_2}$ are nonconvex. Nevertheless, relaxing all the rank constraints gives the following relaxed semidefinite opti-

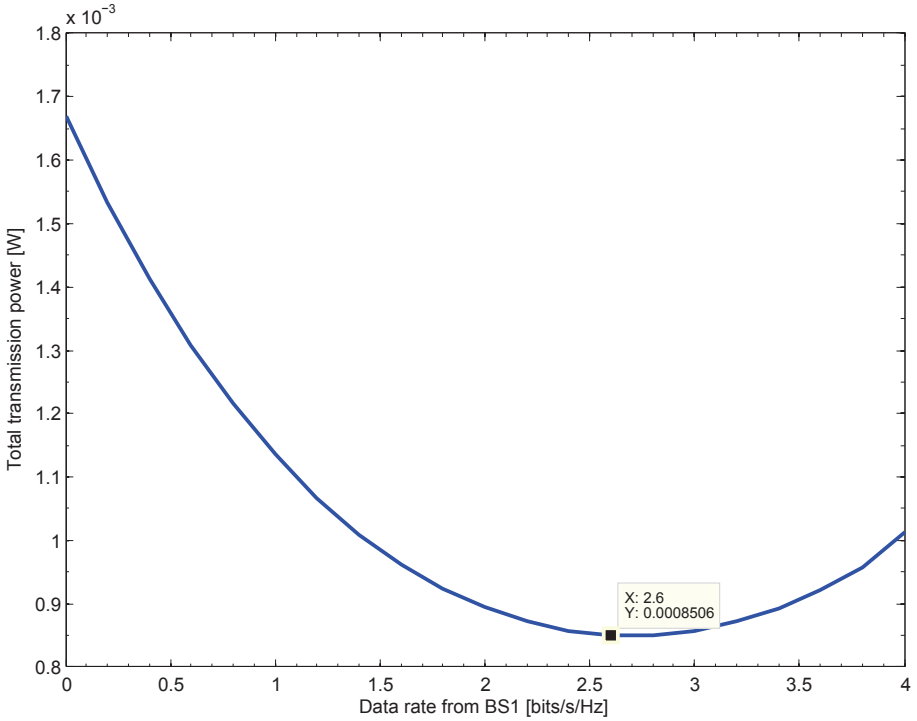

Fig. 3.6 Average achievable data rate at the global user contributed by BS1.

mization problem [57]

$$
\begin{aligned}
\min \sum_{n\in\mathcal{N}}\sum_{l\in\mathcal{L}} & \mathrm{Tr}[\mathbf{W}_{nl}] + \mathrm{Tr}[\mathbf{W}_{1g_1}] + \mathrm{Tr}[\mathbf{W}_{2g_2}] \\
\text{s.t} \quad & \mathrm{Tr}[\mathbf{R}_{nl}\mathbf{W}_{nl}] - \gamma_l I_l \geq \gamma_{nl}\sigma_l^2, \quad \forall l, \\
& \mathrm{Tr}[\mathbf{G}_{1g_1}\mathbf{W}_{1g_1}] - \gamma_{g_1} I_{g_1} \geq \gamma_{g_1}\sigma_{g_1}^2, \quad \forall l, \\
& \mathrm{Tr}[\mathbf{G}_{2g_2}\mathbf{W}_{2g_2}] - \gamma_{g_2} I_{g_2} \geq \gamma_{g_2}\sigma_{g_2}^2, \quad \forall l, \\
& \mathbf{W}_{nl} \succeq 0, \quad \mathbf{W}_{nl} = \mathbf{W}_{nl}^H, \forall n, \forall l, \\
& \mathbf{W}_{1g_1} \succeq 0, \quad \mathbf{W}_{1g_1} = \mathbf{W}_{1g_1}^H, \\
& \mathbf{W}_{2g_2} \succeq 0, \quad \mathbf{W}_{2g_2} = \mathbf{W}_{2g_2}^H,
\end{aligned}
\tag{3.33}
$$

which can be solved to an arbitrary accuracy using SDP solvers like YALMIP [58]. We note that if the (3.33) is feasible, it will provide

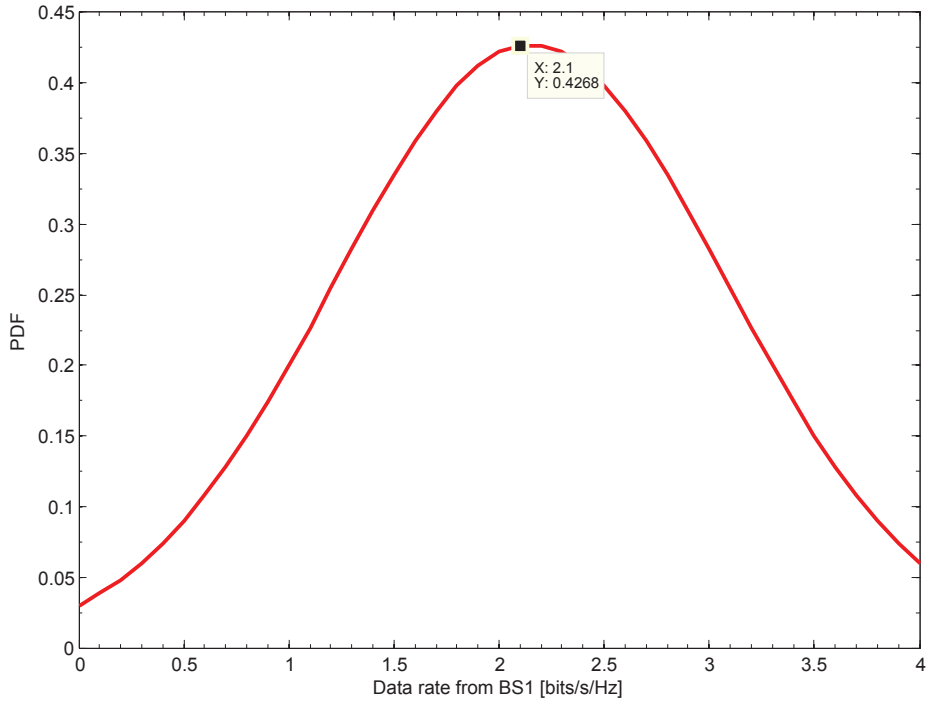

Fig. 3.7 Performance analysis of the proposed SVD based beamformer.

rank-1 matrices $\{\mathbf{W}_{nl}\}_{\forall n,\forall l}$, $\mathbf{W}_{1g_1}$, and $\mathbf{W}_{2g_2}$ [57, 59]. However, if the rank of $\{\mathbf{W}^{\star}_{nl}\}_{\forall n,\forall l}$, $\mathbf{W}^{\star}_{1g_1}$, and $\mathbf{W}^{\star}_{2g_2}$ are greater than one, using the randomization techniques to heuristically find the $\mathbf{w}_{nl}, \forall n, \forall l$, $\mathbf{w}_{1g_1}$, and $\mathbf{w}_{2g_2}$ [59]. Note that if rank of $\{\mathbf{W}^{\star}_{nl}\}_{\forall n,\forall l}$, $\mathbf{W}^{\star}_{1g_1}$, and $\mathbf{W}^{\star}_{2g_2}$ are greater than one, then the heuristic $\{\mathbf{w}_{nl}\}_{\forall n,\forall l}$, $\mathbf{w}_{1g_1}$, and $\mathbf{w}_{2g_2}$ will provide a lower bound for the minimum required transmission power. Apparently, (3.33) is a dual of a dual program (i.e., bidual) of (3.32) [60].

3.7 Numerical Example

Multicell multiuser network with two BSs and five users is proposed. Each BS is equipped with $M = 5$ antennas and it serves two single antenna local users. A global user is equipped with two receive antennas

and it is served by both BSs. All BSs operate on the same frequency henceforth assuming all users experience significant intra-cell and inter-cell interference. Each user has a specific data rate target which needs to be satisfied for a successful connection. The channel vectors $\mathbf{h}_{nl}$ and $\mathbf{H}_{ng}$ were generated as i.i.d Gaussian random variables and the noise variance was set to $\sigma^2 = 1$ for all users. The random channels are generated between users and all BSs with zero mean and unity variance. The data rate targets for a pair of local users at each BS were set to 1.5 bits/s/Hz and 2 bits/s/Hz respectively. The data rate target for the global user was set to 4 bits/s/Hz.

Figure 3.6 shows the total transmission power, for a single channel realization, when the data rate from BS1 to the global user is varied from 0 to 4 bits/s/Hz with step size $\delta = 0.1$ bits/s/Hz. It observed that the minimum total transmission power is achieved when BS1 contribute 2.6 bits/s/Hz of the 4 bits/s/Hz. It is possible that, for a given channel realization, all the data rate to the global user comes from only one BS. In Figure 3.7, the average data rate contributed by BS1 to the global user over 250 random channel realizations were studied . As anticipated, noted that on average, BS1 will contribute 2 bits/s/Hz, whereas the remaining data rate will be contributed by BS2.

3.8 Summary

Multicell multiuser network which simultaneously considers coordinated beamforming and joint transmission is considered. The network consists of single antenna local users and one multi-antenna global user. The

global user is served by more than one BS, whereas the local users are assigned to only one BS at a time. We considered beamforming design using power minimization criterion. For the global user, on average, both BSs equally share the data transfer, however, for the optimality of transmission power, optimum split of data rate is required for instantaneous channel realizations.

In the next chapter, the problem of maximizing the worst-case user signal-to-interference-plus-noise-ratio(SINR) in a multi input single output (MISO) system within the context of energy harvesting is addressed

Chapter 4

SINR Balancing Beamforming for MISO System with Energy Harvesting Constraints

The previous chapter investigated optimization techniques for coordinated multi-cell beamforming in the presence of local users and a global user. This chapter looks at the problem of maximizing the worst-case user signal-to-interference-plus-noise-ratio(SINR) in a multi input single output (MISO) system within the context of energy harvesting. The interference channel is exploited by users for radio frequency energy harvesting (RFEH) while satisfying QoS and power constraints within a framework of beamforming and resource allocations. The power splitting technique where each user divides the received signal into data information and energy charging is considered. The worst-user case

SINR is maximized while satisfying the transmission power and energy harvesting constraints. It has the ability to meet the RFEH constraints.

4.1 Background and Introduction

Radio frequency energy harvesting is being promoted as one of the main energy supply to the Internet of Things (IoT) wireless devices in the near future. With billions of new low power wireless electronic IoT devices expected to appear in the comings years, the necessity for radio frequency (RF) energy harvesting is increasing significantly. RFEH can be used effectively to power the wireless devices when other energy sources are not available. The fact that the radio frequency resources are available everywhere cannot be ignored. RFEH from access points, wide spread cellular base stations and broadcast mast, can offer an alternative solution to powering low energy-IoT devices and could provide enough energy to extend the lifetime of these devices [61]. many researches on RFEH focused on the circuit and antenna design as they are major requirements for RFEH technique [62–64, 61]. Although different protocols and transmission techniques have been developing for various wireless networks with RFEH capabilities, there are limited studies in the literature. A channel learning problem for (MISO) point-to-point wireless energy transfer systems over frequency-selective fading channel) to maximise the energy harvesting is formulated and optimally solved in [65]. A random unitary beamforming-based cooperative beam-selection scheme to enhance the energy harvesting performance at the sensor is proposed in [66]. The energy beamforming is used to enhance

the RF energy transfer efficiency by concentrating the radiated power on target nodes in [67]. The algorithm in [67] is based on the current state of the energy and the data queues and dynamically steers the energy beam to nodes that currently have low energy in the energy queue. A general channel learning design framework for multi-input multi-output(MIMO) wireless energy transfer (WET) based on the energy receiver (ER's) energy feedback over a finite-rate reverse link from the energy receiver to the energy transfer is proposed in [68]. The essential concept of simultaneous wireless transmission of energy and data decoding is discussed in [69]. Different beamforming techniques in a MIMO network that meet quality-of-service (QoS) and energy harvesting constraints for many receivers are studied in [70–72]. In [72], both time switching and power splitting of the decoding information and energy harvesting are studied for simultaneous wireless power and information transfer. This work is extended in [73, 61, 74, 75] for different scenarios.

In this chapter, the focus is on the power splitting technique explained in [76, 77, 72]. We extend the work in [77], that considered only power minimization problem. We propose SINR balancing under power splitting and transmission power constraints. We consider a simple multiple-input single-output (MISO) network to study the optimal solution that maximizes the worst case user SINR within the constraints on total transmitted power and energy harvesting, in the case of splitting the received power at the user side into data and energy harvesting. For different beamforming weights at the base station and known channel state information (CSI) at the user, the power split parameter at each

user (receiver) is optimized. Also, we optimize the transmission power and the energy harvested parameter for each user with the objective of maximizing the worst- user case SINR.

The efficient use of the available resources has become a significant challenge in current wireless networks [78–80]. Various SINR balancing techniques have been developed for downlink beamforming in multi-antenna wireless systems in [81–84]. The SINR-balancing approach introduces fairness to the system so that each user can achieve the same rate [85–88].

The subsequent sections are organized as follows: Section 4.2 presents the system model and assumptions; also it explains the mathematical aspects of the SINR balancing and power splitting. Performance analysis are produced in section 4.3. Section 4.4 concludes with a brief summary.

4.2 System Model and Assumptions

Let us consider a MISO system consisting of M Transmitters (Tx) and M Receivers (RX), each Tx is equipped with N_T antennas. The set of Tx's serve single antenna local users. We assume that all the Tx's operate in the same frequency band and that all users experience considerable intercell interference. Each Tx_i communicates with its corresponding user Rx_i $i = 1,\ldots,M$. It is supposed that the transmitter Tx_i sends signals with power P_i, and its transmitted data symbol denoted as $\mathbf{s}_i(n)$ $= \|\mathbf{s}_i(n)\|^2 = 1$. The transmitted data symbol $\mathbf{s}_i(n)$ is mapped into the antenna array elements by the beamforming vector $\mathbf{v}_i \in \mathbb{C}^{N_T \times 1}$

with $\|\mathbf{v}_i\| = 1$. We assumed that $\mathbf{s}_i(n)$ is a complex Gaussian (CSCG) random variable with zero mean and unit variance.

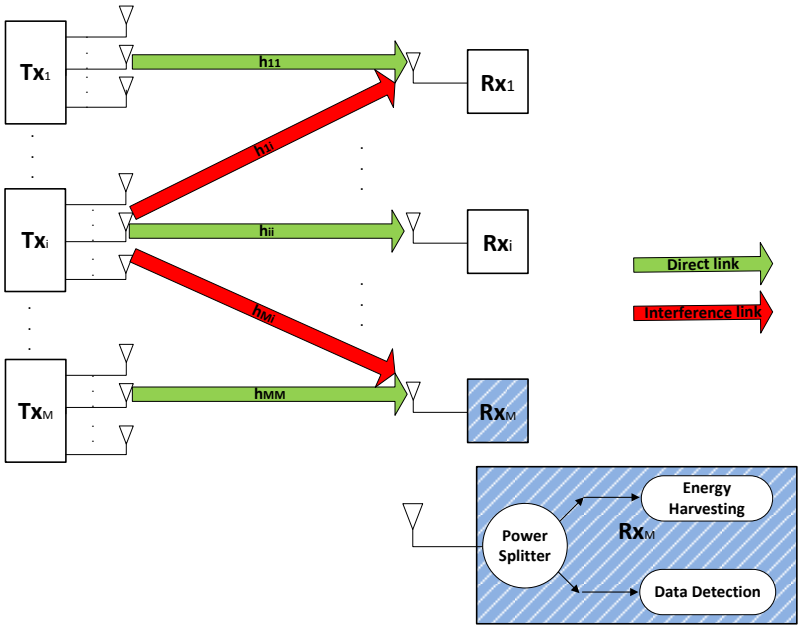

Fig. 4.1 Network topology with date receiver and energy harvesting.

The received signal at user Rx_i can be expressed as

$$r_i(n) = \sqrt{P_i}\mathbf{h}_{i,i}^H \mathbf{v}_i \mathbf{s}_i(n) + \sum_{j \neq i} \sqrt{P_i}\mathbf{h}_{i,j}^H \mathbf{v}_j \mathbf{s}_i(n) + n_i(n), \tag{4.1}$$

where $n_i(n)$ is the additive white Gaussian noise (AWGN) with zero mean and variance σ^2 and $\mathbf{h}_{i,j} \in \mathbb{C}^{N_T \times 1}$ denotes the vector channel from Tx_j to user Rx_i.

The received signal $r_i(n)$ as in (4.1) consists of desired information signal $\sqrt{P_i}\mathbf{h}_{i,i}^H \mathbf{v}_i \mathbf{s}_i$ and the interference $\sum\limits_{j \neq i} \sqrt{P_i}\mathbf{h}_{i,j}^H \mathbf{v}_j \mathbf{s}_j$. The power at Rx_i can be expressed as

$$P_i^r = \sum_{j=1}^{M} |\mathbf{h}_{i,j}^H \mathbf{v}_j|^2 P_j + \sigma^2. \tag{4.2}$$

Each user has RFEH capabilities from the received signal via power splitting technique as explained in [76, 75]. Hence each user separates the received signal into two different parts, first part is used for data detection whereas the latter is used for RFEH. Suppose that the splitting parameter is denoted as $\rho_i \subset (0, 1)$ for any user Rx_i, where portion of the received power will be used for data detection while the rest will be used for RFEH. i.e., $\rho_i \ P_i^r$ is directed towards the data detection while the $(1 - \rho_i)P_i^r$ part is used for radio frequency energy harvesting. Figure. 4.1 shows the MISO topology and the power splitting approach for the i_{th} user. During the baseband conversion, additional circuit noise is appeared due to the phase offsets and non-linearities which is modeled as AWGN with zero mean and variance σ_c^2 [72].

The SINR of the i^{th} user is given by

$$\Gamma_i = \frac{\rho_i P_i |\mathbf{h}_{i,i}^H \mathbf{v}_i|^2}{\rho_i (\sum_{j \neq i} P_j |\mathbf{h}_{i,j}^H \mathbf{v}_j|^2 + \sigma^2) + \sigma_c^2}, \forall i. \tag{4.3}$$

The SINR can be rewritten into an equivalent form by dividing the numerator and the denominator by ρ_i, and using unnormalized beamforming weights $\mathbf{w}_i = \sqrt{P_i}\mathbf{v}_i$ which incorporates beamforming and the power allocation as:

$$\Gamma_i = \frac{|\mathbf{h}_{i,i}^H \mathbf{w}_i|^2}{\sum_{j \neq i} |\mathbf{h}_{i,j}^H \mathbf{w}_j|^2 + \sigma^2 + \sigma_c^2/\rho_i} \forall i. \tag{4.4}$$

4.2.1 Problem Formulation

The beamforming vectors were designed for all users to maximize the SINR subject to each user's transmission power constraint and energy harvesting constraint. When the RF signals arrive at the receiver, the power splitter divides the power P_i^r into two parts as it is shown in Figure. 4.1. The radio frequency energy received at the energy harvesting unit can be stored as electrical energy, and it relies on the conversion efficiency of the i_{th} EH unit [77, 89]. The SINR balancing optimization is performed as

$$\begin{aligned} &\max_{\mathbf{W}} \min_{i}(\Gamma_i), \forall i \\ \text{subject to } &\sum_{i=1}^{M} \|\mathbf{w}_i\|^2 \leq P, \\ &\sum_{j=1}^{M} \left|\mathbf{h}_{i,j}^H \mathbf{w}_j\right|^2 \geq \lambda_i/(1-\rho_i) - \sigma^2 \forall i, \\ &0 \leq \rho_i \leq 1, \forall i, \end{aligned} \tag{4.5}$$

where λ_i is the energy harvesting threshold and P is the maximum transmit power. The second and third term in the denominator of SINR equation $\sigma^2 + \sigma_c^2/\rho_i$ can be expressed as $\sigma^2(\rho_i + 1)/\rho_i$ for $\sigma^2 = \sigma_c^2$. This means that the value of the part $\sigma^2 + \sigma_c^2/\rho_i$ is bigger than $\geq \sigma^2$, taking into consideration that the values of splitting parameters lie in the range $\rho_i \in [0, 1]$.

The right-hand side of the inequality in the energy harvesting constraint should be bigger than zero $\lambda_i/(1-\rho_i) - \sigma^2 > 0$. To achieve that $\lambda_i/(1-\rho_i)$ should be bigger than $> \sigma^2$. $(1-\rho_i) \geq 0$ $\forall \rho_i \in [0, 1]$, so as long as $\lambda_i/(1-\rho_i) - \sigma^2 > 0$ is achieved, the energy harvesting constraint is feasible for a proper value of beamforming. It is good to

mention that making the value $\rho_i = 1$ or very close to one will increase the energy harvesting threshold to highest levels. This will affect the radio frequency energy harvested, so it is crucial to adapt and control the splitting parameters to be able to distribute the power and meet the QoS and the energy harvesting constraints.

4.2.1.1 Feasibility of SINR Balancing optimization problem

In [88], the authors proved that at the optimality problem and SINR balancing, in (4.5) will result into equal SINR for all users. Therefore τ can be used to represent the common SINR values attained by all users. To check the feasibility of the problem (4.6), the proof is needed whether for a given γ_i there exists a $\mathbf{w}_i$.

4.2.1.2 The Connection between SINR Balancing with power optimization

In order to tackle the SINR balancing problem, new matrix variables $\mathbf{W}_i = \mathbf{w}_i \mathbf{w}_i^H, \forall i$ can be introduced. Using both $\{\mathbf{W}_i\}$ and coloration matrix of the channel from M_{th} transmitter to i_{th} user $|\mathbf{h}_{i,i}\mathbf{h}_{i,i}^H|$, the SINR balancing problem (4.5) can be solved using the power optimization problem with bisection method and the formulation can be expressed

$$
\begin{aligned}
&\min_{\mathbf{W}} \sum_{i=1}^{M} \mathrm{Tr}(\mathbf{W}_i) \\
&\text{s.t } \frac{\mathrm{Tr}(\mathbf{h}_{i,i}\mathbf{h}_{i,i}^H \mathbf{W}_i)}{\sum\limits_{j\neq i} \mathrm{Tr}(\mathbf{h}_{i,j}\mathbf{h}_{i,j}^H \mathbf{W}_j) + \sigma^2 + \sigma_c^2/\rho_i} \geq \tau \forall i, \\
&\sum_{j=1}^{M} \mathrm{Tr}(\mathbf{h}_{i,j}\mathbf{h}_{i,j}^H \mathbf{W}_j) \geq \lambda_i/(1-\rho_i) - \sigma^2 \forall i, \\
&\mathbf{W}_i \succeq 0 \\
&0 \leq \rho_i \leq 1, \forall i, \\
&\sum_{i=1}^{M} \mathrm{Tr}(\mathbf{W}_i) \leq P, \forall i,
\end{aligned}
\tag{4.6}
$$

where τ is the $SINR$ target value which $= (\gamma_{min} + \gamma_{max})/2$ and $\gamma_{min} = 0dBm$, $\gamma_{max} = 100dBm$.

Formulation in (4.6) can be further expressed in standard Semi Definite Programming (SDP) form with linear matrix inequalities.

4.2.2 Solution of SINR balancing problem

Problem (4.5) can be solved via bisection method. At every iteration the SINR targets of all users set to τ. The first step to solve the problem in (4.5) is to formulate it as a quasi-convex problem in $\mathbf{w}_i$. So the SINR balancing problem can be solved by the bisection method as explained below:

1. Initialize $\gamma_{min} = SINR_{min}$ and $\gamma_{max} = SINR_{max}$ where $SINR_{min}$ and $SINR_{max}$ refers to the lower and upper SINRs values.

2. Set $\tau = (\gamma_{min} + \gamma_{max})/2$

3. Check the feasibility using equation (4.6)

4. If the problem is feasible then set $\gamma_{min} = \tau$ (replace the lower SINR with the candidate point τ in 2), and store $\mathbf{W}$ as current best solution

5. If the problem is not feasible then set $\gamma_{max} = \tau$ (replace the upper SINR with the candidate point τ in 2).

6. Return the optimal SINR and power harvested values.

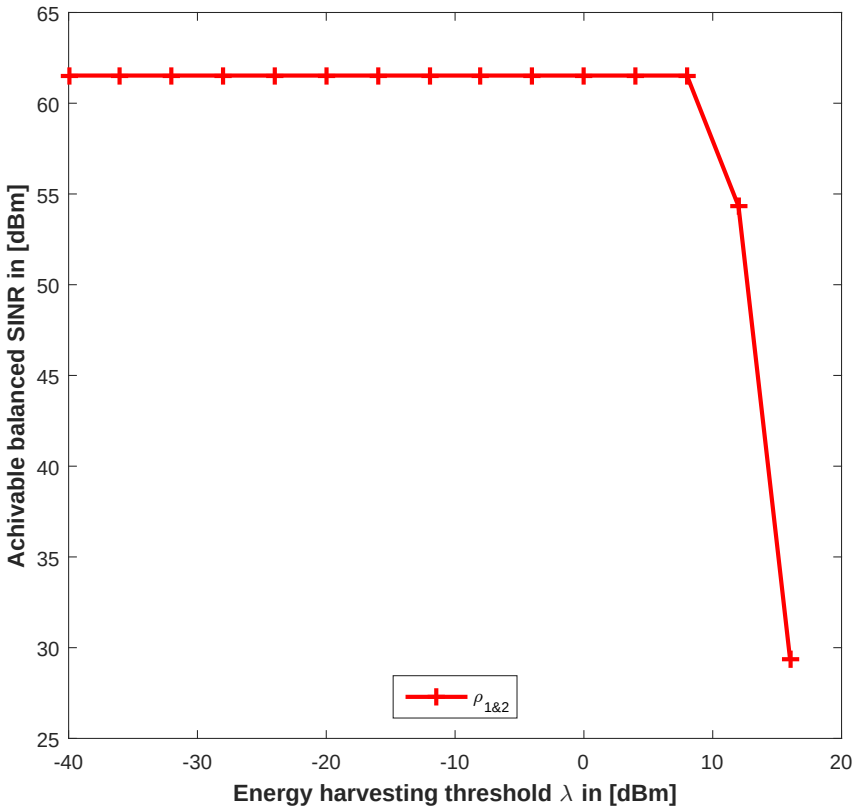

Fig. 4.2 The achievable SINR vs energy harvesting threshold.

4.3 Numerical Example

The SINR balancing problem was evaluated using the network topology as depicted in Fig. 4.1, consider a multicell network with two BSs and two users. Each BS is equipped with $N = 2$ antennas and it serves two users with single antenna. All BSs were assumed to operate on the same frequency and all users experience significant intra-cell and inter-cell interference. The maximum transmit power is set to 0.1 Watt at both transmitters. The $\gamma_{min} = 0$ dBm and $\gamma_{max} = 100$ dBm whereas the energy harvesting threshold is chosen to be in the range of -40 to 40 dBm. The random channels between the users and the BSs are modeled as a sequence of independent and identically distributed (i.i.d.) Gaussian random variables. The noise variance σ^2 is set to be -20 dBm.

Figure 4.2 shows the achievable SINR as evolution on the energy harvesting threshold is varied. The worst-case users' SINR of all users was maximized while satisfying the target SINRs and the energy harvesting power constraints according to (4.6).

Figure.4.3 indicates that the radio frequency harvesting thresholds λ_i for both users are converged and balanced. Also, the RFEH threshold λ_i is achievable for the threshold values from -40 to 16 during the evolution of SINR as it is demonstrated in Fig. 4.3. The achievable energy harvested for the energy harvesting values from 12 to 16 is converged. Results in Fig. 4.2 and Fig. 4.3 are obtained for different energy splitting parameters $\rho_i = (0.2, 0.8)$.

SINR balancing technique persuades energy harvested for all users to be balanced and converged. The SINR-balancing technique has an essential role since its solution introduces a wide range of flexibility to

the system. With energy splitting parameters ρ_i is very close to one the energy harvesting threshold will not be reachable for all λ_i values. Numerical results agree with what has been discussed about the ρ_i values.

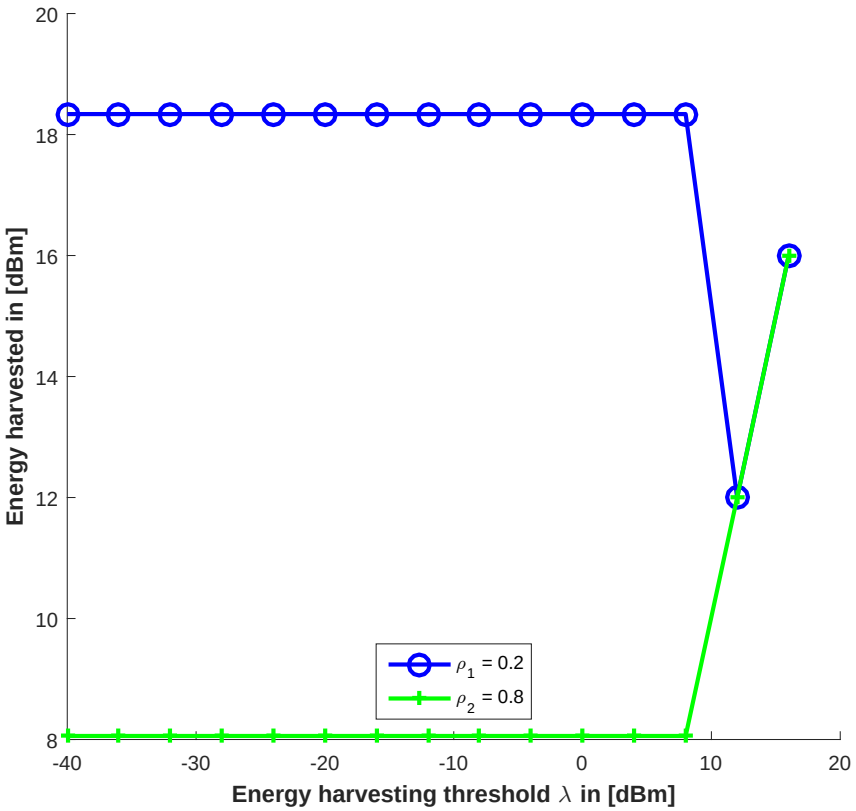

Fig. 4.3 Harvested energy for user (1) and (2) v.s radio frequency energy harvesting threshold.

4.4 Summary

The problem of SINR balancing in MISO network was addressed for two users with two transmitters. The energy splitting technique is used with power and RFEH constraints. Maximization of worst case user SINR has been formulated through an optimization problem under

power and energy harvesting constraints. The performance of the SINR balancing problem with interference was evaluated numerically. Simulation results confirm that SINR balancing technique is able to fairly allocate resources to users while allowing energy harvesting.

The next chapter studies the problem of downlink beamforming design with simultaneous energy and secure information transmission.

Chapter 5

Downlink Beamforming Design with Simultaneous Energy and Secure Information Transmission

In the previous chapter, SINR balancing beamforming for a MISO system with energy harvesting constraints was proposed.

In this chapter, downlink wireless network consisting of WPC system and a SWIPT systems is considered. The SWIPT system simultaneously serves one IR while transferring power to a WD. The wireless powered system consists of the WD and its IR. Both systems operate on the same frequency band. The WD is therefore able to take advantage of the wireless energy transfer from the SWIPT BS, interference power from the BS due to transmission of signals to IRs and the recycled power for energy harvesting. The aim is to minimize the total transmitted

power of the SWIPT BS subject to the SINR target at the information receivers. In order to preserve the secrecy of the information transmitted by BS to IRs on the BS, a set of constraints SINR less than one is introduced.

5.1 Background and Introduction

Radio-frequency (RF) radiation has become a viable source for energy harvesting. It is possible to transfer the energy through wireless medium. The wireless sensors are able of harvest RF energy to power their own transmission [90]. The combination of wireless energy transfer (WET) and wireless information transfer (WIT) has stimulated new studies in wireless communications. For example, SWIPT and WPC have been studied in [91–93] to enable simultaneous RF energy harvesting and information transmission for wireless devices. SWIPT is not only a theoretical possibility but also shown to be practically viable for enabling both wireless data and energy access to mobile devices. The improving energy efficiency on massive multiple-input single-output (MIMO) and small cell were studied in [94]. Joint transmission of energy and information in multiuser systems was studied in [95–98]. Different SWIPT techniques that split the received signal have been discussed in [99]. Coordinated beamforming based SINR balancing techniques were discussed in [52, 100, 101, 87, 55]. In [102], multi-antenna co-channel WET and WIT system was considered. Authors in [103] proposed a wireless powered amplify and forward relaying system under co-channel interference from WET to WIT links. The energy constrained relay

assists the information transmission from the source to the destination using the energy harvested from the source in term of self-energy recycling. The authors in [102] considers spectrum sharing between a multiuser multiple-input multiple-output (MIMO) WET system and a coexisting point-to-point MIMO WIT system, where WET generates interference to WIT and degrades its throughput performance.

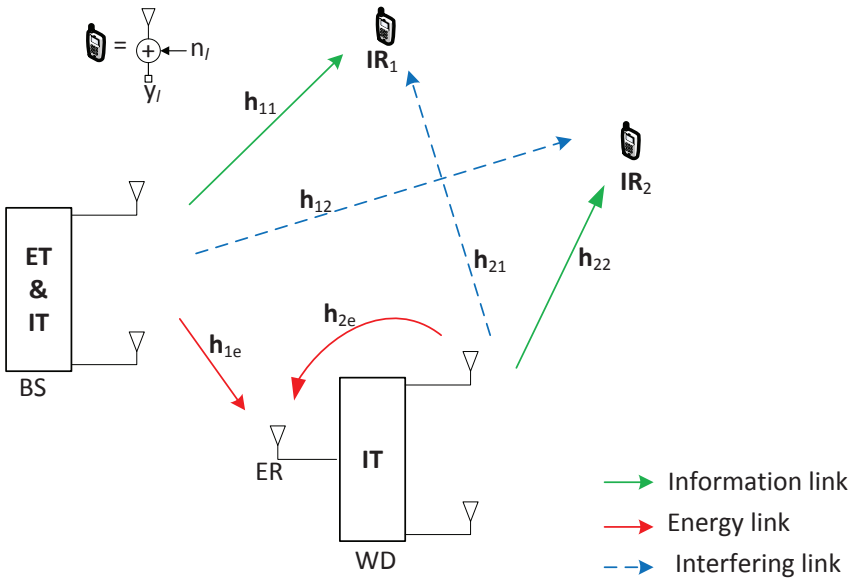

Fig. 5.1 Multiuser system model with energy and information transfer.

5.2 System Model and Assumptions

The SWIPT system consists of one BS, one IR, and one ER located at the WD. The WPC consists of the WD and one IR. The IR_1 and IR_2 were denoted as the receiver of the SWIPT and the WPC systems, respectively. The IR_1 is supposed to receive information from BS, IR_2 is supposed to receive information from WD and WD is supposed

to harvest energy from BS transmissions. Assume that the BS and the WD operate in the same frequency band. Also assume that the transmission at both the transmitters occur simultaneously, hence inducing interference across the systems. The BS and the WD are equipped with multiple antennas and the ER and the IRs are equipped with single antenna as shown in figure 5.1. By using the harvested energy from the ER and the recycled self-energy, the WD transmits information to the $\mathtt{IR}_2$. We denote the number of antennas at the BS as N_B. The WD has $1 + N_W$ antennas in total, one dedicated for energy harvesting and the other N_W antennas are for information transmission.

5.3 System Metric Design

The baseband equivalent channels from the BS to $\mathtt{IR}_1$, $\mathtt{IR}_2$, and the ER are denoted by $\mathbf{h}_{11} \in \mathbb{C}^{N_B \times 1}$, $\mathbf{h}_{12} \in \mathbb{C}^{N_B \times 1}$ and $\mathbf{h}_{1e} \in \mathbb{C}^{N_B \times 1}$, respectively. The channels from the WD to $\mathtt{IR}_1$, $\mathtt{IR}_2$ and the ER are denoted by $\mathbf{h}_{21} \in \mathbb{C}^{N_W \times 1}$, $\mathbf{h}_{22} \in \mathbb{C}^{N_W \times 1}$ and $\mathbf{h}_{2e} \in \mathbb{C}^{N_W \times 1}$, respectively. It is assumed that all the channels are quasi-static flat-fading and remain constant during certain transmission block interval $T > 0$, where T is the coherence time. Also assumed that the BS knows perfectly the CSI of $\mathbf{h}_{11}$ and $\mathbf{h}_{12}$ and the WD knows $\mathbf{h}_{22}$ and $\mathbf{h}_{2e}$. The energy signal transmitted by the BS to the ER is denoted as $\mathbf{x}_e \in \mathbb{C}^{N_B \times 1}$, and the information signal transmitted by the BS to the $\mathtt{IR}_1$ is denoted as $\mathbf{x}_{I1} \in \mathbb{C}^{N_B \times 1}$. The transmitted energy signal $\mathbf{x}_e$ by BS is circularly symmetric complex Gaussian (CSCG) random sequence. We denote the energy covariance matrix at the BS as $\|\mathbf{W}_e\|^2 = \mathbb{E}(\mathbf{x}_e \mathbf{x}_e^H) \succeq \mathbf{0}$, where

$\mathbb{E}(.)$ denotes the statistical expectation, the superscript H denotes the conjugate transpose. The maximum transmit power at the BS denoted as P. The constraint of transmit power at the BS is given by

$$\|\mathbf{w}_e\|^2 + \|\mathbf{w}_1\|^2 \leq P. \tag{5.1}$$

where $\mathbf{h}_{11}^H \mathbf{w}_1 s_1$ is the desirable information signal, $\mathbf{h}_{21}^H \mathbf{w}_2 s_2$ is the interference due to the information signal sent from WD to $\mathtt{IR}_2$, and the $\mathbf{h}_{11}^H \mathbf{w}_e s_e$ is the interference due to the energy signal sent from BS to WD.

The total received signal at the $\mathtt{IR}_1$ user is

$$y_1 = \mathbf{h}_{11}^H \mathbf{w}_1 s_1 + \mathbf{h}_{21}^H \mathbf{w}_2 s_2 + \mathbf{h}_{11}^H \mathbf{w}_e s_e + n_1, \tag{5.2}$$

where $\mathbf{h}_{11}^H \mathbf{w}_1 s_1$ is the desirable information signal, $\mathbf{h}_{21}^H \mathbf{w}_2 s_2$ is the interference due to the information signal sent from WD to $\mathtt{IR}_2$, and the $\mathbf{h}_{11}^H \mathbf{w}_e s_e$ is the interference due to the energy signal sent from BS to WD.

The transmitted information signal by WD to $\mathtt{IR}_2$ can be expressed as $\mathbf{x}_{I2} = \mathbf{w}_2 s_2$, where $\mathbf{w}_2 \in \mathbb{C}^{N_W \times 1}$ denotes the information beamforming vector at the WD and s_2 denotes the desired signal for the $\mathtt{IR}_2$. The total received signal at the $\mathtt{IR}_2$ user is

$$y_2 = \mathbf{h}_{22}^H \mathbf{w}_2 s_2 + \mathbf{h}_{12}^H \mathbf{w}_1 s_1 + \mathbf{h}_{12}^H \mathbf{w}_e s_e + n_2, \tag{5.3}$$

where $\mathbf{h}_{22}^H \mathbf{w}_2 s_2$ is the desirable information signal, $\mathbf{h}_{12} \mathbf{w}_1 s_1$ is the interference due to the information signal sent from BS to $\mathtt{IR}_1$, and the $\mathbf{h}_{1e}^H \mathbf{w}_e s_e$ is the interference due to the energy signal sent from BS to WD.

The total received signal at the ER is

$$y_e = \mathbf{h}_{1e}^H \mathbf{w}_e s_e + \mathbf{h}_{1e}^H \mathbf{w}_1 s_1 + \mathbf{h}_{2e}^H \mathbf{w}_2 s_2 + n_e, \tag{5.4}$$

where $\mathbf{h}_{1e}^H \mathbf{w}_e s_e$ is the desirable information signal, $\mathbf{h}_{1e}^H \mathbf{w}_1 s_1$ is the interference due to the information signal sent from BS to $\mathtt{IR}_1$. Hence, the received signal-to-interference-plus-noise ratio (SINR) at the $\mathtt{IR}_1$ and $\mathtt{IR}_2$ user is given by

$$\mathrm{SINR}_1 = \frac{|\mathbf{h}_{11}^H \mathbf{w}_1|^2}{|\mathbf{h}_{11}^H \mathbf{w}_e|^2 + |\mathbf{h}_{21}^H \mathbf{w}_2|^2 + \sigma_1^2}. \tag{5.5}$$

$$\mathrm{SINR}_2 = \frac{|\mathbf{h}_{22}^H \mathbf{w}_2|^2}{|\mathbf{h}_{12}^H \mathbf{w}_1|^2 + |\mathbf{h}_{12}^H \mathbf{w}_e|^2 + \sigma_2^2}. \tag{5.6}$$

The SINR of the information signal meant for $\mathtt{IR}_1$ at the ER is given by

$$\mathrm{SINR}_e^1 = \frac{|\mathbf{h}_{1e}^H \mathbf{w}_1|^2}{|\mathbf{h}_{1e}^H \mathbf{w}_e|^2 + \sigma_e^2}. \tag{5.7}$$

The SINR of the information signal meant for $\mathtt{IR}_2$ at the $\mathtt{IR}_1$ is given by

$$\mathrm{SINR}_1^2 = \frac{|\mathbf{h}_{21}^H \mathbf{w}_2|^2}{|\mathbf{h}_{11}^H \mathbf{w}_1|^2 + \sigma_1^2}. \tag{5.8}$$

The SINR of the information signal meant for $\mathtt{IR}_1$ at the $\mathtt{IR}_2$ is given by

$$\mathrm{SINR}_2^1 = \frac{|\mathbf{h}_{12}^H \mathbf{w}_1|^2}{|\mathbf{h}_{22}^H \mathbf{w}_2|^2 + \sigma_2^2}. \tag{5.9}$$

The total harvested energy at the WD is expressed as

$$\begin{aligned} P_{\texttt{WD}} &= \eta\mathbb{E}(|\mathbf{h}_{1e}^H\mathbf{w}_e s_e + \mathbf{h}_{2e}^H\mathbf{w}_2 s_2 + \mathbf{h}_{1e}^H\mathbf{w}_1 s_1|^2) \\ &= \eta(|\mathbf{h}_{1e}^H\mathbf{w}_e|^2 + |\mathbf{h}_{2e}^H\mathbf{w}_2|^2 + |\mathbf{h}_{1e}^H\mathbf{w}_1|^2), \end{aligned} \tag{5.10}$$

where $\eta \in (0, 1]$ is a constant denoted the energy harvesting efficiency at the WD. The total harvested energy should be more than the energy requirement for transmission of information from WD. Hence the energy harvesting constraint at the WD is written as

$$\|\mathbf{w}_2\|^2 \leq \eta|\mathbf{h}_{1e}^H\mathbf{w}_e|^2 + \eta|\mathbf{h}_{2e}^H\mathbf{w}_2|^2 + \eta|\mathbf{h}_{1e}^H\mathbf{w}_1|^2, \tag{5.11}$$

which can be rewritten as

$$\mathbf{w}_2^H(\mathbf{I} - \eta\mathbf{h}_{2e}\mathbf{h}_{2e}^H)\mathbf{w}_2 \leq \eta[\mathbf{h}_{1e}^H(\mathbf{w}_e\mathbf{w}_e^H + \mathbf{w}_1\mathbf{w}_1^H)\mathbf{h}_{1e}]. \tag{5.12}$$

$$\mathbf{w}_2\mathbf{I} - \eta(\mathbf{w}_2^H\mathbf{H}_{2e}\mathbf{w}_2) \leq \eta(\mathbf{w}_1^H\mathbf{H}_{1e}\mathbf{w}_1) + \eta(\mathbf{w}_e^H\mathbf{H}_{1e}\mathbf{w}_e). \tag{5.13}$$

$$\mathbf{w}_2\mathbf{I} - \eta(\mathbf{w}_2^H\mathbf{H}_{2e}\mathbf{w}_2) \leq \eta(\mathbf{w}_1^H\mathbf{H}_{1e}\mathbf{w}_1 + \mathbf{w}_e^H\mathbf{H}_{1e}\mathbf{w}_e). \tag{5.14}$$

In order to establish successful connection, the two users $\texttt{IR}_1$ and $\texttt{IR}_2$ have specific date rate requirements. The correlation matrices of the channels from BS and WD transmitters are written as $\mathbf{H}_{11} = \mathbf{h}_{11}\mathbf{h}_{11}^H$, $\mathbf{H}_{1e} = \mathbf{h}_{1e}\mathbf{h}_{1e}^H$, $\mathbf{H}_{12} = \mathbf{h}_{12}\mathbf{h}_{12}^H$, $\mathbf{H}_{21} = \mathbf{h}_{21}\mathbf{h}_{21}^H$, $\mathbf{H}_{2e} = \mathbf{h}_{2e}\mathbf{h}_{2e}^H$ and $\mathbf{H}_{22} = \mathbf{h}_{22}\mathbf{h}_{22}^H$.

5.4 Beamforming Design

The aim is to minimize the total transmission power while guarantee all users their specific SINR requirements. Let us denote the SINR targets for $\mathtt{IR}_1$ and $\mathtt{IR}_2$ as γ_1 and γ_2, respectively. In order to prevent the $\mathtt{ER}$ and both the $\mathtt{IR}_1$ and the $\mathtt{IR}_2$ from decoding the information meant for receivers, we introduce a set of constraints $\mathrm{SINR}_e^1 < \alpha\gamma_1$, $\mathrm{SINR}_1^2 < \alpha\gamma_2$, $\mathrm{SINR}_2^1 < \alpha\gamma_1$, where $\alpha < 1$ to make the interference signal less than the desired signal. Our optimization problem is formulated as

$$
\begin{aligned}
\min\ & \mathrm{Tr}(\mathbf{w}_1\mathbf{w}_1^H) + \mathrm{Tr}(\mathbf{w}_e\mathbf{w}_e^H) \\
\text{s.t}\ & \mathbf{w}_1^H\mathbf{H}_{11}\mathbf{w}_1 \geq \gamma_1(\mathbf{w}_2^H\mathbf{H}_{21}\mathbf{w}_2 + \mathbf{w}_e^H\mathbf{H}_{11}\mathbf{w}_e + \sigma_1^2), \\
& \mathbf{w}_2^H\mathbf{H}_{22}\mathbf{w}_2 \geq \gamma_2(\mathbf{w}_1^H\mathbf{H}_{12}\mathbf{w}_1 + \mathbf{w}_e^H\mathbf{H}_{12}\mathbf{w}_e + \sigma_2^2), \\
& \mathbf{w}_1^H\mathbf{H}_{1e}\mathbf{w}_1 \leq \alpha\gamma_1(\mathbf{w}_e^H\mathbf{H}_{1e}\mathbf{w}_e + \sigma_e^2), \\
& \mathbf{w}_2^H\mathbf{H}_{21}\mathbf{w}_2 \leq \alpha\gamma_2(\mathbf{w}_1^H\mathbf{H}_{11}\mathbf{w}_1 + \mathbf{w}_e^H\mathbf{H}_{11}\mathbf{w}_e + \sigma_1^2), \\
& \mathbf{w}_1^H\mathbf{H}_{12}\mathbf{w}_1 \leq \alpha\gamma_1(\mathbf{w}_2^H\mathbf{H}_{22}\mathbf{w}_2 + \mathbf{w}_e^H\mathbf{H}_{12}\mathbf{w}_e + \sigma_2^2), \\
& \mathbf{w}_2\mathbf{w}_2^H\mathbf{I} - \eta\mathbf{w}_2^H\mathbf{H}_{2e}\mathbf{w}_2 \leq \eta(\mathbf{w}_1^H\mathbf{H}_{1e}\mathbf{w}_1 + \mathbf{w}_e^H\mathbf{H}_{1e}\mathbf{w}_e), \\
& \mathbf{w}_e\mathbf{w}_e^H + \mathbf{w}_1\mathbf{w}_1^H \leq P.
\end{aligned}
\tag{5.15}
$$

The constraints set in (5.15) makes the whole problem nonconvex but after necessary manipulation, the problem can be convexified. Let us denote $\mathbf{W}_1 = \mathbf{w}_1\mathbf{w}_1^H$, $\mathbf{W}_e = \mathbf{w}_e\mathbf{w}_e^H$. We then use the rule

$\mathbf{w}^H\mathbf{H}\mathbf{w} = \mathrm{Tr}[\mathbf{H}\mathbf{w}\mathbf{w}^H] = \mathrm{Tr}[\mathbf{H}\mathbf{W}]$ to rewrite the (18) as

$$
\begin{aligned}
&\min\ \mathrm{Tr}[\mathbf{W}_1] + \mathrm{Tr}[\mathbf{W}_e],\\
&\text{s.t}\ \ \mathrm{Tr}[\mathbf{H}_{11}\mathbf{W}_1] - \gamma_1(\mathrm{Tr}[\mathbf{H}_{21}\mathbf{W}_2] + \mathrm{Tr}[\mathbf{H}_{11}\mathbf{W}_e]) \geq \gamma_1\sigma_1^2,\\
&\qquad \mathrm{Tr}[\mathbf{H}_{22}\mathbf{W}_2] - \gamma_2(\mathrm{Tr}[\mathbf{H}_{12}\mathbf{W}_1] + \mathrm{Tr}[\mathbf{H}_{12}\mathbf{W}_e]) \geq \gamma_2\sigma_2^2,\\
&\qquad \mathrm{Tr}[\mathbf{H}_{1e}\mathbf{W}_1] - \alpha\gamma_1(\mathrm{Tr}[\mathbf{H}_{1e}\mathbf{W}_e]) \leq \alpha\gamma_1\sigma_e^2,\\
&\qquad \mathrm{Tr}[\mathbf{H}_{21}\mathbf{W}_2] - \alpha\gamma_2(\mathrm{Tr}[\mathbf{H}_{11}\mathbf{W}_1] + \mathrm{Tr}[\mathbf{H}_{11}\mathbf{W}_e]) \leq \alpha\gamma_2\sigma_1^2,\\
&\qquad \mathrm{Tr}[\mathbf{H}_{12}\mathbf{W}_1] - \alpha\gamma_1(\mathrm{Tr}[\mathbf{H}_{22}\mathbf{W}_2] + \mathrm{Tr}[\mathbf{H}_{12}\mathbf{W}_e]) \leq \alpha\gamma_1\sigma_2^2, \qquad (5.16)\\
&\qquad \mathrm{Tr}[\mathbf{W}_2] \leq \eta\mathrm{Tr}[\mathbf{H}_{1e}\mathbf{W}_e] + \eta\mathrm{Tr}[\mathbf{H}_{1e}\mathbf{W}_1] + \eta\mathrm{Tr}[\mathbf{H}_{2e}\mathbf{W}_2]\\
&\qquad \mathbf{W}_1 \succeq 0,\ \ \mathbf{W}_1 = \mathbf{W}_1^H,\ \ \mathrm{rank}[\mathbf{W}_1] = 1,\\
&\qquad \mathbf{W}_e \succeq 0,\ \ \mathbf{W}_e = \mathbf{W}_e^H,\ \ \mathrm{rank}[\mathbf{W}_e] = 1,\\
&\qquad \mathbf{W}_2 \succeq 0,\ \ \mathbf{W}_2 = \mathbf{W}_2^H,\ \ \mathrm{rank}[\mathbf{W}_2] = 1,\\
&\qquad \mathrm{Tr}[\mathbf{W}_e] + \mathrm{Tr}[\mathbf{W}_1] \leq P.
\end{aligned}
$$

The ranks of $\mathbf{W}_1$, $\mathbf{W}_e$, and $\mathbf{W}_2$ are nonconvex. Nevertheless, relaxing all the rank constraints gives the following relaxed semidefinite optimization

problem [57]

$$
\begin{aligned}
&\min \ \mathrm{Tr}[\mathbf{W}_1] + \mathrm{Tr}[\mathbf{W}_e], \\
&\text{s.t} \ \ \mathrm{Tr}[\mathbf{H}_{11}\mathbf{W}_1] - \gamma_1(\mathrm{Tr}[\mathbf{H}_{21}\mathbf{W}_2] + \mathrm{Tr}[\mathbf{H}_{11}\mathbf{W}_e]) \geq \gamma_1\sigma_1^2, \\
&\quad \mathrm{Tr}[\mathbf{H}_{22}\mathbf{W}_2] - \gamma_2(\mathrm{Tr}[\mathbf{H}_{12}\mathbf{W}_1] + \mathrm{Tr}[\mathbf{H}_{12}\mathbf{W}_e]) \geq \gamma_2\sigma_2^2, \\
&\quad \mathrm{Tr}[\mathbf{H}_{1e}\mathbf{W}_1] - \alpha\gamma_1\mathrm{Tr}[\mathbf{H}_{12}\mathbf{W}_e] \leq \alpha\gamma_1\sigma_e^2, \\
&\quad \mathrm{Tr}[\mathbf{W}_2] \leq \eta\mathrm{Tr}[\mathbf{H}_{12}\mathbf{W}_1] + \eta\mathrm{Tr}[\mathbf{H}_{12}\mathbf{W}_2] + \eta\mathrm{Tr}[\mathbf{H}_{22}\mathbf{W}_2] \qquad (5.17) \\
&\quad \mathbf{W}_1 \succeq 0, \quad \mathbf{W}_1 = \mathbf{W}_1^H, \\
&\quad \mathbf{W}_e \succeq 0, \quad \mathbf{W}_e = \mathbf{W}_e^H, \\
&\quad \mathbf{W}_2 \succeq 0, \quad \mathbf{W}_2 = \mathbf{W}_2^H, \\
&\quad \mathrm{Tr}[\mathbf{W}_e] + \mathrm{Tr}[\mathbf{W}_1] \leq P,
\end{aligned}
$$

which can be solved using SDP solvers like YALMIP [58]. It is noted that if the (5.17) is feasible, it will provide rank-1 matrices $\mathbf{W}_1$, $\mathbf{W}_e$, and $\mathbf{W}_2$ [57, 59]. However, if the rank of $\mathbf{W}_1^\star$, $\mathbf{W}_e^\star$, and $\mathbf{W}_2^\star$ are greater than one, we can use the randomization techniques to heuristically find the $\mathbf{w}_1$, $\mathbf{w}_e$, and $\mathbf{w}_2$ [59].

5.5 Numerical Example

Considering a multiuser network system with energy and information transmission consisting of one BS and one `WD` as described in Section 5.3. We set the number of transmit antennas at the BS and `WD` as $N_B = N_W = 2$. The energy harvesting efficiency at the `ER` and the noise powers at the `IRs` were set as $\eta = 0.8$ and $\sigma^2 = -90$ dBm, respectively. The channel vectors are randomly generated from i.i.d. Rayleigh fading

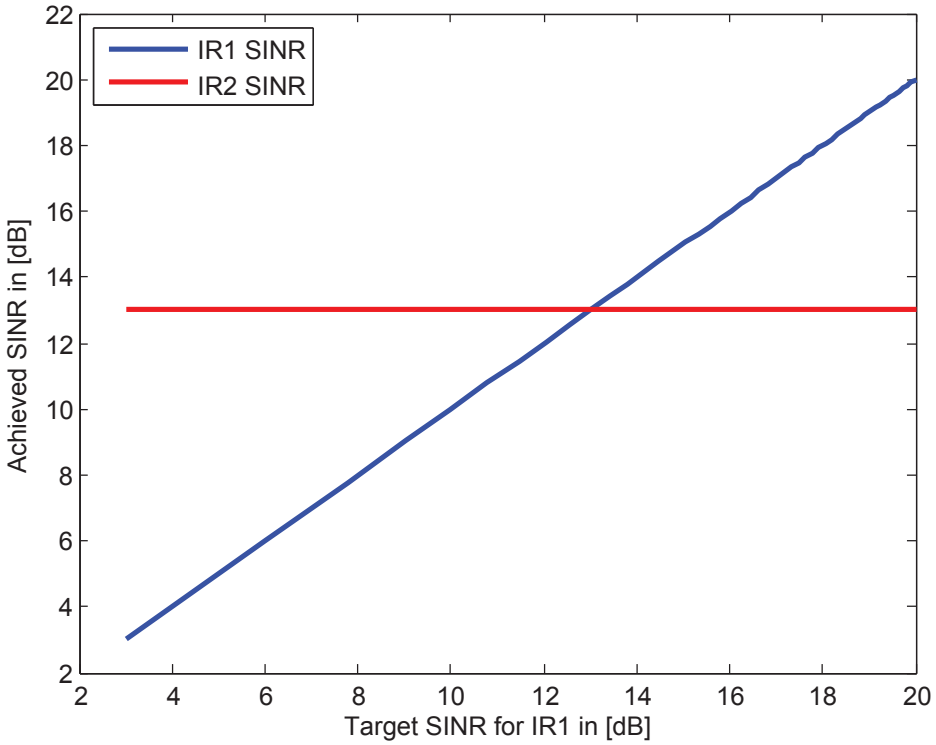

Fig. 5.2 Average achievable SINR at fixed IR2's SINR.

model and the loop channel $\mathbf{h}_{2e}$ was scaled by $\sqrt{\beta}$ with $\beta = -15$ dB. We set $\alpha = 0.8$, the SINR target fixed of $\mathtt{IR}_2$ to $\gamma_2 = 13$ dB while the SINR target of $\mathtt{IR}_1$ was varied between 2 to 20 dB. The results in figure 5.2 show that both IRs are able to achieve their SINR targets. In figure 5.3, the harvested energy by the ER and the allocated power to the IRs is illustrated. We observe that at low SINR targets, the harvested power at the ER is equal to the power allocated to $\mathtt{IR}_1$. At very high target SINRs, the harvested power at the ER surpasses the power allocated to $\mathtt{IR}_1$. The power allocated to $\mathtt{IR}_2$, is less than the harvested power at the ER when the SINR targets of $\mathtt{IR}_2$ are low. The SINR target fixed of $\mathtt{IR}_1$ to $\gamma_1 = 13$ dB while the SINR target of $\mathtt{IR}_2$ was varied between 2 to 20 dB. The results in figure 5.4 show that both IRs are able to achieve their SINR targets. In figure 5.5, the harvested

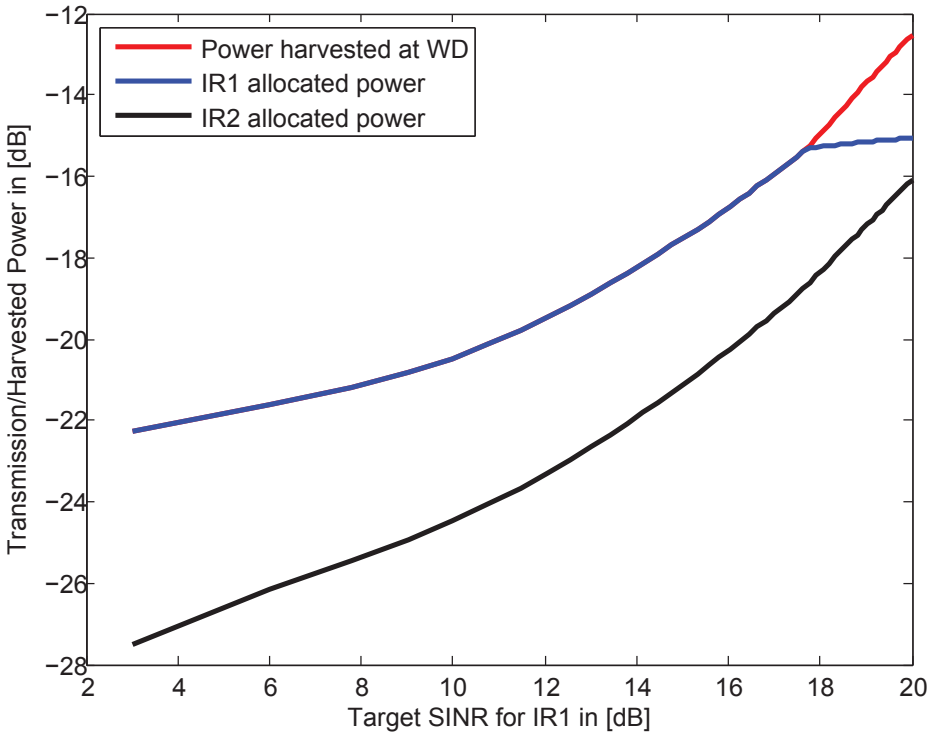

Fig. 5.3 Power harvested and power allocated for IR1 and IR2 at fixed SINR at IR2.

energy by the ER and the allocated power to the IRs are illustrated. We observe that at high SINR targets, the harvested power at the ER is equal to the power allocated to $\mathtt{IR}_1$. At very low target SINRs, the harvested power at the ER surpasses the power allocated to $\mathtt{IR}_1$. The power allocated to $\mathtt{IR}_2$, is less than the harvested power at the ER when the SINR targets of $\mathtt{IR}_2$ are high.

5.6 Summary

Downlink energy and information transmission in a multiuser transmission system is proposed. The system consisting of a WPC system and a SWIPT system. ET's energy beamforming and WD's information

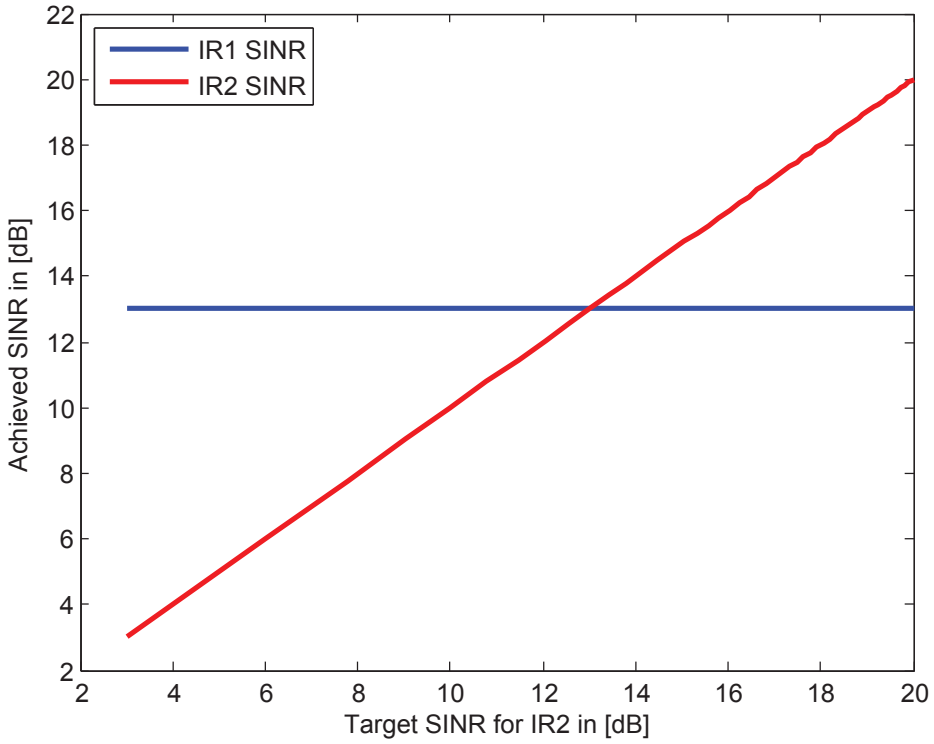

Fig. 5.4 Average achievable SINR at fixed IR1's SINR.

beamforming were designed, to minimize the total transmitted power subject to the SINR constraints at $\mathtt{IR}_1$ and $\mathtt{IR}_2$. This work provided a joint wireless energy transfer and wireless information transfer design with two information receivers and one energy receiver. The optimization constraint also introduced a mechanism to control the SINR of the information signal at the energy receiver to enhance security. In the next chapter, a technique for secrecy rate maximization in wireless information and power transfer in MIMO channels is proposed.

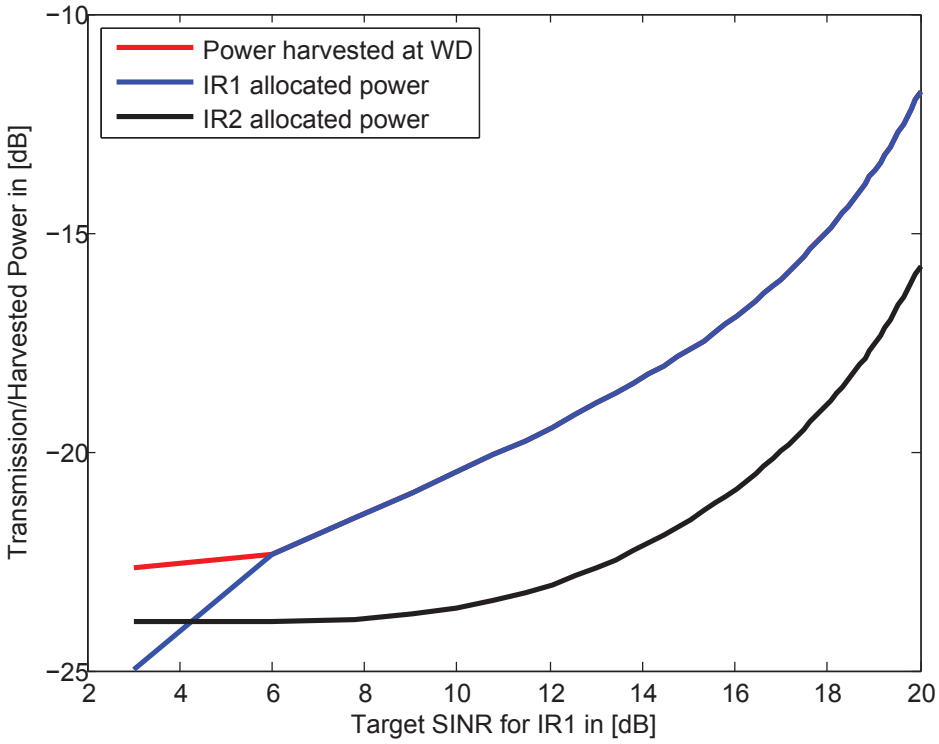

Fig. 5.5 Power harvested and power allocated for IR1 and IR2 at fixed SINR at IR1.

Chapter 6

Secrecy Wireless Information and Power Transfer in MIMO Channels

The previous chapter looked at the problem of downlink beamforming design with simultaneous energy and information transmission. In this chapter, sum secrecy rate optimization techniques for a system that consist of simultaneous wireless information and power transfer SWIPT and wireless powered communication WPC was considered. The SWIPT system simultaneously serves one information receiver (IR1) while transferring power to a wireless device WD. A second information receiver (IR2) that is served by the WD is also considered. The WD is charged by the wireless energy signal power from the SWIPT basestation (BS) and the recycled energy harvested by one antenna Energy Receiver (ER) located at the WD. It is a requirement that IR1 should not be able to decode signal intended for IR2 and vice versa,

hence for this purpose IR1 is treated as eavesdropper for WD and IR2 is considered as eavesdropper for BS. Optimization methods for maximizing secrecy rates are proposed. The secrecy rate maximization problem is non-convex due to the non-concavity of the secrecy rate function. Hence two alternative algorithms are proposed to reformulate the optimization as a convex problem, namely a null-space method based optimization and Taylor series approximated optimization.

6.1 Introduction

The simultaneous wireless information and power transfer (SWIPT) system has drawn considerable attention due to the battery limited wireless devices and consideration for green communications [104–106]. It is possible to simultaneously transfer energy through wireless medium and send information. The wireless devices are able to harvest RF energy to power their own transmission [107]. Because of the open nature of wireless signals and channels, some other information receivers and energy receivers may able to decode information signal which will result in information leakage. Authors in [108] illustrated that the physical layer (PHY) security can be an effective alternative to provide secure communications based on the interference and channel noise. The information signal can be used as a power source to increase the harvested energy at the WD, and establish a secured data transmission between a transmitter and a legitimate receiver [109–111]. The achievable rate-energy for SWIPT with many user interference channel is studied in [112]. The authors in [113] studied the secure

communication for MISO SWIPT system from energy harvesting and secrecy rate maximization. In [70], the coordinating basestations were investigated by employing semidefinite programing based transmitter beamforming design and performing optimum data rate split for the global user in order to minimise the transmission power. Taylor expansion and zero-forcing algorithms are used in [114] for solving the sum power constrained beamforming design for the purpose of maximizing the sum secrecy-rate. The authors in [115] maximize the minimum harvested energy among energy harvesting (EH) receiver guaranteeing the secrecy transmission to the legitimate user in SWIPT system for a MISO secrecy channel. In [116], optimal transmit covariance matrix designs were developed and solved based on the convex optimization approach for MISO secrecy system with the presence of a multiple-antenna eavesdroppers. In addition, authors in [117] proposed a robust jamming scheme for MISO secrecy channel by considering the worst-case performance. In [118], the author solved the secrecy rate maximization and power minimization problems for the MIMO secrecy channel with an eavesdropper with multiple-antenna. The authors in [119] investigated secrecy rate optimization technique for a MIMO communication system incorporating a multiantenna cooperative jammer and multiantenna eavesdropper.

In this chapter, a SWIPT scenario of a MIMO secrecy channel overheard by a multiple-antenna eavesdropper was considered. For this secrecy network, two information receivers served by different transmitters, each transmitter treats the receiver of the other transmitter as an eavesdropper. The goal is to achieve secure communications over

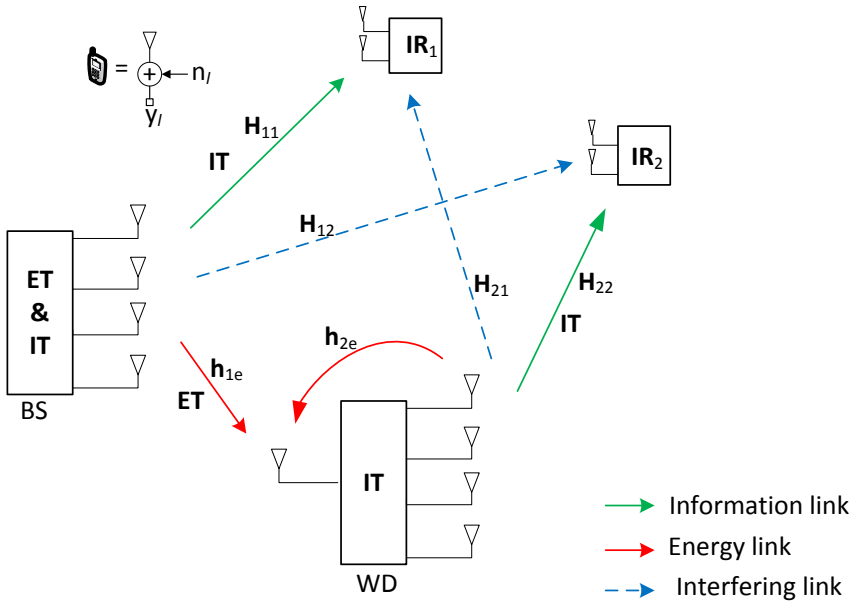

Fig. 6.1 Multiuser SWIPT and WPC system model with two IRs and Eavesdroppers

the two information receivers by designing secrecy rate maximization problems subject to maximum transmission power constraints for BS and WD. In order to eliminate the non-convexity of the secrecy rate maximization problem, two different approaches, namely orthogonal projection based maximization and Taylor series approximation of the secrecy rate function are proposed.

6.2 System Model and Assumptions

Secrecy network as shown in Fig. 6.1 was presented, where a transmitters establishes a MIMO communication link with a legitimate user for data transmission in the presence of a multipleantenna eavesdropper. There are two sub-systems, a SWIPT system and a WPC systems.

The SWIPT system consists of one BS, one IR, and one ER located at the WD. The WPC consists of the WD and one IR. The $\mathtt{IR}_1$ and $\mathtt{IR}_2$ were denoted as the information receivers of SWIPT and the WPC systems, respectively. The BS transmits energy and information to the ER and $\mathtt{IR}_1$ respectively while the WD transmits information to $\mathtt{IR}_2$. It is assumed that the BS and the WD operate in the same frequency band. A further assumption is that the transmissions at both transmitters occur simultaneously, hence inducing interference across the systems. The BS, the WD and the IR1, IR1 are equipped with multiple antennas, whereas the ER is equipped with a single antenna as shown in Fig. 6.1. By using the harvested energy from the ER and the recycled self-energy, the WD transmits information to the $\mathtt{IR}_2$. The antennas at the BS were denoted as N_B, the antennas at the $\mathtt{IR}_1$ as M_1 and the antennas at the $\mathtt{IR}_2$ as M_2. The WD has $1 + N_W$ antennas in total, with one antenna for energy harvesting and the other N_W antennas for information transmission.

6.2.1 System Metric Design

The baseband equivalent channels from the BS to $\mathtt{IR}_1$, $\mathtt{IR}_2$, and the ER are denoted by $\mathbf{H}_{11} \in \mathbb{C}^{N_B \times M_1}$, $\mathbf{H}_{12} \in \mathbb{C}^{N_B \times M_2}$ and $\mathbf{h}_{1e} \in \mathbb{C}^{N_B \times 1}$, respectively. The channels from the WD to $\mathtt{IR}_1$, $\mathtt{IR}_2$ and the ER are denoted by $\mathbf{H}_{21} \in \mathbb{C}^{N_W \times M_1}$, $\mathbf{H}_{22} \in \mathbb{C}^{N_W \times M_2}$ and $\mathbf{h}_{2e} \in \mathbb{C}^{N_W \times 1}$, respectively. It is assumed that all the channels are quasi-static flat-fading and remain constant during each transmission block with $T > 0$, where T is the coherence time. It is assumed that the BS and the WD know perfectly the CSI of $\mathbf{H}_{11}$, $\mathbf{H}_{12}$ and $\mathbf{H}_{22}$ and $\mathbf{h}_{2e}$. The energy signal

transmitted by the BS to the ER is denoted as $\mathbf{x}_e \in \mathbb{C}^{N_B \times 1}$, and the information signal transmitted by the BS to the $\mathtt{IR}_1$ is denoted as $\mathbf{x}_1 \in \mathbb{C}^{N_B \times 1}$, and the information signal transmitted by the WD to the $\mathtt{IR}_2$ is denoted as $\mathbf{x}_2 \in \mathbb{C}^{N_W \times M_2}$. The energy covariance matrix at the BS is denoted as $\mathbf{Q}_e = \mathbb{E}\{\mathbf{x}_e \mathbf{x}_e^H\}$, and the information signal covariance matrix at the BS as $\mathbf{Q}_1 = \mathbb{E}\{\mathbf{x}_1 \mathbf{x}_1^H\}$. The information signal covariance matrix at the WD as $\mathbf{Q}_2 = \mathbb{E}\{\mathbf{x}_2 \mathbf{x}_2^H\}$. The maximum transmit power at the **BS** is limited to P_{BS} as follows:

$$\mathrm{Tr}(\mathbf{Q}_e) + \mathrm{Tr}(\mathbf{Q}_1) \leq P_{BS}. \tag{6.1}$$

The signal $\mathbf{x}_e$ carries no information and unknown to the ER and both $\mathtt{IR}_1$ and $\mathtt{IR}_2$. The energy signal $\mathbf{x}_e$ sent by BS to ER is independent of the information signals $\mathbf{x}_2$ and $\mathbf{x}_1$ sent by WD and BS, respectively.

The total received signal at $\mathtt{IR}_1$ user is

$$\mathbf{y}_1 = \mathbf{H}_{11}\mathbf{x}_1 + \mathbf{H}_{21}\mathbf{x}_2 + \mathbf{H}_{11}\mathbf{x}_e + \mathbf{n}_1, \tag{6.2}$$

where $\mathbf{H}_{11}\mathbf{x}_1$ consists of the desirable information signal, $\mathbf{H}_{21}\mathbf{x}_2$ is the interference due to the information signal sent from WD to $\mathtt{IR}_2$, and the $\mathbf{H}_{11}\mathbf{x}_e$ is the interference due to the energy signal sent from BS to WD.

The total received signal at the $\mathtt{IR}_2$ user is

$$\mathbf{y}_2 = \mathbf{H}_{22}\mathbf{x}_2 + \mathbf{H}_{12}\mathbf{x}_1 + \mathbf{H}_{12}\mathbf{x}_e + \mathbf{n}_2, \tag{6.3}$$

where $\mathbf{H}_{22}\mathbf{x}_2$ consists of the desirable information signal, $\mathbf{H}_{12}\mathbf{x}_1$ is the interference due to the information signal sent from BS to $\mathtt{IR}_1$, and

the $\mathbf{H}_{12}\mathbf{x}_e$ is the interference due to the energy signal sent from BS to WD. The vectors $\mathbf{n}_1 \in \mathbb{C}^{M_1 \times 1}$ and $\mathbf{n}_2 \in \mathbb{C}^{M_2 \times 1}$ are the noises at the $\mathtt{IR}_1$ and the $\mathtt{IR}_2$ and they are CSCG random variable with zero mean and identity covariance matrices, respectively.

The total received signal at the ER located at the WD is

$$\mathbf{y}_e = \mathbf{h}_{1e}\mathbf{x}_1 + \mathbf{h}_{1e}\mathbf{x}_e + \mathbf{h}_{2e}\mathbf{x}_2 + \mathbf{n}_e, \tag{6.4}$$

where $\mathbf{h}_{1e}\mathbf{x}_1$ consists of the desirable information signal, $\mathbf{h}_{1e}\mathbf{x}_e$ consists of the energy signal, $\mathbf{h}_{2e}\mathbf{x}_2$ the interference due to the information signal sent from WD to $\mathtt{IR}_2$, $\mathbf{n}_e$ is the noises at the ER.

The total energy harvested at the WD is expressed as

$$P_{WD} = \eta\mathbb{E}(|\mathbf{h}_{1e}^H\mathbf{x}_e + \mathbf{h}_{2e}^H\mathbf{x}_2 + \mathbf{h}_{1e}^H\mathbf{x}_1|^2), \tag{6.5}$$

where $\eta \in (0, 1]$ is a constant denoting the energy harvesting efficiency at the WD. The total harvested energy should be more than the energy requirement for transmission of information from WD. Hence the energy harvesting constraint at the WD is written as:

$$\|\mathbf{w}_2\|^2 \leq \eta|\mathbf{h}_{1e}^H\mathbf{w}_e|^2 + \eta|\mathbf{h}_{2e}^H\mathbf{w}_2|^2 + \eta|\mathbf{h}_{1e}^H\mathbf{w}_1|^2, \tag{6.6}$$

where $\mathbf{w}_1$, $\mathbf{w}_2$ and $\mathbf{w}_e$ are the beamformer weights used for transmitting information signals and energy signals from the BS and WD. To establish successful connection, the two users $\mathtt{IR}_1$ and $\mathtt{IR}_2$ have specific date rate requirements. Two channel matrices of the BS and WD

transmitters are defined as $\mathbf{H}_{1e}$ =$\mathbf{h}_{1e}\mathbf{h}_{1e}^{H}$, $\mathbf{H}_{2e}$ =$\mathbf{h}_{2e}\mathbf{h}_{2e}^{H}$.

Equation (6.6) can be further reformulated as:

$$\begin{aligned}
\mathbf{w}_2^H(\mathbf{I}-\eta\mathbf{h}_{2e}\mathbf{h}_{2e}^H)\mathbf{w}_2 &\leq \eta[\mathbf{h}_{1e}^H(\mathbf{w}_e\mathbf{w}_e^H+\mathbf{w}_1\mathbf{w}_1^H)\mathbf{h}_{1e}].\\
\mathbf{w}_2\mathbf{I}-\eta(\mathbf{w}_2^H\mathbf{H}_{2e}\mathbf{w}_2) &\leq \eta(\mathbf{w}_1^H\mathbf{H}_{1e}\mathbf{w}_1)+\eta(\mathbf{w}_e^H\mathbf{H}_{1e}\mathbf{w}_e).\\
\mathbf{w}_2\mathbf{I}-\eta(\mathbf{w}_2^H\mathbf{H}_{2e}\mathbf{w}_2) &\leq \eta(\mathbf{w}_1^H\mathbf{H}_{1e}\mathbf{w}_1+\mathbf{w}_e^H\mathbf{H}_{1e}\mathbf{w}_e). \qquad (6.7)
\end{aligned}$$

$\mathbf{W}$=$\mathbf{w}\mathbf{w}^H$ and hence $\mathbf{w}^H\mathbf{H}\mathbf{w} = \mathrm{Tr}[\mathbf{H}\mathbf{w}\mathbf{w}^H] = \mathrm{Tr}[\mathbf{H}\mathbf{W}]$,

rewrite the (6.7) as

$$\mathrm{Tr}[\mathbf{W}_2] \leq \eta\mathrm{Tr}[\mathbf{H}_{1e}\mathbf{W}_e]+\eta\mathrm{Tr}[\mathbf{H}_{1e}\mathbf{W}_1]+\eta\mathrm{Tr}[\mathbf{H}_{2e}\mathbf{W}_2]. \qquad (6.8)$$

The sum secrecy rate maximization (R_{IR1} +R_{IR2}) were proposed with respect to $\mathbf{Q_1}$, $\mathbf{Q_e}$ and $\mathbf{Q_2}$ using two different approaches such as, Taylor series and null space approach. The optimization problem for the Taylor series approach with respect to all $\mathbf{Q_1}$, $\mathbf{Q_e}$ and $\mathbf{Q_2}$ on the same time which can be formulated as:

$$\begin{aligned}
\max_{Q_1,Q_e,Q_2}\ & (\ R_{IR1}+\ R_{IR2})\\
\text{s.t}\quad & \mathrm{Tr}(\mathbf{Q}_2) \leq P_{WD},\\
& R_{IR2} \geq Z,\\
& \mathrm{Tr}(\mathbf{Q}_1)+\mathrm{Tr}(\mathbf{Q}_e) \leq P_{BS},\\
& \mathbf{Q}_2 \succeq 0, \mathbf{Q}_1 \succeq 0, \mathbf{Q}_e \succeq 0, \qquad (6.9)
\end{aligned}$$

where R_{IR1} and R_{IR2} are the secrecy rate at the $\mathtt{IR}_1$ and $\mathtt{IR}_2$ respectively. The second approach is the null space which is simple and not optimum solution, when we ensure that the transmitted signal orthogonal on the eavesdropper channel as explained in the following sections.

6.3 Null-Space Optimization Method

According to the null-space scheme, it is ensured that the transmitted signal $\mathbf{x}_1$ from BS is orthogonal to channels $\mathbf{H}_{12}$ and $\mathbf{h}_{1e}$ i.e. $\mathbf{w}_1$ is chosen in the null space of the matrices $\mathbf{H}_{12}$ and $\mathbf{h}_{1e}$, this can be achieved as follows:

$$\mathbf{H}_1 = [\mathbf{H}_{12} \quad \mathbf{h}_{1e}] = \mathbf{U_1}\Sigma_1\mathbf{V_1}^H, \tag{6.10}$$

where $\mathbf{H}_1 \in \mathbb{C}^{N_B \times (M_2+1)}$ is the new null space channel matrix that $\mathbf{w}_1$ is orthogonal to; $\mathbf{H}_{12} \in \mathbb{C}^{N_B \times M_2}$ and $\mathbf{h}_{1e} \in \mathbb{C}^{N_B \times 1}$. Let $\mathbf{w}_1 = \mathbf{V}_{11}[\alpha_{M_2+2}, ..., \alpha_{N_B}]^T$, where $\mathbf{V}_{11} \in \mathbb{C}^{N_B \times (N_B-(M_2+1))}$ is the null space matrix of $\mathbf{H}_1$ obtained through SVD from the last $N_B-(M_2+1)$ column of $\mathbf{V}_1^H$ (6.10); and $\alpha_{M_2+2}...\alpha_{N_B} \in \mathbb{C}^{(N_B-(M_2+1))\times 1}$ are eigenvalues and $\alpha_{M_2+2} \gg \alpha_{N_B}$

$$\begin{aligned}\mathbf{w}_1 &= \alpha_4\mathbf{v}_4 + \alpha_5\mathbf{v}_5 + ..\alpha_{10}\mathbf{v}_{10} \\ &= [\alpha_4\alpha_5..\alpha_{10}][\mathbf{v}_4\mathbf{v}_5..\mathbf{v}_{10}]^T,\end{aligned} \tag{6.11}$$

where $\alpha_4...\alpha_{10}$ is the eigenvalues and $\mathbf{v}_4...\mathbf{v}_{10}$ is the null space vectors, while $\mathbf{v}_1...\mathbf{v}_3$ is the signal space vectors.

The data rate and secrecy rate at $\mathtt{IR}_1$ are same as

$$R_{IR1} = \log \left| \sigma_1^2 \mathbf{I} + \mathbf{H}_{11} \mathbf{W}_1 \mathbf{H}_{11}^H \right|, \tag{6.12}$$

where $\mathbf{W_1} = \mathbf{w}_1 \mathbf{w}_1^H$, $\mathbf{w}_1 = \mathbf{v}_1 \alpha$, (6.12) can be formulated as:

$$R_{IR1} = \log \left| \sigma_1^2 \mathbf{I} + \mathbf{H}_{11} \mathbf{v}_1 \alpha \alpha^H \mathbf{v}_1^H \mathbf{H}_{11}^H \right|. \tag{6.13}$$

At the same time, the transmitted signal $\mathbf{x}_2$ transmitted from WD is orthogonal on channel $\mathbf{H}_{21}$ i.e. $\mathbf{w}_2$ is chosen in the null space of the matrix $\mathbf{H}_{21}$. Transmission of signal in this way ensures explicitly that the information signal intended for a receiver does not reach other unintended receivers. This is obtained thus:

$$\mathbf{H}_2 = [\mathbf{H}_{21}] = \mathbf{U_2} \Sigma_2 \mathbf{V_2}^H, \tag{6.14}$$

where $\mathbf{H}_2 \in \mathbb{C}^{N_W \times M_1}$ is the new null space channel matrices that $\mathbf{w}_2$ is orthogonal on it, $\mathbf{H}_{21} \in \mathbb{C}^{N_W \times M_1}$. Let $\mathbf{w}_2 = \mathbf{V}_{22}[\upsilon_{M_1+1} ... \upsilon_{N_W}]^T$, where $\mathbf{V}_{22} \in \mathbb{C}^{N_W \times (N_W - M_1)}$ is the null space matrix of $\mathbf{H}_2$ obtained through SVD from the last $N_W - M_1$ column of $\mathbf{V}_2^H$ (6.14); and $\upsilon_{M_1+1} ... \upsilon_{N_W} \in \mathbb{C}^{(N_W - M_1) \times 1}$ are eigenvalues and $\upsilon_{M_1+1} \gg \upsilon_{N_W}$

$$\begin{aligned} \mathbf{w}_2 &= \upsilon_3 \mathbf{v}_3 + \upsilon_4 \mathbf{v}_4 + .. \upsilon_{10} \mathbf{v}_{10} \\ &= [\upsilon_3 \upsilon_4 .. \upsilon_{10}][\mathbf{v}_3 \mathbf{v}_4 .. \mathbf{v}_{10}]^T, \end{aligned} \tag{6.15}$$

where $\upsilon_3 ... \upsilon_{10}$ is the eigenvalues and $\mathbf{v}_3 ... \mathbf{v}_{10}$ is the null space vectors, while $\mathbf{v}_1 ... \mathbf{v}_2$ is the signal space vectors.

The data rate and secrecy rate at $\mathtt{IR}_2$ are same as

$$R_{IR2} = \log \left| \sigma_2^2 \mathbf{I} + \mathbf{H}_{22} \mathbf{W}_2 \mathbf{H}_{22}^H \right|, \tag{6.16}$$

where $\mathbf{W_2} = \mathbf{w}_2 \mathbf{w}_2^H$, $\mathbf{w}_2 = \mathbf{v}_2 \upsilon$, (6.16) is formulated as:

$$R_{IR1} = \log \left| \sigma_1^2 \mathbf{I} + \mathbf{H}_{11} \mathbf{v}_2 \upsilon \upsilon^H \mathbf{v}_1^H \mathbf{H}_{11}^H \right|. \tag{6.17}$$

The transmitted energy signal $\mathbf{x}_e$ from BS is orthogonal on channels $\mathbf{H}_{11}$ and $\mathbf{H}_{12}$ i.e. $\mathbf{w}_e$ is chosen in the null space of the matrices $\mathbf{H}_{11}$ and $\mathbf{H}_{12}$, this can be achieved as:

$$\mathbf{H}_e = [\mathbf{H}_{11} \quad \mathbf{H}_{12}] = \mathbf{U_e} \Sigma_e \mathbf{V_e}^H \tag{6.18}$$

where $\mathbf{H}_e \in \mathbb{C}^{N_B \times (M_2 + M_1)}$ is the new null space channel matrices that $\mathbf{w}_e$ is orthogonal on it, $\mathbf{H}_{11} \in \mathbb{C}^{10 \times 2}$ and $\mathbf{H}_{12} \in \mathbb{C}^{10 \times 2}$. Let $\mathbf{w}_e = \mathbf{V}_{ee}[\gamma_{(M_2+M_1+1)} ... \gamma_{N_B}]^T$, where $\mathbf{V}_{ee} \in \mathbb{C}^{N_B \times (N_B - (M_2+M_1))}$ is the null space matrix of $\mathbf{H}_e$ obtained through SVD from the last $N_B - (M_2 + M_1)$ column of $\mathbf{V}_e^H$ (6.18); and $\gamma_{(M_2+M_1+1)} ... \gamma_{N_B} \in \mathbb{C}^{N_B - (M_2+M_1) \times 1}$ are eigenvalues and $\gamma_{(M_2+M_1+1)} \gg \gamma_{N_B}$.

$$\begin{aligned}\mathbf{w}_e &= \gamma_5\mathbf{v}_5 + \gamma_6\mathbf{v}_6 + ..\gamma_{10}\mathbf{v}_{10} \\ &= [\gamma_5\gamma_6..\gamma_{10}][\mathbf{v}_5\mathbf{v}_6..\mathbf{v}_{10}]^T \end{aligned} \tag{6.19}$$

where $\gamma_5...\gamma_{10}$ is the eigenvalues and $\mathbf{v}_5...\mathbf{v}_{10}$ is the null space vectors, while $\mathbf{v}_1...\mathbf{v}_4$ is the signal space vectors.

The goal in this section is to obtain the optimal vector and maximize the sum data rate at $(R_{IR1} + R_{IR2})$ with respect to α, υ and γ subject to total transmit power and harvested energy constraints with extra constraint $(R_{IR2} \geq Z)$

The sum date rate is similar to the sum secrecy rate at null space method as follow:

$$\begin{aligned} R_{IR1} + R_{IR2} = &\log\left|\sigma_1^2\mathbf{I} + \mathbf{H}_{11}\mathbf{W}_1\mathbf{H}_{11}^H\right| + \\ &\log\left|\sigma_2^2\mathbf{I} + \mathbf{H}_{22}\mathbf{W}_2\mathbf{H}_{22}^H\right|, \end{aligned} \tag{6.20}$$

(6.20) can be formulated as:

$$\begin{aligned} R_{IR1} + R_{IR2} = &\log\left|\sigma_1^2\mathbf{I} + \mathbf{H}_{11}\mathbf{v}_1\alpha\alpha^H\mathbf{v}_1^H\mathbf{H}_{11}^H\right| + \\ &\log\left|\sigma_2^2\mathbf{I} + \mathbf{H}_{22}\mathbf{v}_2\upsilon\upsilon^H\mathbf{v}_2^H\mathbf{H}_{22}^H\right|. \end{aligned} \tag{6.21}$$

The sum secrecy rate at the information receivers $\mathtt{IR}_1$ and $\mathtt{IR}_2$ is maximized with respect to α, υ and γ as shown on the following optimization problem

$$\begin{aligned}
\max_{\upsilon,\gamma,\alpha} \quad & (\ R_{IR1} + \ R_{IR2}) \\
\text{s.t} \quad & \mathrm{Tr}(\mathbf{v}_1 \alpha \alpha^H \mathbf{v}_1^H) + \mathrm{Tr}(\mathbf{v}_e \gamma \gamma^H \mathbf{v}_e^H) \leq P_{BS}, \\
& \mathrm{Tr}(\mathbf{v}_2 \upsilon \upsilon^H \mathbf{v}_2^H) \leq P_{WD}, \\
& R_{IR2} \geq Z, \\
& \upsilon \succeq 0, \gamma \succeq 0, \alpha \succeq 0. \qquad (6.22)
\end{aligned}$$

6.4 Taylor Series Based Approximation

The optimization in (6.9) is not convex due to the nonconvex objective function. Hence, the objective function is approximated based on a Taylor series expansion to become convex which is presented in the following sections.

The achievable secrecy rate at IR1 is defined as follows:

$$\begin{aligned}
R_{IR1} = & \log \Big| \mathbf{I} + \mathbf{H}_{11} \mathbf{Q}_1 \mathbf{H}_{11}^H \\
& \times \left(\mathbf{H}_{11} \mathbf{Q}_e \mathbf{H}_{11}^H + \mathbf{H}_{21} \mathbf{Q}_2 \mathbf{H}_{21}^H + \sigma_1^2 \right)^{-1} \Big| \\
& - \log \Big| \mathbf{I} + \mathbf{H}_{12} \mathbf{Q}_1 \mathbf{H}_{12}^H \\
& \times \left(\mathbf{H}_{12} \mathbf{Q}_e \mathbf{H}_{12}^H + \mathbf{H}_{22} \mathbf{Q}_2 \mathbf{H}_{22}^H + \sigma_2^2 \right)^{-1} \Big|. \qquad (6.23)
\end{aligned}$$

Equation (6.23) can be further reformulated as (6.24) using logarithm quotient rule.

$$\begin{aligned} R_{IR1} =& \log\left|\mathbf{H}_{11}\mathbf{Q}_e\mathbf{H}_{11}^H + \mathbf{H}_{21}\mathbf{Q}_2\mathbf{H}_{21}^H + \sigma_1^2\mathbf{I} + \mathbf{H}_{11}\mathbf{Q}_1\mathbf{H}_{11}^H\right| \\ & - \log\left|\mathbf{H}_{11}\mathbf{Q}_e\mathbf{H}_{11}^H + \sigma_1^2\mathbf{I} + \mathbf{H}_{21}\mathbf{Q}_2\mathbf{H}_{21}^H\right| \\ & - \log\left|\mathbf{H}_{12}\mathbf{Q}_e\mathbf{H}_{12}^H + \mathbf{H}_{22}\mathbf{Q}_2\mathbf{H}_{22}^H + \sigma_2^2\mathbf{I} + \mathbf{H}_{12}\mathbf{Q}_1\mathbf{H}_{12}^H\right| \\ & + \log\left|\mathbf{H}_{12}\mathbf{Q}_e\mathbf{H}_{12}^H + \mathbf{H}_{22}\mathbf{Q}_2\mathbf{H}_{22}^H + \sigma_2^2\mathbf{I}\right|. \end{aligned} \tag{6.24}$$

The objective function is approximated based on a Taylor series expansion at a given transmit covariance matrix.

The desired secrecy rate function to be maximized is given in (6.24). However, this function is non-convex due to the second and third terms in right hand side (RHS) of (6.24). Taylor series approximation can be used to approximate the second and third terms in RHS of (6.24). The second term in RHS of (6.24) is given by:

$$\begin{aligned} \mathrm{T}_1 =& \log\left|\mathbf{H}_{11}\mathbf{Q}_e\mathbf{H}_{11}^H + \mathbf{H}_{21}\mathbf{Q}_2\mathbf{H}_{21}^H + \sigma_1^2\mathbf{I}\right| \simeq \\ & \log\left|\mathbf{H}_{11}\tilde{\mathbf{Q}}_\mathbf{e}\mathbf{H}_{11}^H + \mathbf{H}_{21}\mathbf{Q}_2\mathbf{H}_{21}^H + \sigma_1^2\mathbf{I}\right| \\ & + \mathrm{Tr}\left[\left(\mathbf{H}_{11}\tilde{\mathbf{Q}}_\mathbf{e}\mathbf{H}_{11}^H + \mathbf{H}_{21}\tilde{\mathbf{Q}}_\mathbf{2}\mathbf{H}_{21}^H + \sigma_1^2\mathbf{I}\right)^{-1}\right. \\ & \left.\times\, \mathbf{H}_{11}\mathbf{Q}_e\mathbf{H}_{11}^H + \mathbf{H}_{21}\mathbf{Q}_2\mathbf{H}_{21}^H\right] \\ & - \mathrm{Tr}\left[\left(\mathbf{H}_{11}\tilde{\mathbf{Q}}_\mathbf{e}\mathbf{H}_{11}^H + \mathbf{H}_{21}\tilde{\mathbf{Q}}_\mathbf{2}\mathbf{H}_{21}^H + \sigma_1^2\mathbf{I}\right)^{-1}\right. \\ & \left.\times\, \mathbf{H}_{11}\tilde{\mathbf{Q}}_\mathbf{e}\mathbf{H}_{11}^H + \mathbf{H}_{21}\tilde{\mathbf{Q}}_\mathbf{2}\mathbf{H}_{21}^H\right]. \end{aligned} \tag{6.25}$$

The third term in RHS of (6.24) is given by :

$$\begin{aligned}
\mathrm{T}_2 = &\log\left|\mathbf{H}_{12}\mathbf{Q}_e\mathbf{H}_{12}^H + \mathbf{H}_{22}\mathbf{Q}_2\mathbf{H}_{22}^H + \sigma_2^2\mathbf{I} + \mathbf{H}_{12}\mathbf{Q}_1\mathbf{H}_{12}^H\right| \simeq \\
&\log\left|\mathbf{H}_{12}\tilde{\mathbf{Q}}_\mathbf{e}\mathbf{H}_{12}^H + \mathbf{H}_{12}\tilde{\mathbf{Q}}_\mathbf{1}\mathbf{H}_{12}^H + \mathbf{H}_{22}\tilde{\mathbf{Q}}_\mathbf{2}\mathbf{H}_{22}^H + \sigma_2^2\mathbf{I}\right| \\
&+ \mathrm{Tr}\left[\left(\mathbf{H}_{12}\tilde{\mathbf{Q}}_\mathbf{e}\mathbf{H}_{12}^H + \mathbf{H}_{12}\tilde{\mathbf{Q}}_\mathbf{1}\mathbf{H}_{12}^H + \mathbf{H}_{22}\tilde{\mathbf{Q}}_\mathbf{2}\mathbf{H}_{22}^H + \sigma_2^2\mathbf{I}\right)^{-1}\right. \\
&\left.\times\left(\mathbf{H}_{12}\mathbf{Q}_e\mathbf{H}_{12}^H + \mathbf{H}_{12}\mathbf{Q}_1\mathbf{H}_{12}^H + \mathbf{H}_{22}\mathbf{Q}_2\mathbf{H}_{22}^H\right)\right] \\
&- \mathrm{Tr}\left[\left(\mathbf{H}_{12}\tilde{\mathbf{Q}}_\mathbf{e}\mathbf{H}_{12}^H + \mathbf{H}_{12}\tilde{\mathbf{Q}}_\mathbf{1}\mathbf{H}_{12}^H + \mathbf{H}_{22}\tilde{\mathbf{Q}}_\mathbf{2}\mathbf{H}_{22}^H + \sigma_2^2\mathbf{I}\right)^{-1}\right. \\
&\left.\times\left(\mathbf{H}_{12}\tilde{\mathbf{Q}}_\mathbf{e}\mathbf{H}_{12}^H + \mathbf{H}_{12}\tilde{\mathbf{Q}}_\mathbf{1}\mathbf{H}_{12}^H + \mathbf{H}_{22}\tilde{\mathbf{Q}}_\mathbf{2}\mathbf{H}_{22}^H\right)\right] \qquad (6.26)
\end{aligned}$$

Substituting (6.25) and (6.26) into (6.24) gives:

$$\begin{aligned}
R_{IR1} = &\log\left|\mathbf{H}_{11}\mathbf{Q}_e\mathbf{H}_{11}^H + \mathbf{H}_{21}\mathbf{Q}_2\mathbf{H}_{21}^H + \sigma_1^2\mathbf{I} + \mathbf{H}_{11}\mathbf{Q}_1\mathbf{H}_{11}^H\right| \\
&+ \log\left|\mathbf{H}_{12}\mathbf{Q}_e\mathbf{H}_{12}^H + \mathbf{H}_{22}\mathbf{Q}_2\mathbf{H}_{22}^H + \sigma_2^2\mathbf{I}\right| - T_1 - T_2, \qquad (6.27)
\end{aligned}$$

where, T_1 and T_2 are the Taylor series approximation results of term two and three respectively in (6.24).

Now, the secrecy rate at $\mathtt{IR}_2$ will approximate similar to the approximation way of secrecy rate approximation at $\mathtt{IR}_1$.

The achievable secrecy rate at the $\mathtt{IR}_2$ is defined as follows:

$$\begin{aligned} R_{IR2} = &\log \Big| \mathbf{I} + \mathbf{H}_{22}\mathbf{Q}_2\mathbf{H}_{22}^H \\ &\times \left(\mathbf{H}_{12}\mathbf{Q}_e\mathbf{H}_{12}^H + \mathbf{H}_{12}\mathbf{Q}_1\mathbf{H}_{12}^H + \sigma_2^2\right)^{-1} \Big| \\ &- \log \Big| \mathbf{I} + \mathbf{H}_{21}\mathbf{Q}_2\mathbf{H}_{21}^H \\ &\times \left(\mathbf{H}_{11}\mathbf{Q}_1\mathbf{H}_{11}^H + \mathbf{H}_{11}\mathbf{Q}_e\mathbf{H}_{11}^H + \sigma_1^2\right)^{-1} \Big|. \end{aligned} \tag{6.28}$$

Equation (6.28) can be further reformulated as (6.29) using logarithm quotient rule.

$$\begin{aligned} R_{IR2} = &\log \left| \mathbf{H}_{12}\mathbf{Q}_e\mathbf{H}_{12}^H + \mathbf{H}_{12}\mathbf{Q}_1\mathbf{H}_{12}^H + \sigma_2^2\mathbf{I} + \mathbf{H}_{22}\mathbf{Q}_2\mathbf{H}_{22}^H \right| \\ &- \log \left| \mathbf{H}_{12}\mathbf{Q}_e\mathbf{H}_{12}^H + \sigma_2^2\mathbf{I} + \mathbf{H}_{12}\mathbf{Q}_1\mathbf{H}_{12}^H \right| \\ &- \log \left| \mathbf{H}_{11}\mathbf{Q}_1\mathbf{H}_{11}^H + \mathbf{H}_{11}\mathbf{Q}_e\mathbf{H}_{11}^H + \sigma_1^2\mathbf{I} + \mathbf{H}_{21}\mathbf{Q}_2\mathbf{H}_{21}^H \right| \\ &+ \log \left| \mathbf{H}_{11}\mathbf{Q}_1\mathbf{H}_{11}^H + \mathbf{H}_{11}\mathbf{Q}_e\mathbf{H}_{11}^H + \sigma_1^2\mathbf{I} \right|. \end{aligned} \tag{6.29}$$

The objective function is approximated based on a Taylor series expansion at a given transmit covariance matrix.

The desired secrecy rate function to be maximized is given in (6.29). However, this function is non-convex due to the second and third terms in RHS of (6.29). Taylor series approximation can be used to approximate the second and third terms in RHS of (6.29). Firstly, the second term in RHS of (6.29) approximation is described as follows:

$$
\begin{aligned}
\mathrm{T}_3 = &\log\left|\mathbf{H}_{12}\mathbf{Q}_e\mathbf{H}_{12}^H + \mathbf{H}_{12}\mathbf{Q}_1\mathbf{H}_{12}^H + \sigma_2^2\mathbf{I}\right| \simeq \\
&\log\left|\mathbf{H}_{12}\tilde{\mathbf{Q}}_\mathbf{e}\mathbf{H}_{12}^H + \mathbf{H}_{12}\tilde{\mathbf{Q}}_\mathbf{1}\mathbf{H}_{12}^H + \sigma_2^2\mathbf{I}\right| \\
&+ \mathrm{Tr}\Bigg[\left(\mathbf{H}_{12}\tilde{\mathbf{Q}}_\mathbf{e}\mathbf{H}_{12}^H + \mathbf{H}_{12}\tilde{\mathbf{Q}}_\mathbf{1}\mathbf{H}_{12}^H + \sigma_2^2\mathbf{I}\right)^{-1} \\
&\times (\mathbf{H}_{12}\mathbf{Q}_e\mathbf{H}_{12}^H + \mathbf{H}_{12}\mathbf{Q}_1\mathbf{H}_{12}^H)\Bigg] \\
&- \mathrm{Tr}\Bigg[\left(\mathbf{H}_{12}\tilde{\mathbf{Q}}_\mathbf{e}\mathbf{H}_{12}^H + \mathbf{H}_{12}\tilde{\mathbf{Q}}_\mathbf{1}\mathbf{H}_{12}^H + \sigma_2^2\mathbf{I}\right)^{-1} \\
&\times (\mathbf{H}_{12}\tilde{\mathbf{Q}}_\mathbf{e}\mathbf{H}_{12}^H + \mathbf{H}_{12}\tilde{\mathbf{Q}}_\mathbf{1}\mathbf{H}_{12}^H)\Bigg]. \qquad (6.30)
\end{aligned}
$$

The third term in RHS of (6.29) is approximated using Taylor series approximation as:

$$
\begin{aligned}
\mathrm{T}_4 = &\log\left|\mathbf{H}_{11}\mathbf{Q}_1\mathbf{H}_{11}^H + \mathbf{H}_{21}\mathbf{Q}_2\mathbf{H}_{21}^H + \sigma_1^2\mathbf{I} + \mathbf{H}_{11}\mathbf{Q}_e\mathbf{H}_{11}^H\right| \simeq \\
&\log\left|\mathbf{H}_{11}\tilde{\mathbf{Q}}_\mathbf{1}\mathbf{H}_{11}^H + \mathbf{H}_{11}\tilde{\mathbf{Q}}_\mathbf{e}\mathbf{H}_{11}^H + \mathbf{H}_{21}\tilde{\mathbf{Q}}_\mathbf{2}\mathbf{H}_{21}^H + \sigma_1^2\mathbf{I}\right| \\
&+ \mathrm{Tr}\Bigg[\left(\mathbf{H}_{11}\tilde{\mathbf{Q}}_\mathbf{1}\mathbf{H}_{11}^H + \mathbf{H}_{11}\tilde{\mathbf{Q}}_\mathbf{e}\mathbf{H}_{11}^H + \mathbf{H}_{21}\tilde{\mathbf{Q}}_\mathbf{2}\mathbf{H}_{21}^H + \sigma_1^2\mathbf{I}\right)^{-1} \\
&\times (\mathbf{H}_{11}\mathbf{Q}_1\mathbf{H}_{11}^H + \mathbf{H}_{11}\mathbf{Q}_e\mathbf{H}_{11}^H + \mathbf{H}_{21}\mathbf{Q}_2\mathbf{H}_{21}^H)\Bigg] \\
&- \mathrm{Tr}\Bigg[\left(\mathbf{H}_{11}\tilde{\mathbf{Q}}_\mathbf{1}\mathbf{H}_{11}^H + \mathbf{H}_{11}\tilde{\mathbf{Q}}_\mathbf{e}\mathbf{H}_{11}^H + \mathbf{H}_{21}\tilde{\mathbf{Q}}_\mathbf{2}\mathbf{H}_{21}^H + \sigma_1^2\mathbf{I}\right)^{-1} \\
&\times (\mathbf{H}_{11}\tilde{\mathbf{Q}}_\mathbf{1}\mathbf{H}_{11}^H + \mathbf{H}_{11}\tilde{\mathbf{Q}}_\mathbf{e}\mathbf{H}_{11}^H + \mathbf{H}_{21}\tilde{\mathbf{Q}}_\mathbf{2}\mathbf{H}_{21}^H)\Bigg]. \qquad (6.31)
\end{aligned}
$$

Substituting (6.30) and (6.31) into (6.29), R_{IR2} of (6.29) becomes:

$$R_{IR2} = \log\left|\mathbf{H}_{12}\mathbf{Q}_e\mathbf{H}_{12}^H + \mathbf{H}_{12}\mathbf{Q}_1\mathbf{H}_{12}^H + \sigma_2^2\mathbf{I} + \mathbf{H}_{22}\mathbf{Q}_2\mathbf{H}_{22}^H\right| + \log\left|\mathbf{H}_{11}\mathbf{Q}_1\mathbf{H}_{11}^H + \sigma_1^2\mathbf{I}\right| - T_3 - T_4, \tag{6.32}$$

where, T_3 and T_4 are the Taylor series approximation results of term two and three respectively in (6.29).

After the previous Taylor series approximation steps, the equation (6.9) becomes convex. The $\mathbf{Q_1}$, $\mathbf{Q_e}$ and $\mathbf{Q_2}$ can be obtained by solving problem (6.9) based on updating $\tilde{\mathbf{Q}}_\mathbf{1}$, $\tilde{\mathbf{Q}}_\mathbf{e}$ and $\tilde{\mathbf{Q}}_\mathbf{2}$.

The direct Taylor series approximated optimization problem as below can be solved as presented in algorithm 1.

$$\begin{aligned} \max_{Q_1,Q_e,Q_2} \; & (\, R_{IR1} + \; R_{IR2}) \\ \text{s.t} \quad & \mathrm{Tr}(\mathbf{Q}_2) \le P_{WD}, \\ & R_{IR2} \ge Z, \\ & \mathrm{Tr}(\mathbf{Q}_1) + \mathrm{Tr}(\mathbf{Q}_e) \le P_{BS}, \\ & \mathbf{Q}_2 \succeq 0, \mathbf{Q}_1 \succeq 0, \mathbf{Q}_e \succeq 0. \end{aligned} \tag{6.33}$$

6.5 Simulation Results

The BS and WD are equipped with N_B =N_W =10 antennas with one antenna on ER located at the WD. The $\mathtt{IR}_1$ and $\mathtt{IR}_2$ receivers are

1: Set initialization values for transmit covariance matrices: $\tilde{\mathbf{Q}}_1$, $\tilde{\mathbf{Q}}_e$, $\tilde{\mathbf{Q}}_2$.
2: **for** i=1:10 **do**
3: - Obtain $\mathbf{Q}_1^*$, $\mathbf{Q}_e^*$ and $\mathbf{Q}_2^*$ from optimization problem (6.33).
4: $\tilde{\mathbf{Q}}_1 \leftarrow \mathbf{Q}_1^*$,
5: $\tilde{\mathbf{Q}}_e \leftarrow \mathbf{Q}_e^*$ and
6: $\tilde{\mathbf{Q}}_2 \leftarrow \mathbf{Q}_2^*$
7: **end for**

Algorithm 1: Direct approximated Sum Secrecy Rate Maximization

equipped with $M_1 = M_2 = 2$ antennas each. The energy harvesting efficiency at the ER and the noise powers at the information receivers $\mathtt{IR}_1$ and $\mathtt{IR}_2$ were set as $\eta = 0.4$ and $\sigma^2 = -90$ dBm, respectively. The channel vectors are randomly generated from i.i.d. Rayleigh fading model and the loop channel $\mathbf{h}_{2e}$ was scaled by $\sqrt{\beta}$ with $\beta = -15$ dB.

The results in Figure. 6.2 shows the transmitted power regarding the information signal (P_1) and the energy signal (P_e) from the BS. It is evident that the proposed system opts to allocate the majority of the available power towards the legitimate receiver $\mathtt{IR}_1$ in order to obtain the maximum secrecy rate possible. Whereas, the power allocated to WD for energy harvesting is evidently lower and both converge after 10 iterations.

The comparison between the power transmitted by WD for $\mathtt{IR}_2$ information receiver (P_2) and the harvested energy at WD were depicted in Figure. 6.3. As expected, the result confirm that the constraints harvested energy greater than P_2 satisfies the optimization problem. Both converge after 10 iterations. Figure. 6.4 shows the achieved sum secrecy rate by direct Taylor series approach scheme with different secrecy rate values constraint Z at IR2, $R_{IR2} >= Z$ to ensure the

transmitted power by BS shared to all receivers and also for the QoS, the smaller Z the higher the sum secrecy rate.

As shown in Figure. 6.5, the convergence of the secrecy rate for the $\mathtt{IR}_1$ and $\mathtt{IR}_2$ at direct Taylor series approach with the constraint secrecy rate at $\mathtt{IR}_2$ =0.45 b/s/Hz. It is shown that the sum secrecy rate is equal to the sum of both receivers secrecy rates and also the secrecy rate at IR2 is equal to the value of Z which is the optimal value. As observed in Fig. 6.6, the comparison between the sum secrecy rates at direct optimization schemes using (6.33) and null space scheme using (6.22). It's clear that the direct Taylor series approach outperforms the null space scheme.

6.6 Summary

A secure SWIPT over the two-user MIMO interference channels with two eavesdroppers have been investigated. First, A null-space based scheme was considered, where the transmit covariance matrix of the BS and WD ensures that the transmitted signal lies in the null space of the channels between the BS and $\mathtt{IR}_2$ and that between the WD and the $\mathtt{IR}_1$. Secondly, the Taylor series expansion is used to reformulate the secrecy rate maximization problems and the secrecy sum-rate maximization problems of both BS and WD into convex form. The simulation results demonstrate the efficient security performance of the proposed system and the comparison between both systems. The sum-rate maximization optimization based direct method outperforms the sum-rate maximization optimization based iterative method. Furthermore,

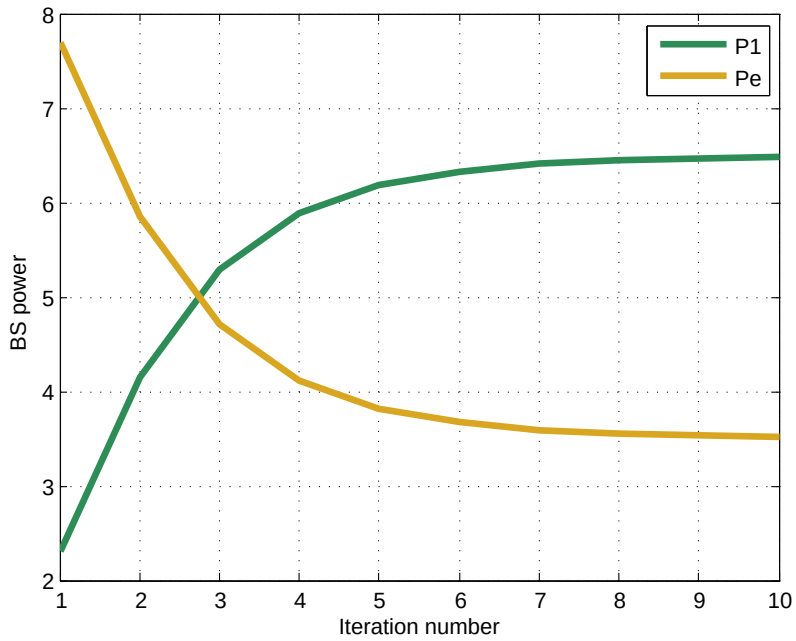

Fig. 6.2 Comparison between the power transmitted by BS for $\mathtt{IR}_1$ information receiver P1 and the wireless power Pe transmitted by BS for ER at WD. Both converge after 10 iterations and confirm the constraints that sum of P1 and Pe equal to the Pmax.

it is evident that the incentive of the BS is to guarantee safe information transmission, since it opts to use most of the available power for the communication signal.

In the next chapter, concluding remarks fro this thesis are drawn and future research directions discussed.

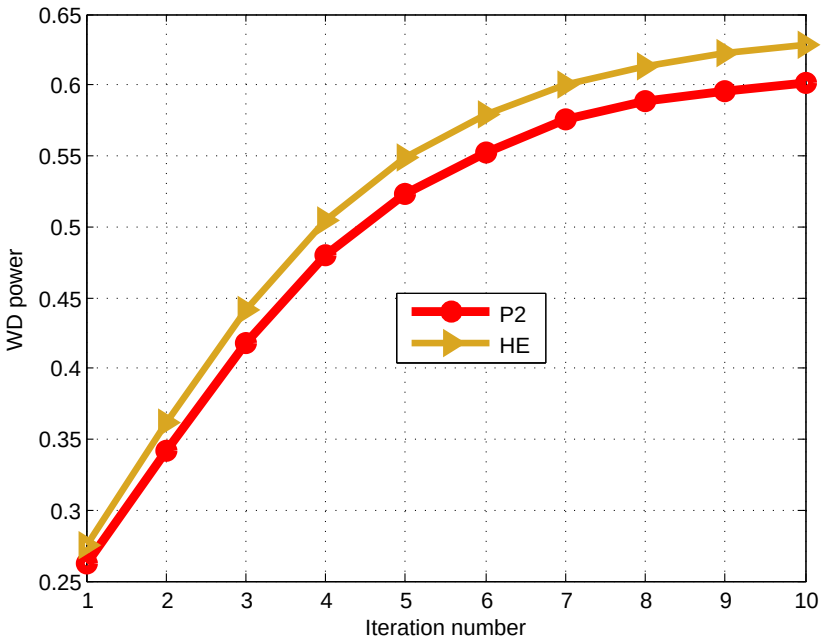

Fig. 6.3 Comparison between the power P2 transmitted by WD for $\mathtt{IR}_2$ information receiver and the harvested energy HE at the WD. As expected, the result confirm that the constraints harvested energy greater than P2 satisfies the optimization problem.

6.7 Appendix

6.8 Secrecy Rate Approximation Proof

The proof for the achievable secrecy rate of (6.23) and (6.28) is provided using Taylor series expansion. For a MIMO secrecy channel with a multi-antenna eavesdropper, the secrecy rate can be expressed as [120]:

$$R = \log\left|\mathbf{I} + \frac{1}{\sigma_e^2}\mathbf{H}_e\mathbf{Q}_l\mathbf{H}_e^H\right| - \log\left|\mathbf{I} + \frac{1}{\sigma_l^2}\mathbf{H}_l\mathbf{Q}_l\mathbf{H}_l^H\right| \tag{6.34}$$

From (6.34) above, it is observe that the expression is the difference of the two nonconvex concave functions. In order to convert R into a

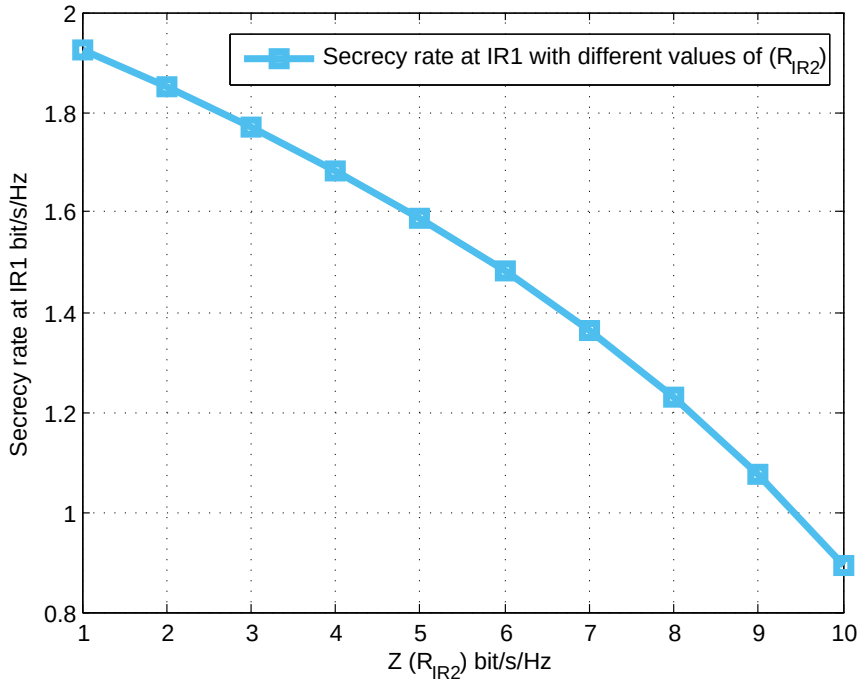

Fig. 6.4 Achieved secrecy rate by direct Taylor series approach scheme with different secrecy rate values constraint Z at $\mathtt{IR}_2$, $R_{IR2} >= Z$ to ensure the transmitted power by BS shared to all receivers and also for the QoS, the smaller Z the higher secrecy rate at $\mathtt{IR}_1$.

concave function, various approximations are available to do this with different accuracy levels. For example, this concave function could be approximated using the quadratic Taylor series approximation or using the difference of convex programming technique [118]. Given a function $g(\mathbf{Y})$, an affine Taylor series approximation of $g(\mathbf{Y}) : \mathbb{R}^{M\times N} \rightarrow \mathbb{R}$ can be expressed at $\tilde{\mathbf{Y}}$ as:

$$g(\mathbf{Y}) = g(\tilde{\mathbf{Y}}) + \text{vec}\left(g'(\tilde{\mathbf{Y}})\right) \text{vec}(\mathbf{Y} - \tilde{\mathbf{Y}}). \tag{6.35}$$

When (6.35) is applied along with the property $\partial(\log|\mathbf{Y}|) = \text{Tr}(\mathbf{Y}^{(1-)}\partial\mathbf{Y})$, the second term of equation(6.34) can be approximated using Taylor

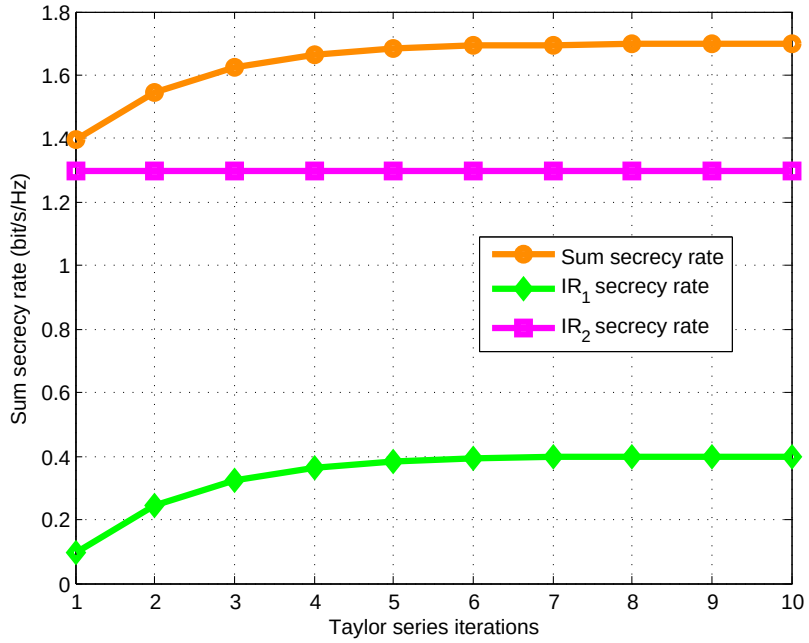

Fig. 6.5 Convergence of the secrecy rate for the $\mathtt{IR}_1$ and $\mathtt{IR}_2$ at direct approach with the constraint secrecy rate at $\mathtt{IR}_2$ =1.3 b/s/Hz. It is shown that the sum secrecy rate is equal to the sum of both receivers secrecy rates and also the secrecy rate at $\mathtt{IR}_2$ is equal to the value of Z which is the optimal value.

series expansion as

$$\begin{aligned}
&\log\left|\mathbf{I}+\frac{1}{\sigma_l^2}\mathbf{H}_l\mathbf{Q}_l\mathbf{H}_l^H\right| \approx \log\left|\mathbf{I}+\frac{1}{\sigma_l^2}\mathbf{H}_l\tilde{\mathbf{Q}}_l\mathbf{H}_l^H\right| \\
&+\mathrm{vec}\left[\mathbf{H}_l\left(\mathbf{I}+\frac{1}{\sigma_l^2}\mathbf{H}_l\tilde{\mathbf{Q}}_l\mathbf{H}_l^H\right)^{(-1)}\mathbf{H}_l^H\right] \\
&\times \mathrm{vec}(\mathbf{Q}_l-\tilde{\mathbf{Q}}_l) \\
&=\log\left|\mathbf{I}+\frac{1}{\sigma_l^2}\mathbf{H}_l\tilde{\mathbf{Q}}_l\mathbf{H}_l^H\right| \\
&+\mathrm{Tr}\left[\frac{1}{\sigma_l^2}\left(\mathbf{I}+\frac{1}{\sigma_l^2}\mathbf{H}_l\tilde{\mathbf{Q}}_l\mathbf{H}_l^H\right)^{(-1)}\mathbf{H}_l\mathbf{Q}_l\mathbf{H}_l^H\right] \\
&-\mathrm{Tr}\left[\frac{1}{\sigma_l^2}\left(\mathbf{I}+\frac{1}{\sigma_l^2}\mathbf{H}_l\tilde{\mathbf{Q}}_l\mathbf{H}_l^H\right)^{(-1)}\mathbf{H}_l\tilde{\mathbf{Q}}_l\mathbf{H}_l^H\right]. \qquad (6.36)
\end{aligned}$$

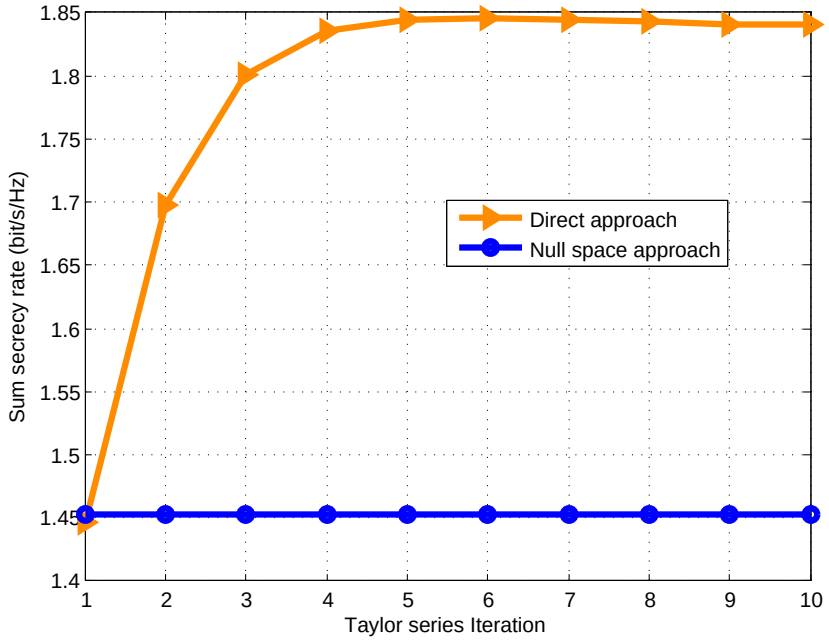

Fig. 6.6 Comparison between the sum secrecy rates at direct Taylor series optimization schemes and null space scheme, the direct Taylor series approach performance overcome the null space scheme performance.

Proof complete. ■

Chapter 7

Conclusion and Future Work

In this chapter, the contributions of this thesis along with concluding remarks are summarized in Section 7.1 and Section 7.2 features suggestions for future work.

7.1 Conclusions

In this thesis, mathematical optimization techniques were proposed and investigated towards achieving reliable data communication in wireless multi-antenna communication systems.

In Chapter 3, a multicell multiuser network that simultaneously considers coordinated beamforming and joint transmission was studied. This approach consisted of a network of single antenna local users and one multi-antenna global user. The global user was served by more than one BS, whereas the local users were assigned to only one BS at a time. A beamforming design using power minimization criterion was also considered. It was shown that for the global user, on average, both BSs equally share the data transfer, however, for the

optimality of transmission power, optimum split of data rate is required for instantaneous channel realizations.

In Chapter 4, the problem of SINR balancing in MISO network was addressed for two users with two Base stations. An energy splitting technique was used with power and RFEH constraints. Maximization of worst case user SINR was formulated through an optimization problem under power and energy harvesting constraints. The performance of the SINR balancing problem with interference was evaluated numerically. Results from simulation confirm that SINR balancing technique was able to fairly allocate resources to users while allowing energy harvesting.

Chapter 5 investigated a downlink energy and information transmission problem in a multiuser transmission system. The system consisted of a WPC system and an SWIPT system. The ET's energy beamforming and WD's information beamforming were designed to minimize the total transmitted power subject to the SINR constraints at IR1 and IR2. As a result, a joint wireless energy transfer and wireless information transfer design was achieved with two information receivers and one energy receiver. The optimization constraint also introduced a mechanism to control the SINR of the information signal at the energy receiver in order to enhance security.

Lastly, in Chapter 6, an approach for secure communications of SWIPT over the two-user MIMO interference channel when two eavesdroppers are present was proposed. Firstly, a null-space-based scheme of BS and WD transmitters were implemented. By imposing orthogonality among the interfering channels of the system, two sub-optimal secrecy rate optimization problems regarding IR1 and IR2 were de-

signed. Taylor series expansion was used to reformulate the secrecy rate maximization problems of both BS and WD into convex form. Performance was demonstrated using simulation results which confirmed efficient security performance of the proposed system and the comparison between both systems.

7.2 Future Work

The work presented in this thesis can be extended further in several research directions. Potential future research areas of stem from firstly, massive MIMO systems which is a new research into higher channel count MIMO systems. It indicates that increasing the number of antennas can significantly improve gains in spectral efficiency and capacity and can reduce energy consumption at the base station. Second is high mobility. Mobility is more difficult to achieve in Massive MIMO setups than in conventional wireless systems. Since Massive MIMO relies on up-to-date channel-state information to pinpoint each user via beamforming, the shorter channel coherence time of a mobile user may prevent accurate beamforming. The channel coherence time is dependent on the speed of the user device, and the faster the device movies, the more often the channel state information must be updated. In other words, a user equipment (UE) could move faster than the beam could update or track. This is especially challenging in time division duplex setups. Thirdly, 5G wireless communication network. This is an area which has attracted more and more attention in recent years. 5G denotes the next major phase of mobile telecommunications standards

beyond the current 4G/IMT-Advanced standards, which provide much more than just fast data speeds on mobile devices, envisioned as the key to providing seamless communications. Lastly, is IoT. This involves having a structure where everyday physical objects, each having unique identifiers, are connected to the Internet without the need for human interaction. In order for concepts such as this to be self-sustainable, there is the need to have energy-aware devices that are potentially capable of harvesting their required energy from ambient sources.

The work in Chapter 3 can be extended to multiple non-static global users so that the beamforming optimization becomes that of a dynamic optimization problem. This will then require a reformulation of the channel decomposition equation and semi definite programming equation. Once this is achieved, the possibility of attaining optimum power split between the global and local users would then be investigated.

Investigating the SINR balancing with increased number of MISO systems in Chapter 4 could be of interest. Performance of such a model could be evaluated with additional constraints such as SWIPT. Power splitting technique and other performance measures could also be studied with the presence of different interference models such as ISI and channel interference.

A downlink beamforming design with SWIPT in the presence of eavesdropper and QoS constraints is a possible research direction for the work in Chapters 5 and 6. This would be considered with the aim of minimization of total transmitted power of the SWIPT BS subject to secrecy rate due to eavesdropper and the SINR target at the information receivers.

References

[1] S. Boyd and L. Vandenberghe, *Convex optimization*. Cambridge university press, 2004.

[2] D. Tse and P. Viswanath, *Fundamentals of wireless communication*. Cambridge university press, 2005.

[3] H. Bölcskei, "Fundamentals of wireless communication," *Tc*, vol. 1, pp. 4–17, 2012.

[4] A. Goldsmith, *Wireless communications*. Cambridge university press, 2005.

[5] U. Dalal, *Wireless communication*. Oxford University Press, Inc., 2010.

[6] Z. Chu, "Transmit optimization techniques for physical layer security," 2016.

[7] G. J. Foschini, "Layered space-time architecture for wireless communication in a fading environment when using multi-element antennas," *Bell labs technical journal*, vol. 1, no. 2, pp. 41–59, 1996.

[8] E. Telatar, "Capacity of multi-antenna gaussian channels," *Transactions on Emerging Telecommunications Technologies*, vol. 10, no. 6, pp. 585–595, 1999.

[9] G. J. Foschini and M. J. Gans, "On limits of wireless communications in a fading environment when using multiple antennas," *Wireless personal communications*, vol. 6, no. 3, pp. 311–335, 1998.

[10] E. Biglieri, R. Calderbank, A. Constantinides, A. Goldsmith, A. Paulraj, and H. V. Poor, *MIMO wireless communications*. Cambridge university press, 2007.

[11] M. D. Renzo, H. Haas, and P. M. Grant, "Spatial modulation for multiple-antenna wireless systems: a survey," *IEEE Communications Magazine*, vol. 49, no. 12, pp. 182–191, December 2011.

[12] J. Mietzner, R. Schober, L. Lampe, W. H. Gerstacker, and P. A. Hoeher, "Multiple-antenna techniques for wireless communications-a comprehensive literature survey," *IEEE communications surveys & tutorials*, vol. 11, no. 2, 2009.

[13] E. Hossain, M. Rasti, H. Tabassum, and A. Abdelnasser, "Evolution toward 5g multi-tier cellular wireless networks: An interference management perspective," *IEEE Wireless Communications*, vol. 21, no. 3, pp. 118–127, 2014.

[14] V. Raghunathan, S. Ganeriwal, and M. Srivastava, "Emerging techniques for long lived wireless sensor networks," *IEEE Communications Magazine*, vol. 44, no. 4, pp. 108–114, 2006.

[15] L. R. Varshney, "Transporting information and energy simultaneously," in *Information Theory, 2008. ISIT 2008. IEEE International Symposium on.* IEEE, 2008, pp. 1612–1616.

[16] R. Zhang and C. K. Ho, "Mimo broadcasting for simultaneous wireless information and power transfer," *IEEE Transactions on Wireless Communications*, vol. 12, no. 5, pp. 1989–2001, 2013.

[17] P. Grover and A. Sahai, "Shannon meets tesla: Wireless information and power transfer," in *Information Theory Proceedings (ISIT), 2010 IEEE International Symposium on.* IEEE, 2010, pp. 2363–2367.

[18] M. Bloch and J. Barros, *Physical-layer security: from information theory to security engineering.* Cambridge University Press, 2011.

[19] L. Liu, R. Zhang, and K.-C. Chua, "Secrecy wireless information and power transfer with miso beamforming," in *Global Communications Conference (GLOBECOM), 2013 IEEE.* IEEE, 2013, pp. 1831–1836.

[20] D. W. K. Ng, E. S. Lo, and R. Schober, "Robust beamforming for secure communication in systems with wireless information and power transfer," *IEEE Transactions on Wireless Communications*, vol. 13, no. 8, pp. 4599–4615, 2014.

[21] Q. Li, W.-K. Ma, and A. M.-C. So, "Robust artificial noise-aided transmit optimization for achieving secrecy and energy harvesting," in *Acoustics, Speech and Signal Processing (ICASSP), 2014 IEEE International Conference on.* IEEE, 2014, pp. 1596–1600.

[22] R. Feng, Q. Li, Q. Zhang, and J. Qin, "Robust secure transmission in miso simultaneous wireless information and power transfer system," *IEEE Transactions on Vehicular Technology*, vol. 64, no. 1, pp. 400–405, 2015.

[23] D. W. K. Ng and R. Schober, "Max-min fair wireless energy transfer for secure multiuser communication systems," in *Information Theory Workshop (ITW), 2014 IEEE*. IEEE, 2014, pp. 326–330.

[24] M. Tian, X. Huang, Q. Zhang, and J. Qin, "Robust AN-aided secure transmission scheme in MISO channels with simultaneous wireless information and power transfer," *IEEE Signal Processing Letters*, vol. 22, no. 6, pp. 723–727, 2015.

[25] Z. Chu, Z. Zhu, M. Johnston, and S. Y. Le Goff, "Simultaneous wireless information power transfer for miso secrecy channel," *IEEE Transactions on Vehicular Technology*, vol. 65, no. 9, pp. 6913–6925, 2016.

[26] Q. Zhang, X. Huang, Q. Li, and J. Qin, "Cooperative jamming aided robust secure transmission for wireless information and power transfer in miso channels," *IEEE Transactions on Communications*, vol. 63, no. 3, pp. 906–915, 2015.

[27] M. Zhang, Y. Liu, and R. Zhang, "Artificial noise aided secrecy information and power transfer in ofdma systems," *IEEE Transactions on Wireless Communications*, vol. 15, no. 4, pp. 3085–3096, 2016.

[28] S. Plevel, S. Tomazic, T. Javornik, and G. Kandus, "Mimo: Wireless communications," *Encyclopedia of Wireless and Mobile Communications*, 2008.

[29] N. Shinohara, "Development of Rectenna with Wireless Communication System," in *the 5th European Conference on Antennas and Propagation, Rome, Italy, April 2011*, 2011, pp. 3970–3973.

[30] P. Kamalinejad, C. Mahapatra, Z. Sheng, S. Mirabbasi, V. C. M. Leung, and Y. L. Guan, "Wireless energy harvesting for the internet of things," *IEEE Communications Magazine*, vol. 53, no. 6, pp. 102–108, June 2015.

[31] Z. Popovic, "Cut the cord Low power far field wireless powering," *IEEE Microwave Magazine*, pp. 55–62, Apr. 2013.

[32] L. R. Varshney, "Transporting information and energy simultaneously," in *Information Theory, 2008. ISIT 2008. IEEE International Symposium on.* IEEE, 2008, pp. 1612–1616.

[33] I. Krikidis, S. Timotheou, S. Nikolaou, G. Zheng, D. W. K. Ng, and R. Schober, "Simultaneous wireless information and power transfer in modern communication systems," *IEEE Communications Magazine*, vol. 52, no. 11, pp. 104–110, 2014.

[34] T. Arakawa, A. C. Marcum, J. V. Krogmeier, and D. J. Love, "Simultaneous wireless information and power transfer over inductively coupled circuits," in *Acoustics, Speech and Signal Processing (ICASSP), 2017 IEEE International Conference on.* IEEE, 2017, pp. 3769–3773.

[35] J. Huang, C. C. Xing, and C. Wang, "Simultaneous wireless information and power transfer: Technologies, applications, and research challenges," *IEEE Communications Magazine*, vol. 55, no. 11, pp. 26–32, NOVEMBER 2017.

[36] A. Khisti and G. W. Wornell, "Secure transmission with multiple antennas—part ii: The mimome wiretap channel," *IEEE Transactions on Information Theory*, vol. 56, no. 11, pp. 5515–5532, 2010.

[37] ——, "Secure transmission with multiple antennas i: The misome wiretap channel," *IEEE Transactions on Information Theory*, vol. 56, no. 7, pp. 3088–3104, 2010.

[38] K. Cumanan, Z. Ding, B. Sharif, G. Y. Tian, and K. K. Leung, "Secrecy rate optimizations for a mimo secrecy channel with a multiple-antenna eavesdropper," *IEEE Transactions on Vehicular Technology*, vol. 63, no. 4, pp. 1678–1690, 2014.

[39] L. Zhang, R. Zhang, Y.-C. Liang, Y. Xin, and S. Cui, "On the relationship between the multi-antenna secrecy communications and cognitive radio communications," *IEEE Transactions on Communications*, vol. 58, no. 6, pp. 1877–1886, 2010.

[40] J. Li and A. P. Petropulu, "On ergodic secrecy rate for gaussian miso wiretap channels," *IEEE Transactions on Wireless communications*, vol. 10, no. 4, pp. 1176–1187, 2011.

[41] Z.-Q. Luo and W. Yu, "An introduction to convex optimization for communications and signal processing," *IEEE Journal on selected areas in communications*, vol. 24, no. 8, pp. 1426–1438, 2006.

[42] Q. Ke and T. Kanade, "Quasiconvex optimization for robust geometric reconstruction," *IEEE Transactions on Pattern Analysis and Machine Intelligence*, vol. 29, no. 10, pp. 1834–1847, Oct 2007.

[43] E. Björnson, M. Kountouris, and M. Debbah, "Massive MIMO and Small Cells: Improving Energy Efficiency by Optimal Soft-Cell Coordination," in *2013 20th International Conference on Telecommunications, ICT 2013*, 2013, pp. 1–5.

[44] N. Bhushan, J. Li, D. Malladi, R. Gilmore, D. Brenner, A. Damnjanovic, and R. Teja, "Network Densification : The Dominant Theme for Wireless Evolution into 5G," *IEEE Communications Magazine*, no. February, pp. 82–89, Feb. 2014.

[45] F. Rashid-Farrokhi, K. J. R. Liu, and L. Tassiulas, "Transmit Beamforming and Power Control for Cellular Wireless Systems," *IEE Journal on selected areas in communications*, vol. 16, no. 8, pp. 1437–1450, Oct. 1998.

[46] M. Schubert and H. Boche, "Solution of the Multiuser Downlink Beamforming Problem With Individual SINR Constraints," *IEEE Transactions on Vehicular Technology*, vol. 53, no. 1, pp. 18–28, Jan. 2004.

[47] D. W. H. Cai, T. Q. S. Quek, C. W. Tan, and S. H. Low, "Max-Min SINR Coordinated Multipoint Downlink Transmission — Duality and Algorithms," *IEEE Transactions on Signal Processing*, vol. 60, no. 10, pp. 5384–5395, Oct. 2012.

[48] D. Senaratne and C. Tellambura, "Generalized Singular Value Decomposition for Coordinated Beamforming in MIMO Systems," in *IEEE Globecom 2010 proceedings*, 2010, pp. 0–5.

[49] K. Dawui and D. Slock, "Multiuser-MIMO Downlink TX-RX Design Based on SVD Channel Diagonalization and Multiuser Diversity," in *Conference Record of the Thirty-Ninth Asilomar Conference onSignals, Systems and Computers, 2005.*, no. 1, 2005, pp. 1493–1497.

[50] H. Dahrouj and W. Yu, "Coordinated Beamforming for the Multicell Multi-antenna Wireless System," *IEEE Transactions on Wireless Communications*, vol. 9, no. 5, pp. 1748–1759, May 2010.

[51] E. Björnson and E. Jorswieck, "Optimal Resource Allocation in Coordinated Multi-Cell Systems," *Foundation and Trends in Communications and Information Theory*, vol. 9, no. 2012, pp. 113–381, 2013.

[52] Y. Rahulamathavan, S. Member, and K. Cumanan, "A Mixed SINR-Balancing and SINR-Target-Constraints-Based Beamformer Design Technique for Spectrum-Sharing Networks," *IEEE Transactions on Vehicular Technology*, vol. 60, no. 9, pp. 4403–4414, 2011.

[53] J. Zhao, T. Q. S. Quek, S. Member, Z. Lei, and S. Member, "Coordinated Multipoint Transmission with Limited Backhaul Data Transfer," *IEEE Transactions on Wireless Communications*, vol. 12, no. 6, pp. 2762–2775, 2013.

[54] B. Basutli and S. Lambotharan, "Distributed beamformer design under mixed SINR balancing and SINR -target-constraints," in *2015 IEEE International Conference on Digital Signal Processing (DSP)*, July 2015, pp. 530–534.

[55] G. Bournaka, Y. Rahulamathavan, K. Cumanan, S. Lambotharan, and F. Lazarakis, "Base station beamforming technique using multiple signal-to-interference plus noise ratio balancing criteria," *IET Signal Processing*, vol. 9, no. August 2014, pp. 248–259, 2015.

[56] C. Chan-Byoung, I. Hwang, J. R. W. Heath, and V. Tarokh, "Interference Aware-Coordinated Beamforming in a Multi-Cell System," *IEEE Transactions on Wireless Communications*, vol. 11, no. 10, pp. 3692–3703, Oct. 2012.

[57] M. Bengtsson and B. Ottersten, "Optimal Downlink Beamforming Using Semidefinite Optimization," in *In proceedings of 37th*

Annual Allerton Conference on Communication, Stockholm, 1999, pp. 987–996.

[58] J. Efberg, "YALMIP : A toolbox for modeling and optimization in MATLAB," in *IEEE International Symposium on Computer Aided Control Sysytems Design*, Tapei, 2004, pp. 284–289.

[59] L. Zhi-Quan, M. Wing-Kin, S. A. Man-Cho, Y. Ye, and Z. Shuzhong, "Semidefinite Relaxation of Quadratic Optimization Problems," *IEEE Signal Processing Magazine*, no. May, pp. 20–34, May 2010.

[60] S. Boyd and L. Vandenberghe, *Convex Optimization*, 3rd ed. University Press, Cambridge UK, 2004, vol. 25.

[61] L. Liu, R. Zhang, and K.-C. Chua, "Wireless information transfer with opportunistic energy harvesting," *IEEE Transactions on Wireless Communications*, vol. 12, no. 1, pp. 288–300, 2013.

[62] S. Ulukus, E. Erkip, P. Grover, K. Huang, O. Simeone, A. Yener, and M. Zorzi, "Guest editorial: Wireless communications powered by energy harvesting and wireless energy transfer, part ii," *IEEE Journal on Selected Areas in Communications*, vol. 33, no. 8, pp. 1477–1479, Aug 2015.

[63] Z. Hadzi-Velkov, I. Nikoloska, G. K. Karagiannidis, and T. Q. Duong, "Wireless networks with energy harvesting and power transfer: Joint power and time allocation," *IEEE Signal Processing Letters*, vol. 23, no. 1, pp. 50–54, 2016.

[64] S. Ulukus, A. Yener, E. Erkip, O. Simeone, M. Zorzi, P. Grover, and K. Huang, "Energy harvesting wireless communications: A

review of recent advances," *IEEE Journal on Selected Areas in Communications*, vol. 33, no. 3, pp. 360–381, 2015.

[65] Y. Zeng and R. Zhang, "Optimized training for net energy maximization in multi-antenna wireless energy transfer over frequency-selective channel," *IEEE Transactions on Communications*, vol. 63, no. 6, pp. 2360–2373, 2015.

[66] T. Wu and H.-C. Yang, "RF energy harvesting with cooperative beam selection for wireless sensors," *IEEE Wireless Communications Letters*, vol. 3, no. 6, pp. 585–588, 2014.

[67] D. I. K. Kae Won Choi, "Stochastic optimal control for wireless poweredcommunication networks," *IEEE Transactions on Wireless Communications, Vol. 15, NO. 1, January 2016*, vol. 15, no. 1, pp. 686–699, 2016.

[68] J. Xu and R. Zhang, "A general design framework for mimo wireless energy transfer with limited feedback," *Signal Processing, IEEE Transactions on*, vol. PP, no. 99, pp. 1–1, 2016.

[69] P. Grover and A. Sahai, "Shannon meets tesla: Wireless information and power transfer," in *2010 IEEE International Symposium on Information Theory*, June 2010, pp. 2363–2367.

[70] R. Elsabae, B. Basutli, K. Ghanem, Y. Gong, and S. Lambotharan, "Coordinated multicell beamforming with local and global data rate constraints," in *2016 24th European Signal Processing Conference (EUSIPCO)*, Aug 2016, pp. 1388–1392.

[71] C. Song, C. Ling, J. Park, and B. Clerckx, "MIMO broadcasting for simultaneous wireless information and power transfer:

Weighted MMSE approaches," in *Globecom Workshops (GC Wkshps), 2014*. IEEE, 2014, pp. 1151–1156.

[72] R. Zhang and C. K. Ho, "MIMO broadcasting for simultaneous wireless information and power transfer," *IEEE Transactions on Wireless Communications*, vol. 12, no. 5, pp. 1989–2001, 2013.

[73] Z. Xiang and M. Tao, "Robust beamforming for wireless information and power transmission," *IEEE Wireless Communications Letters*, vol. 1, no. 4, pp. 372–375, 2012.

[74] I. Krikidis, S. Timotheou, and S. Sasaki, "RF energy transfer for cooperative networks: Data relaying or energy harvesting?" *IEEE Communications Letters*, vol. 16, no. 11, pp. 1772–1775, 2012.

[75] J. Xu, L. Liu, and R. Zhang, "Multiuser MISO beamforming for simultaneous wireless information and power transfer," *IEEE Transactions on Signal Processing*, vol. 62, no. 18, pp. 4798–4810, 2014.

[76] S. Timotheou, I. Krikidis, and B. Ottersten, "MISO interference channel with QoS and RF energy harvesting constraints," in *IEEE International Conference on Communications (ICC), 2013*. IEEE, 2013, pp. 4191–4196.

[77] S. Timotheou, I. Krikidis, G. Zheng, and B. Ottersten, "Beamforming for MISO interference channels with QoS and RF energy transfer," *IEEE Transactions on Wireless Communications*, vol. 13, no. 5, pp. 2646–2658, 2014.

[78] T. Le, K. Mayaram, and T. Fiez, "Efficient far-field radio frequency energy harvesting for passively powered sensor networks,"

Solid-State Circuits, IEEE Journal of, vol. 43, no. 5, pp. 1287–1302, 2008.

[79] Q. Ye, B. Rong, Y. Chen, M. Al-Shalash, C. Caramanis, and J. G. Andrews, "User association for load balancing in heterogeneous cellular networks," *IEEE Transactions on Wireless Communications*, vol. 12, no. 6, pp. 2706–2716, 2013.

[80] W. Yu and T. Lan, "Transmitter optimization for the multi-antenna downlink with per-antenna power constraints," *IEEE Transactions on Signal Processing*, vol. 55, no. 6, pp. 2646–2660, 2007.

[81] H. Park, S.-H. Park, J.-S. Kim, and I. Lee, "SINR balancing techniques in coordinated multi-cell downlink systems," *IEEE Transactions on Wireless Communications*, vol. 12, no. 2, pp. 626–635, 2013.

[82] A. Tölli, H. Pennanen, and P. Komulainen, "SINR balancing with coordinated multi-cell transmission." in *WCNC*, 2009, pp. 386–391.

[83] L. Liu and R. Zhang, "Downlink SINR balancing in C-RAN under limited fronthaul capacity," in *IEEE International Conference on Acoustics, Speech and Signal Processing (ICASSP) 2016*. IEEE, 2016, pp. 3506–3510.

[84] J. Zhang, Z. K. M. Ho, E. Jorswieck, and M. Haardt, "SINR balancing for non-regenerative two-way relay networks with interference neutralization," in *IEEE International Conference on Acoustics, Speech and Signal Processing (ICASSP) 2014*. IEEE, 2014, pp. 7604–7608.

[85] C. W. Tan, M. Chiang, and R. Srikant, "Maximizing sum rate and minimizing MSE on multiuser downlink: Optimality, fast algorithms and equivalence via max-min SINR," *IEEE Transactions on Signal Processing*, vol. 59, no. 12, pp. 6127–6143, 2011.

[86] H. T. Do and S.-Y. Chung, "Linear beamforming and superposition coding with common information for the gaussian MIMO broadcast channel," *IEEE Transactions on Communications*, vol. 57, no. 8, pp. 2484–2494, 2009.

[87] B. Basutli and S. Lambotharan, "Distributed beamformer design under mixed SINR balancing and SINR-target-constraints," in *Digital Signal Processing (DSP), 2015 IEEE International Conference on*. IEEE, 2015, pp. 530–534.

[88] C. Masouros and G. Zheng, "Exploiting known interference as green signal power for downlink beamforming optimization," *IEEE Transactions on Signal Processing*, vol. 63, no. 14, pp. 3628–3640, 2015.

[89] A. Dolgov, R. Zane, and Z. Popovic, "Power management system for online low power RF energy harvesting optimization," *IEEE Transactions on Circuits and Systems I: Regular Papers*, vol. 57, no. 7, pp. 1802–1811, 2010.

[90] O. Ozel, K. Tutuncuoglu, J. Yang, S. Ulukus, and A. Yener, "Transmission with energy harvesting nodes in fading wireless channels: Optimal policies," *IEEE Journal on Selected Areas in Communications*, vol. 29, no. 8, pp. 1732–1743, 2011.

[91] R. Zhang and C. K. Ho, "Mimo broadcasting for simultaneous wireless information and power transfer," *IEEE Transactions on Wireless Communications*, vol. 12, no. 5, pp. 1989–2001, 2013.

[92] H. Ju and R. Zhang, "Throughput maximization in wireless powered communication networks," *IEEE Transactions on Wireless Communications*, vol. 13, no. 1, pp. 418–428, 2014.

[93] Y. Che, J. Xu, L. Duan, and R. Zhang, "Multiantenna wireless powered communication with cochannel energy and information transfer," *IEEE Communications Letters*, vol. 19, no. 12, pp. 2266–2269, 2015.

[94] E. Bjornson, M. Kountouris, and M. Debbah, "Massive mimo and small cells: Improving energy efficiency by optimal soft-cell coordination," in *Telecommunications (ICT), 2013 20th International Conference on*. IEEE, 2013, pp. 1–5.

[95] S. Dadallage, C. Yi, and J. Cai, "Joint beamforming, power, and channel allocation in multiuser and multichannel underlay miso cognitive radio networks," *IEEE Transactions on Vehicular Technology*, vol. 65, no. 5, pp. 3349–3359, 2016.

[96] G. Zheng, C. Masouros, I. Krikidis, and S. Timotheou, "Exploring green interference power for wireless information and energy transfer in the miso downlink," in *Communications (ICC), 2015 IEEE International Conference on*. IEEE, 2015, pp. 149–153.

[97] Q. Shi, L. Liu, W. Xu, and R. Zhang, "Joint transmit beamforming and receive power splitting for miso swipt systems," *IEEE Transactions on Wireless Communications*, vol. 13, no. 6, pp. 3269–3280, 2014.

[98] J. Park and B. Clerckx, "Joint wireless information and energy transfer in a two-user mimo interference channel," *IEEE Transactions on Wireless Communications*, vol. 12, no. 8, pp. 4210–4221, 2013.

[99] I. Krikidis, S. Timotheou, S. Nikolaou, G. Zheng, D. W. K. Ng, and R. Schober, "Simultaneous wireless information and power transfer in modern communication systems," *IEEE Communications Magazine*, vol. 52, no. 11, pp. 104–110, 2014.

[100] J. Zhao, T. Q. Quek, and Z. Lei, "Coordinated multipoint transmission with limited backhaul data transfer," *IEEE Transactions on Wireless Communications*, vol. 12, no. 6, pp. 2762–2775, 2013.

[101] Y. Wu and S. Lambotharan, "A coordinated multicell beamforming technique with multiple interference constraints," 2013.

[102] J. Xu, S. Bi, and R. Zhang, "Multiuser mimo wireless energy transfer with coexisting opportunistic communication," *IEEE Wireless Communications Letters*, vol. 4, no. 3, pp. 273–276, 2015.

[103] Y. Zeng and R. Zhang, "Full-duplex wireless-powered relay with self-energy recycling," *IEEE Wireless Communications Letters*, vol. 4, no. 2, pp. 201–204, 2015.

[104] S. Bi, C. K. Ho, and R. Zhang, "Wireless powered communication: opportunities and challenges," *IEEE Communications Magazine*, vol. 53, no. 4, pp. 117–125, April 2015.

[105] L. R. Varshney, "Transporting information and energy simultaneously," in *2008 IEEE International Symposium on Information Theory*, July 2008, pp. 1612–1616.

[106] X. Zhou, R. Zhang, and C. K. Ho, "Wireless information and power transfer: Architecture design and rate-energy tradeoff," *IEEE Transactions on Communications*, vol. 61, no. 11, pp. 4754–4767, November 2013.

[107] Z. Ding, C. Zhong, D. W. K. Ng, M. Peng, H. A. Suraweera, R. Schober, and H. V. Poor, "Application of smart antenna technologies in simultaneous wireless information and power transfer," *IEEE Communications Magazine*, vol. 53, no. 4, pp. 86–93, April 2015.

[108] X. Chen, C. Zhong, C. Yuen, and H. H. Chen, "Multi-antenna relay aided wireless physical layer security," *IEEE Communications Magazine*, vol. 53, no. 12, pp. 40–46, Dec 2015.

[109] L. Dong, Z. Han, S. Member, A. P. Petropulu, and H. V. Poor, "Improving Wireless Physical Layer Security via Cooperating Relays," *IEEE Transactions on Signal Processing*, vol. 58, no. 3, pp. 1875–1888, 2010.

[110] Y. Liang, H. V. Poor, and L. Ying, "Networks : Stability and Utility Maximization," *IEEE Transactions on information forensics and secrity*, vol. 6, no. 3, pp. 682–692, Sep. 2011.

[111] X. Tang, R. Liu, P. Spasojevic, and H. V. Poor, "Interference Assisted Secret Communication ´ ,," *IEEE Transactions on information theory*, vol. 57, no. 5, pp. 3153–3167, 2011.

[112] J. Park and B. Clerckx, "Joint wireless information and energy transfer in a k -user mimo interference channel," *IEEE Transactions on Wireless Communications*, vol. 13, no. 10, pp. 5781–5796, Oct 2014.

[113] L. Liu, R. Zhang, and K. C. Chua, "Secrecy wireless information and power transfer with miso beamforming," *IEEE Transactions on Signal Processing*, vol. 62, no. 7, pp. 1850–1863, April 2014.

[114] P. Zhao, M. Zhang, H. Yu, H. Luo, and W. Chen, "Robust beamforming design for sum secrecy rate optimization in mu-miso networks," *IEEE Transactions on Information Forensics and Security*, vol. 10, no. 9, pp. 1812–1823, Sept 2015.

[115] Z. Zhu, Z. Wang, Z. Chu, S. Huang and F. Zhou, "Max-min Fair Harvested Energy Based Beamforming Designs for MISO SWIPT Secrecy System," in *2016 IEEE International Conference on Ubiquitous Wireless Broadband (ICUWB)*, 2016, pp. 1–4.

[116] J. Li, A. P. Petropulu, and A. A. G. Miso, "On Ergodic Secrecy Rate for Gaussian MISO Wiretap Channels," *IEEE Transaction on Wireless Communications,*, vol. 10, no. 4, pp. 1176–1187, 2011.

[117] J. Huang and A. L. Swindlehurst, "Robust secure transmission in miso channels based on worst-case optimization," *IEEE Transactions on Signal Processing*, vol. 60, no. 4, pp. 1696–1707, April 2012.

[118] K. Cumanan, R. Zhang, and S. Lambotharan, "A new design paradigm for mimo cognitive radio with primary user rate constraint," *IEEE Communications Letters*, vol. 16, no. 5, pp. 706–709, May 2012.

[119] Z. Chu, K. Cumanan, Z. Ding, M. Johnston, and S. Y. L. Goff, "Secrecy rate optimizations for a mimo secrecy channel with a cooperative jammer," *IEEE Transactions on Vehicular Technology*, vol. 64, no. 5, pp. 1833–1847, May 2015.

[120] A. Khisti and G. W. Wornell, "Secure Transmission With Multiple Antennas I : The MISOME Wiretap Channel," *IEEE Transactions on information theory*, vol. 56, no. 7, pp. 3088–3104, 2010.